1984

Ultrastructure of Wheat (Triticum aestivum) Leaf Cells Infected with Leaf Rust (Puccinia recondita), and Wheat Streak Mosaic Virus

Saleh H. Shrief

ULTRASTRUCTURE OF WHEAT (TRITICUM AESTIVUM) LEAF CELLS INFECTED WITH LEAF RUST (PUCCINIA RECONDITA), AND WHEAT STREAK MOSAIC VIRUS

BY

SALEH H. SHRIEF

A thesis submitted
in partial fulfillment of the requirements for the
degree Doctor of Philosophy, Major in
Agronomy, South Dakota
State University

1984

ULTRASTRUCTURE OF WHEAT (TRITICUM AESTIVUM) LEAF CELLS INFECTED WITH LEAF RUST (PUCCINIA RECONDITA), AND WHEAT STREAK MOSAIC VIRUS

This thesis is approved as a creditable and independent investigation by a candidate for the degree, Doctor of Philosophy, and is acceptable for meeting the thesis requirements for this degree. Acceptance of this thesis does not imply that the conclusions reached by the candidate are necessarily the conclusions of the major department.

Thesis Adviser Date

Date

ACKNOWLEDGEMENTS

I wish to express my sincere appreciation to Dr. Wayne S. Gardner, my major adviser, who provided direction, knowledge, and a great deal of his time in assistance in completing this study. Without his enthusiastic and personal interest in my success, completion of this thesis would have been impossible. I would like to thank Dr. Maurice L. Horton, and the Plant Science Department for giving me the opportunity to conduct this research. Sincere thanks are extended to Dr. George Buchenau and Dr. Charles R. McMullen who provided many valuable suggestions and constructive comments, and to the rest of my graduate committee for their time and support.

Special thanks to my wife Suad for her patience, support and prayers throughout the time, and to my children Alaedean, Hazem and Lubna for their understanding, and putting up with their student father. I would like to thank Mrs. Naomi Boone for a wonderful job in typing this thesis.

TABLE OF CONTENTS

ULTRASTRUCTURE OF WHEAT (TRITICUM AESTIVUM) LEAF CELLS

INFECTED WITH LEAF RUST (PUCCINIA RECONDITA),

AND WHEAT STREAK MOSAIC VIRUS

Abstract

SALEH H. SHRIEF

Under the supervision of Dr. Wayne S. Gardner

Puccinia recondita ultrastructure resembles that of other rust species. The urediospore infection was characterized by the formation of a specialized structure, the haustorium, within the leaf cells. The haustorium contains organelles such as nuclei, mitochondria, microbodies, ribosomes, lipid bodies, and vacuoles. A haustorial neck connects the haustorium with the haustorial mother cell, and contains a neck band made up of darkly stained material. The neck band was located at the last one third of its length toward the haustorium. The haustorial mother cell was situated intercellularly, and closely adhering to the cell wall, but contained few organelles, and the nucleus was never evident. The intercellular hyphae were packed with organelles. The hyphal cells were separated by septa which were perforated and nonperforated. Nuclei, and nucleoli were frequently found in intercellular hyphae. In the septal pore region, mitochondria, microbodies, and glycogen bodies, appear to be bounded by a membrane which separates it from the cytoplasm. Rod and spherical shaped virus-like particles (VLPs) were observed in several haustoria and intercellular hyphae. Most of the VLPs examined were different from the wheat streak mosaic virus, (WSMV), and existed in fungal haustoria, and intercellular

hyphae infecting wheat tissues that were either infected or not infected with WSMV. The VLPs detected in one haustorium, were indistinguishable from the virus particles infecting the host cell outside the haustorium. The fungal plasmalemma in the haustoria, haustorial necks, intercellular hyphae and urediospores, were repeatedly folded, and formed conspicuous invaginated membranous structures which occurred either connected to or next to the plasma membrane. It is proposed that those membranous structures be called "Invaginated Fungal Plasmalemma" (IFP). Crystalline and noncrystalline containing microbodies were found in haustoria, intercellular hyphae and urediospores. Their number ranged from two to nine per fungal propagule, but generally they were more abundant in haustoria. Crystalline and noncrystalline microbodies appeared together in several haustoria. Attempts to transmit WSMV by urediospores were unsuccessful, even though VLPs were detected in the fungal propagules.

INTRODUCTION

Wheat leaf rust caused by Puccinia recondita Rob. ex Desm. f. sp. tritici syns. P. rubiogo - vera (DC) Wint., P. triticina Eriks. may be the most widely distributed of wheat diseases. An estimated yield loss of 55% on susceptible cultivars has been reported by Johnston, (49), and Burleigh et al., (9).

The ultrastructure of rust fungi has been extensively reviewed by Bracker (7), Bushnell (10), and Littlefield and Heath (56). However, studies on the ultrastructure of wheat leaf rust are few. This does not justify the important impact this fungus has in cereal production. Studies available on P. recondita of wheat are mostly on ultrastructure of the different types of spores. Gold et al., (33), followed the pycnial and aecial spore formation on Thalictrum speciosissimum Loeft. (Meadow rue), an alternate host for wheat leaf rust fungus, and provided both scanning, and transmission electron micrographs of these spores. Salako (81), found no difference in ultrastructure between urediospores of P. recondita killed by infra-red radiation, and dry, fresh but viable urediospores. A description of fungal haustoria was given in Russian with few electron micrographs showing limited details by Peresypkin et al., (71). Other aspects such as septa and setal-pore appartus of uredial mycelium were described by Ehrlich et al., (23), and some aspects of mitosis and cell division in some cereal rust fungi, including leaf rust, have been reported by Harder, (36, 37).

Wheat streak mosaic virus (WSMV) causes an important wheat disease. It occurs throughout central and western North America,

eastern Europe and parts of the USSR (89). In the United States it is most prevalent in the central great plains where the losses in winter wheat range from insignificant to complete. The virus infects wheat systemically, and in later infections may involve only the flag leaf and the awns. The symptoms vary in severity with cultivar. Wheat streak mosaic virus and leaf rust are known to occur together in nature, and their combined effects on wheat yield had been reported by Raju et al. (75). However, ultrastructure of wheat infected with both pathogens has not been studied, and the need for such studies is obviously great.

The association of virus with fungi has long been assumed, but experimental proof was not evident until 1962 when virus particles were shown in the diseased mushroom Agaricus bisporus, by Hollings (46). Since then a great deal of work has been published, and reviewed by Lemke (52), and Ghabrial (32). To date, viruses and virus-like particles (VLPs) have been reported in more than 100 species of fungi belonging to all major groups (32). The terms (VLPs) and mycoviruses are commonly used to describe the relationship of virus to fungi, and also used to in reference to those particles that are shown in electron micrographs of fungal structures, but have never been isolated and characterized. The term mycovirus is applied to those particles that have been isolated and their morphology and nucleoprotein composition are known. The term VLPs is favored by some workers to be used in all cases since the mycoviruses are not conclusively proven to be infectious in purified forms.

The presence of VLPs in many plant pathogenic fungi has been confirmed in several studies. McDonald and Heath (68), found rod-

shaped and spherical virus-like particles in the cowpea rust fungus. Yarwood, and Hect-Poinar (92) described VLPs found in five species of rusts and two species of powdery mildews, but attempts to transmit and produce virus-like infection were unsuccessful. Wechmar, (88) reported that urediospores of P. graminis tritici transmitted brome mosaic virus, (BMV) and typical virus symptoms appeared 5-6 days after inoculation. She thought of an internal association between BMV and the urediospores, and did not exclude the possibility that the virus multiplied within the urediospores. Recently, Erasmus et al., (26) confirmed Wechmar's (88) results of transmission, adding that leaf rust transmitted BMV also. However, Erasmus et al., (27) showed that brome mosaic virus was carried externally on the urediospores, and the rust transmitted virus produced atypical symptoms on the inoculated wheat plants.

The effect of viruses on plant hosts has been studied, and ultrastructural changes were found to occur as host responses to infections. Kim and Fulton (50) reported that cell wall overgrowth and pronounced formation of paramural bodies occurred in bean leaves at early stages of infection by bean pod mottle virus. McMullen et al., (69) found similar results of paramural bodies and associated cell-wall thickenings in barley leaves infected with barley stripe mosaic virus, and cell wall thickenings observed in wheat streak mosaic virus infected wheat cells (70). Studies on ultrastructure of multiple infection, where a mixture of plant viruses were simultaneously applied to host cells, are limited. Carr and Kim (12) reported that bean leaf cells infected with two morphologically distinct viruses, formed nuclear inclusions, of two types, spheres and filaments, characteristic of each

virus. The effects of viruses on their fungal hosts, or a combined effect of a virus and a fungal pathogen on a plant host are not as well understood. However, the systemic fungicide Triadimefon applied to leaves of wheat infected with P. recondita and broad bean infected with Uromyces vicia fabae caused incomplete and multiperforated septa (74). An extensive wall thickening in the intercellular mycelia following both root and leaf application of the fungicide was observed also.

Invaginated Fungal Plasmalemma (IFP). Membrane structures between the plasma lemma and cell wall of plants and fungi are seen quite often in electron micrographs of several published reports, but they were either ignored or received very little attention. Those spongy structures that are continuous with the cell wall and their interior limits defined by the plasma membrane were first fully described, and named lomasomes by Moor and McAlear (67), who concluded based on their surveys, that lomasomes occur only in fungi. This observation however, was proven to be erroneous. Since Manocha and Shaw (57), reported that lomasomes occurred in the mesophyll cells of wheat, and Barton (3), showed a micrograph of charasomes (a lomasome-like structure) in the alga Chara vulgaris.

The vesicular and membranous structures observed by Marchant and Robards (62) are present in different parts of many fungi from all major groups. The main exception is the mature spores, or the cells from which they arise as noted by Moor and McAlear (67), and Marchant and Robards (62). Paramural body, a general term, was suggested by Marchant and Robards (62) to be used for all membranous and vesicular structures which were associated with the plasma membrane regardless of

their origin. These paramural bodies were then separated into two groups based on their derivation. The lomasomes are derived from cytoplasmic membranes, whereas structures formed mainly from the plasmalemma were called plasmalemmasomes. Van Dyke and Hooker (87) observed that the plasma membrane of P. sorghi infecting maize, was arranged in a concentric manner, and the tubular configuration of the extensions of the fungal plasma membrane were then called lomasomes.

The term membrane complexes was used by Ramberg and McLaughlin (76), in reference to those organelles that had an occasional association to the plasma membrane, but were randomly distributed throughout the cytoplasm. Tubular complexes, as described by Rijo and Sargent (80), in the coffee leaf rust, were not lomasomes since they were not always associated with the plasmalemma.

The terminology of those membranous structures found in fungal cells is extensive, and most of these names refer to the same structure. Multivesicular bodies was used to refer to a coiled membrane found in an immature urediospore of U. phaseoli of bean rust by Pring (73). The same membrane-type structure was called mylein figure in Scopulariopsis breviculis by Cole and Aldrich (19), and membrane complex in U. appendiculatus of bean by Hardwick et al., (41), and in P. coronata of oats by Harder (37, 38). Abu-zinada et.al., (1), found that the vacuole of U. fabae infecting faba bean, contained tubular and vesicular elements, which often aggregated into multivesicular bodies, which are totally different from those reported by Pring (73).

The function of all the above described membrane systems is as confused as their terminology. Some interpreted them as golgi bodies or

dictyosomes such as Littlefield and Heath (56), or behave in a similar way as golgi bodies by Wilsenach and Kessel (91), or structures that serve the functions of a golgi apparatus by Rajo and Sargent, (80). Peyton and Bowen (72), suggested that the formation of membranous structures (lomasomes) were the result of an elaboration of the plasma membrane. Wilsenach and Kessel (91), suggested that the invaginated fungal plasmalemmas (lomasomes) were associated with the formation of cell wall material due to its location between the two membranes of the endoplasmic reticulum.

Microbodies. Plant microbodies have received much attention since their discovery. Several review articles have been written on microbodies of plants by Beeves (4), Gerhardt (31), and a more specific review dealt with microbodies in plant pathogenic fungi by Maxwell et al., (65). The most recent review by Huang et al. (47) discussed several aspects of both plant as well as fungal peroxisomes.

Microbodies were first recognized in fungi in 1966 by Mollenhauer et al., (66). Several electron microscopic studies from all major taxa of fungi at different stages of development showed that microbodies are common to fungal cells (65). However, when permanganate was used as a fixative for plant tissues, several names were assigned to morphologically describe, and identify microbodies such as: cytosomes, spherosomes, lysosomes, side-body matrix, stuben bodies, woronin bodies, etc.

Examination of thin section of glutaraldehyde-fixed tissues by electron microscopy revealed that plant microbodies are round to oval having a diameter of 0.2 - 1.7 um, a coarse granular or fibrillar

matrix bound by a single membrane and they may contain amorphous or crystalline inclusions (30, 47). Maxwell et al., (63) found microbodies in the hyphal tips of Sclerotinia sclerotiorum, with similar characteristics as described above.

Recently Huang et al., (47) described how the term microbody should be used. Microbody is used as a general name, and not to imply any specific function. It can be used in reference to any or all classes of peroxisomes, or to describe such organelles observed with the electron microscope when their enzyme content has never been tested.

The occurrence and distribution of microbodies within fungal cells depends on the species and the cell type. In plant cells a similar trend of variation in the number of microbodies ranged from one microbody to several hundreds of microbodies per cell (31).
In the haustoria and the intercellular hyphae of obligate plant pathogenic fungi, microbodies were generally scarce, but microbodies were abundant in hyphae of necrotrophic fungi colonizing dead plant tissues (65), and in hyphae of fungi grown on carbon-rich media (64).

The purpose of this study was to explore different ultrastructural aspects of P. recondita, such as the haustorium, intercellular hyphae, and urediospores. Penetration sites at different wheat cell types were sought. Various types of organelles, which were thought to exist in fungal cells, but were never shown in leaf rust such as microbodies, and membranous structures formed as an invagination of the fungal plasmalemma were investigated. The study was conducted to describe the relationship between P. recondita and wheat streak mosaic virus, to determine whether virus-like particle could be found in the

fungal propagules, and to test the transmission of WSMV by urediospores of the leaf rust.

MATERIALS AND METHODS

Urediospores of the leaf rust Puccinia recondita were obtained from naturally infected winter wheat plants, that were brought in from South Dakota Agriculture Experiment Station, in Brookings, South Dakota and kept in the greenhouse to be used as a source of inoculum. Wheat streak mosaic virus was obtained from Dr. W. S. Gardner, where it is maintained on winter wheat in the greenhouse. Winoka, a hard red winter wheat (Triticum aestivum) cultivar that is known to be susceptible to WSMV and P. recondita, was used throughout the study. Seeds of Winoka were vernalized in a cold room where the temperatures was 32° C - 38° C for 6 weeks. The seedlings were transplanted into 10 cm pots. A week after transplanting, the seedlings were dusted with corundum and finger-inoculated with the juice from wheat leaves infected with WSMV. The flag leaves of virus-infected plants were inoculated with freshly harvested urediospores suspended in water. The rust inoculation was done by rubbing the flag leaf between the index finger and the thumb after dipping them in the spore suspension. The inoculated plants were covered with plastic bags wetted on the inner side to maintain high relative humidity for 24 hours. Plants were kept on greenhouse benches after removal of the plastic bags. The flag leaves, infected with WSMV, P. recondita, both pathogens, and healthy checks were collected for electron microscopy. The leaves from each treatment were sliced by putting the infected area of the leaf on a drop of 2.5% glutaraldehyde (GA), in 0.1M (pH 7.1) potassium phosphate buffer placed on the top cover of plastic petri dish filled with crushed ice. The infected areas were then cut into approximately 1 x 5 mm portions. The leaf pieces

were transferred into glass vials containing 6 ml of the buffered GA, and kept in ice bath on the laboratory bench for 60 minutes. The vials were drained using a Pasteur pipet. One ml of 1% phosphate-buffered osmic acid (OsO_4) was added to each vial. After 60 minutes the OsO_4 was removed. The tissues were dehydrated in a series of cold acetone starting at 25% for 15 minutes, repeated twice, followed by 50% and repeated twice. Four ml of 2,2-Dimethoxypropane (DMP) (acidified with two drops of concentrated HCl per 100 ml) was added to each vial and repeated after 15 minutes at room temperature. The tissues were soaked for two hours in epoxy plastic medium mixture with frequent stirring (69). The soaked pieces were transferred into "micron" molds containing the same medium. The molds were placed in a 60 C oven for 24 hours for plastic polymerization. This schedule of tissue preparation was followed throughout the study. Manual trimming of the blocks was carried out by the use of a device (Fig. 37), designed during the study. It consists of a round disc 9.375 mm thick cut from acrylic sheets of plexiglass or a "methyl methacrylate". A hole was drilled at its center to hold an embedded specimen block in place. The disc was mounted on a small wooden table in which a hole was cut to fit the plexiglass disc. The entire device was made to fit the stage of a binocular microscope made by "Swift Instruments International S. A. Stereo Eighty". The light source, from above and below the stage passes through the plexiglass piece, and through the epoxy block. An additional top light source can be used if necessary on either side of the block.

Thin sections were cut with either glass or diamond knives in a

Porter-Blum MT-2 ultramicrotome. The sections were mounted on bare 300 mesh ultra-high transmission "Thin Bar" copper grids (Ladd Research Industries, Inc.). The mounted sections were stained in 2% uranyl acetate for 2 hours, rinsed in glass distilled water, and drained before they were stained in lead citrate for one minute (69). The stained sections were viewed with a Hitachi HU-12 transmission electron microscope operated at 75 KV. The images were recorded on Du Pont Cronar film or Kodak high contrast film 4489, and developed in Kodak Developer (D-19). In the transmission experiments of WSMV with urediospores, ten-day old wheat seedlings were inoculated as above, first with the virus, and after the symptoms appeared, they were inoculated with urediospores of the leaf rust fungus. Urediospores were then collected from the virus diseased seedlings and applied to another set of disease-free seedlings. Materials for electron microscopy were prepared as mentioned before.

RESULTS

Host-Virus-Fungus Interaction. Nearly 1,000 electron-micrographs of P. recondita and wheat streak mosaic virus infected wheat tissues were examined, including micrographs of intercellular hyphae, urediospores and cytoplasm containing haustoria, combinations of haustoria and virus particles alone or haustoria, virus particles and inclusion bodies together within the same cell. The frequency of electron micrographs which contain haustoria and virus particles in the host cytoplasm was high. However only seven micrographs containing haustoria, virus particles and inclusion bodies were observed. Inclusion bodies of wheat streak mosaic virus such as pinwheels, laminated aggregates, and scrolls were observed in wheat leaf mesophyll cells infected with the virus (Figs. 1-A and 1-B), and virus particles were not detected in those sections. Host cell nuclei and chloroplasts were not affected by the virus. The double membrane around the chloroplasts as well as the thylakoid membranes retained their normal structure. The inclusion bodies in both sections were distributed in the cytoplasm between chloroplasts and nuclei. The occurrence of WSMV was not limited to the mesophyll cells of wheat, but its presence was detected in epidermal cells (Fig. 16) and in the guard cells.

Some nuclei were pycnotic in wheat mesophyll cells doubly infected where fungal haustoria, and the virus particles or haustoria and inclusion bodies were present (Figs. 13 & 14).

Examination of sections from wheat leaves infected with both wheat streak mosaic virus and leaf rust showed that tremendous amounts of virus particles were present in close proximity to the haustorial

wall in the mesophyll cell (Figs. 13-A and 14). The virus occurrence was evident throughout the cytoplasm but the frequency of pinwheels, scrolls or other inclusion bodies was relatively low in those sections that exhibited haustoria and large amounts of virus particles.

Fungal Virus-Like Particles. The existence of virus-like particles in haustoria invading the mesophyll cells was observed in several sections (Figs. 2-A, 2-B, 3-B, 4-B, 13-A and 14). The particles were of different sizes and shapes and were present mostly in the fungal cytoplasm. Short rod-type particles similar to the ones present in the haustoria (Figs. 7-A and 14) were observed in an intercellular hyphae (Fig. 7-B). The fungal vacuole (Fig. 4-B) apparently contains short-rods and spherical particles enclosed in a membrane. The arrangement of the particles viewed in Fig. 7-B where the short rods were intercrossing each other and forming a net-type was not seen in others. Fig. 7-A, shows particles of shorter rods than Fig. 7-B, but they are more or less parallel to each other and perpendicular to a membrane. Particles in different planes of cross and longitudinal sections were apparent in serial sections of the haustorium (Figs. 13-A and 14). The particles present in the cytoplasm near the nuclear envelope are indistinguishable from the virus particles viewed outside the haustorium in the host cytoplasm. At the same location (Fig. 14-A) the particles viewed in longitudinal sections, stained darker than the endoplasmic reticulum and are localized to that part of the fungal cytoplasm. The haustorial lobe (Fig. 3) contains long rod-shaped particles in its cytoplasm. Those particles closely adhere to each other, and each particle appears to consist of two finer particles,

longitudinally connected. A small group of particles were found in a haustorium (Fig. 12), which were distinct in their appearance from other organelles and were more darkly stained than the ribosomes, and arranged in a small chevron-like structure not common for endoplasmic reticulum. Virus-like particles were observed only in haustoria invading the host mesophyll cells.

Ultrastructure of Haustoria. The haustoria of P. recondita varied in shape considerably, but the most common appeared to be flattened cylinders (Figs. 8, 12, 16, 22-B) or spheres (Figs. 2-A, 4-A, 7-A, 9, 10, 11, 13, 23-A). The haustorium is delimited by a single-zone wall separated from the protoplasm by a well defined plasma membrane which appears to undulate in certain areas, and intensifies to form the invaginated fungal plasmalemma (IFP) that will be discussed under a separate section. The haustorial wall had a denser-electron appearance and stained darker than the haustorial contents (Figs. 13-A, 14, 15, 16, 18-B). The haustoria are shown to penetrate several types of host cells such as subsidiary (Fig. 25), epidermal (Figs. 16, 24), and most of them were found in the mesophyll (Figs. 2-A, 4-A, 5-A, 6-A, 8, 9, 10, 11, 12, 13, 15, 17, 18, 22, and 23). No difference between the fine structure of haustoria in the epidermal cells and haustoria in the mesophyll cells was observed. Haustoria contained mitochondria, microbodies, an abundance of ribosomes, lipid bodies vacuoles that may contain several different vesicles, and a nucleus surrounded by a double membrane. Nucleoli were not found in sections of haustoria examined.

The haustoria are surrounded and separated from the host cell

contents by the extrahaustorial matrix which is bounded by the host plasmalemma (extrahaustorial sheath) (Fig. 16). Variable amounts of electron dense deposits were observed in the matrix region, sometimes continuous with the haustorial wall (Figs. 10, 12, 13-A, 15, 16). A remarkable increase in the size of the matrix region and the dissolution of the contents occurred (Fig. 10), the density of the fungal wall appears to be less in this side than others accompanied by disorganization of the fungal plasma membrane inside the haustorium. An apparent expansion of the matrix caused a stretch in the extrahaustorial sheath. The host cytoplasm around the haustoria (Figs. 5-A, 8, 9, 10) shows different types of endoplasmic reticulum arrangements including formation of tubular vesicles and endoplasmic reticulum complexes. The tubular vesicles bounded by the plasmalemma of the host (Fig. 6-A) and the haustorial wall are apparently connected at one site. The membranous structure formed in the haustorium appeared to be connected, through an opening in the wall of the haustorium, to some of the ends of the tubular vesicles on the outside (Fig 6-B). This type of opening was not seen in any other haustoria examined. An unusually dense matrix in the extrahaustorial matrix at the distal end of the haustorium from the host nucleus is shown in Fig. 5-A. Upon enlargement (Fig. 5-B) the matrix shows a few shorter tubes and a large number of granular structures. The matrix is continuous with the haustorial wall.

The complete penetration site of P. recondita is composed of three major parts: the haustorial mother cell, the connecting channel or the haustorial neck, and the haustorium (Figs. 22 and 23). The

haustorial mother cell (HMC), is present outside the invaded host cell, is tightly appressed against it, has no specific shape, and maybe determinate (Figs. 20, 22-B) or branched (Figs. 22-C, 23-A). In all the penetration sites examined no septa between the haustorium and HMC were seen. The wall of the haustorial mother cell thickens on both sides of the penetration pore (Figs. 18, 20, 22, 23-A, 23-B). Organelles such as mitochondria, glycogen particles, and large vacuoles are most commonly observed in the HMC, and no nuclei or nucleoli were found. Serial sections of the penetration of a host cell wall are shown in Fig. 20. The sections are arranged to illustrate the possible events involved during penetration. There was no abrupt eruption of the host cell wall or the fungal wall at the penetration pore where the haustorial neck passed through (Figs. 20-A, 20-B, 20-C, 22-B, 22-C, 23-A, 23-B) while there was a sudden erruption in the thickened area of the haustorial mother cell wall in Fig. 24-A. The haustorial neck was generally similar in all penetration sites. It was continuous with the inner layers of the haustorial mother cell, but its wall becomes thinner at the penetration pore (Figs. 20-A, 22-C, 23-B). The wall of the haustorial neck appears to thicken and differentiate into an electron dense band at about the last one-third of its length toward the haustorium. This electron dense band is present in most of the haustorial necks (Figs. 22-C, 23-A, 23-B), and may appear only on one side (Fig. 17). A collar which consists of an accumulation of deposited material in the host cell around the penetration site and bounded by the host plasma membrane is most frequently seen. Several collar shapes are shown (Figs. 23-A, 23-B). Less developed collars

appear in Figs. 22-B and 22-C. Host cell organelles such as chloroplasts and mitochondria aggregate around the penetration sites (Figs. 17, 20A-F, 22-B, 22-C, 23-A, 23-B).

Mitochondria and plasmalemma bounded vesicles occurred in an epidermal host cell (Fig. 24-B). The fungal cytoplasm in the haustoria appears to be continuous with that of the haustorial mother cell through the haustorial neck, and the passage of fungal organelles and membrane is clearly shown (Figs. 17, 20-A, 20-B, 22-B, 23-A, 23-B).

Fine Structure of Intercellular Hyphae. An elaborate system of hyphae grew in the intercellular spaces of wheat mesophyll cells during the development stages of P. recondita (Figs. 4-A, 7-B, 8, 11, 26, 27-D, 28, and 31). The intercellular hyphae were usually close to the host cell walls where a deposited material present between the host cells and fungal walls apparently kept them in close contact (Figs. 19, 29, 31).

The intercellular hyphae contain well-developed mitochondria of elongated, oval or round shapes, which may invaginate part of the cytoplasm (Figs. 29, 31, 32). In addition organelles such as endoplasmic reticulum, ribosomes, lipid drops, and vacuoles were commonly found. The plasmalemma which appears heavily extended and folded in various parts forms the invaginated fungal plasmalemma (Fig. 11, 19-A, 26, 28, 29, 30, 31, and 32). Microbodies, some with crystals (Fig. 7-B, 27-A, B, and C), were also observed. The nuclear condition of the intercellular hyphae was dikaryotic (Figs. 11 and 27-B) and nucleoli were rare in the sections examined (Fig. 30). Perforated septa with a typical pore at different developmental stages are shown

in Figs. 11, 26-C, and 27-B. The pore apparatus is clearly shown in Fig. 27-B, where diaphragm-like plugs occur in the pore area of the uredial mycelium. A differentiated region of the cytoplasm bounded by a membrane contains mitochondria, microbodies mostly with crystals, glycogen particles, and a membrane system of unknown nature (Fig. 27-B). Another type of perforated septa, but without the septal pore apparatus, and the membrane bound regions appears in Figs. 11, 26-C and 27-D. Complete (non-perforated) septa occur in the intercellular hyphae (Figs. 4-A, 7-B, 24-A, 27-A, 27-B, 28-A, 30, and 31). The septum in Fig. 27-A is similar to the septum in Fig. 27-B except the former lacks septal pore and the apparatus. Other complete septa observed had neither septal pore nor the septal pore apparatus, and the movement of materials from cell to cell is not evident.

Organelles of unknown nature in the intercellular hyphae are evident in several sections, such organelles as in Fig. 7-B where an aggregation of circular bodies with darker centers, and apparently associated with an endoplasmic-like membrane existed in the cytoplasm of an intercellular hypha. A "cap-like bulge" developed at the area of a thickened wall of an intercellular hypha (Fig. 24-A), at which a penetration of the host cell wall might have occurred. This was apparently due to an expansion of the material in the area of contact between the fungal wall and the host cell wall and the cause of the apparent massive erruption is not known. A typical dictyosome was not observed in any stage of the fungus, however, small structures near an invaginated fungal plasmalemma (Fig. 30) appeared similar to a dictyosome in a differentiated area of an intercellular hyphae.

Invaginated Fungal Plasmalemma. Invaginations of fungal plasmalemma (IFP) were present in all fungal cells of P. recondita such as haustoria, intercellular hyphae, haustorial mother cells, uredial hyphae and urediospores. In haustoria (Figs. 2-A, 4-B, 15, 16, 18-A) and in the haustorial neck (Figs. 17 and 18-B), the fungal plasmalemma extended and apparently infolded further to form different membranous configurations. The occurrence of invaginated fungal plasmalemma in the intercellular hyphae (Figs. 12, 19-A, 26-A and C, 28-A, 29, 30, 31, and 32), clearly shows the high frequency of its presence especially in the actively growing vegetative hyphae (Figs. 28, 29, 30, 31 and 32). The fungal plasma membrane invagination occurred less frequently in some haustorial mother cells (Fig. 20-D) and uredial mycelium (Figs. 27-A and D). The occurrence of IFP in the urediospores of wheat leaf rust is confirmed in Figs. 35-B and 36. The membrane invagination resulted in the formation of a complex structure located near the plasmalemma of the spore and apparently linked to it.

Although the IFP was present in all examined stages of the leaf rust, its occurrence was most common in the vegetative intercellular hyphae and haustoria. The degree of enfolding of the membrane and the amount of membrane involved in the formation of the IFP appears to be highest in the haustoria and the haustorial-neck bearing IFP (Figs. 15, 16, 17, and 18-B). The direct association of the fungal plasmalemma to the invaginated membrane is shown clearly (Figs. 2-A, 15, 17, 19, 29, 30, 31, and 32) where the IFP is connected at both ends or at least continuous at one end with the fungal plasma membrane (Figs. 16, 18-B, 28-A, and 36). There is no clear relationship between the fungal

plasma membrane and the membranous structures (Figs. 4-B, 11, 16) that appear next to but obviously not connected to the plasmalemma.

Fungal Microbodies. Microbodies were observed in all stages examined of P. recondita infected wheat. Almost all microbodies in the fungal propagules have an oval to round shape bounded by a single membrane. The population density of microbodies is variable among the different parts of the fungus. The least number of microbodies observed is two in Figs. 7-A, 10, 12, 27-C, and 36, and as many as nine in Figs. 7-B, 8, 9, and 27-A.

The distribution of the microbodies was not restricted to certain propagules such as the haustoria or the intercellular hyphae. Crystal containing microbodies were more abundant in the haustoria. No microbodies of any type were detected in the haustorial mother cell.

Microbodies were found in close proximity to the fungal mitochondria, frequently inseparable from the endoplasmic reticulum (ER) (Figs. 7-A, 7-B, 8 and 27), and only with ER (Figs. 9 and 10). Visual observation on the size of the microbodies indicates that the leaf rust mitochondria are always larger than the microbodies. On the contrary, host microbodies are generally larger than host mitochondria, and are generally associated with each other (Figs. 8, 12, 16 and 26-C). Microbodies were not present in all intercellular hyphae or haustoria examined. None of the sections of the vegetative hyphae (Figs. 28, 29, 30, 31, 32), contain microbodies, while the uredial mycelium (Fig. 27-A, B and C), and the older intercellular hyphae (Figs. 7-B) contained several microbodies.

Ultrastructure of Urediospores. Urediospore development based

on the morphological difference between the spines at different stages, and their positions from the spore surface are shown (Figs. 33. 34, and 35). Typically, mature urediospores have a high concentration of mitochondria, a pair of nuclei, an increased accumulation of lipid content, ribosomes, and an increase in the cytoplasm density. Fig. 33 demonstrates the successive development of urediospores marked by spine location from the spore wall as well as other structural differences as the spores mature. In Figs. 33-A, 33-B, spines are still below the surface, but an apparent spore wall thickening is evident.

Endoplasmic reticulum and a flap of endoplasmic reticulum-like membrane occur at the base of the spines in maturing urediospores (Figs. 33-B, and 34). The spines start to emerge out of the cavity but are not fully developed (Fig. 33-C). Spore wall thickenings accompany the development of a wall barrier at the base of the spine (Fig. 34-B), separating it from the fungal plasmalemma. A marked increase in the wall thickness of the urediospore (Fig. 33-D), and fully emerged spines from the surface coupled with lipid accumulation may indicate an advanced maturity stage.

The nuclei of the urediospores were round (Fig. 35-B), or oval (Fig. 35-A), and occupied more or less the center of the spores. The nuclear envelope was double, and invaginated at various locations (Fig. 36). The nuclear pores were not evident in some planes of sectioning. A nucleolus was evident at the periphery of the same nuclei (Fig. 35-A). Cytoplasm was more dense, and ribosomes more numerous in some urediospores (Figs. 35-B, and 36). Some urediospores had a high lipid content (Fig. 35-A). A membrane system is located in the periphery of

the spore next to the fungal plasmalemma and is apparently an invagination of the plasma membrane (Figs. 35-B, and 36). Another type of membrane aggregates near the base of the spine (Fig. 34-B) but its link to the plasmalemma is not as envident as in Fig. 35-B.

Microbodies were observed in the cytoplasm of the urediospore (Fig. 36), near the nuclei. Crystals or any other type of inclusions were not detected in urediospore microbodies examined.

DISCUSSION AND CONCLUSIONS

Host Responses. Several host-parasite interaction characteristics observed in this study agree with other results reported by Ehrlich and Ehrlich (22), Shaw and Manocha (82), Manocha and Shaw (59), Van Dyke and Hooker (87), and Skipp et al., (83). The host endoplasmic reticulum was frequently observed to form tubular vesicles around the haustorium (Fig. 6-A), those vesicles are similar to P. coronata avenae described by Harder (39), and appear to be originated from the extrahaustorial sheath, but clearly they are connected with the haustorial wall in more than one site. A remarkable aggregation of endoplasmic reticulum complex (ERC) (Figs. 8, 10), consists of a lattice-arrangement in cross section made up of large tubules, and small tubules which contain darkly stained material at their centers. The ERC arrangement is similar to wheat - P. graminis tritici reported by Harder et al. (40), but only comparable with P. coronata - oat, which lacked the lattice arrangement, but had tubular complexes (15). Based on the above mentioned arrangement, Chong and Harder (15) predicted that those tubular complexes are pathogen specific. This would be true if P. recondita - wheat interaction reported here resulted in a response other than the lattice arrangement, therefore, it appears that the tubular complex is specific to the host and not to the pathogen. Another type of host response to the presence of haustorial lobes (Fig. 5-A) is marked by an increase in the presence of endoplasmic reticulum seen at different areas in the host cytoplasm around the haustorium. Chong et al., (14) reported similar observations for P. coronata. However, a clump of material that appears to be in the extra haustorial

matrix, but in direct contact with the haustorial wall, is shown at the other end of the haustorium. An enlargement of the clump next to the haustorium reveals that it consists of granular and tubular texture, and is continuous with the haustorial wall. Coffey and Wilson (18) showed a similar penetration matrix with granular texture, different from either the fungal or host cells and bounded by the host plasmalemma, and probably constituted the extra haustorial matrix in Phytophthora infestans infecting potato cultivars.

Ultrastructure of Wheat Leaf Rust Haustoria. The ultrastructure of P. recondita is generally comparable and follows closely to other rust fungi described by Ehrlich and Ehrlich (22), Shaw and Manocha (82), Van Dyke and Hooker (87), Zimmer (93), Hardwick et al. (41), Coffey et al., (16, 17), Littlefield and Bracker (55), Abu-Zinada et al., (1), and Heath and Heath (42). However, there are few differences which may be attributed to the host-pathogen systems, the methodology and techniques utilized and their effects on the fungus, or both factors combined.

The haustorium of wheat leaf rust is basically a branch of a hypha that penetrates the wall and develops in the host cell lumen and is separated by the host plasmalemma from the cell protoplasm. The shape and size of the haustorial body varied from one infection site to another, and no typical appearance of the haustoria can be associated with any host cell type. Haustoria contain organelles such as mitochondria which may be scattered around, (Figs. 2-A, 4-A, 6-A, 8, 10, 11), arranged around the plasma membrane (Figs. 12, 13, 16) or packed together in one side of the haustorium (Figs. 5-A, 15). The

mitochondrial membrane is double (Fig. 16), and parallel plate-like cristae are formed on its inner layer, and appeared similar to those described for P. graminis tritici by Williams and Ledingham, (90), Shaw and Manocha (82) and P. sorghi by Van Dyke and Hooker (87), and P. carthami by Zimmer (93). Several mitochondria appeared excessively stretched and possibly dividing (Figs. 8,15). The haustoria contain other organelles, such as ribosomes, endoplasmic reticulum, vacuoles, microbodies, and lipid bodies. No haustorial dictyosomes were observed in any of the sections, this is generally the case in uredinales (7) and agrees with observations in many other fungi by Wilsenach and Kessel (91) Littlefield and Bracker (55), and Coffey et al., (16, 17). The haustoria are connected to the intercellular hyphae or a haustorial mother cell by the haustorial neck that usually bears a distinctive band of a darkly-stained fungal wall about two-thirds its length toward the haustorium (Figs. 17, 22-C, 23-A, 23-B). The neck band was first described by Rice (79) and its occurrence in many other rusts was shown by Hardwick et al., (41), Coffey et al., (16, 17), Littlefield and Bracker (55), Rijo and Sargent (80), Abu-Zinada et al., (1), Heath (43), Harder (39) Littlefield and Heath (56), Chong and Harder (13) Al-Khesragi and Losel (2), Gray et al., (34) and Takatoshi et al., (84). The neckband was shown to be of a fungal origin by Hardwick et al., (41), and Heath (43) showed that it possess certain ultrastructural similarities to the casparian strip of the endodermal cells. Septa between haustoria and haustorial mother cell as reported by Heath and Heath (42) for U. phaesoli were never seen for P. recondita. The movement of organelles through the haustorial neck is obvious (Figs.

17, 23-B, 22-C), and the cytoplasm appears to be continuous through the neck (Figs. 20-B, 23-A, 23-B). The plasma membrane of the neck was occasionally invaginated (Figs. 17, 18) but other membranous structures (Figs. 18-B, 23-A, 23-B) are seen in the neck which are similar to structures observed by Coffey et al., (16), and Abu-Zinada et al., (1). The haustorial neck was constricted at the penetration pore of the host cell wall, and its wall appeared thinner at that site than the other areas below and above it (Figs. 22-C, 23-B). Several types of well-developed collars (Figs. 21, 22-C, 23-A, 23-B), apparently of host cell wall material, were found around the penetration sites and encircling the upper portion of the haustorial neck. A microfibrill material, apparently different from host cell wall but similar to the collar and obviously continuous with it is clearly seen (Fig. 23-A) deposited between the host plasma membrane and the host cell wall on one side of the host cell.

This type of deposit has never been observed in other rust infections. The collar however, was not present in younger penetration sites (Fig. 22-B). This is not surprising since collars are more frequent in older infections (16). The host plasma membrane lies between the inner surface of the collar and the haustorial neck (Fig. 23-B). The host plasma membrane is in direct contact with the haustorium at the neck region, and then it doubled back along the neck and around the body of the haustorium, where it constitutes the sheath membrane according to Coffey et al., (16). Littlefield and Heath (56) called it an extrahaustorial membrane. To avoid confusing the abbreviation of the extrahaustorial membrane with that of the extrahaustorial matrix, I used

extrahaustorial sheath instead of the extrahaustorial membrane. The host plasma membrane (extrahaustorial sheath) is separated from the haustorial wall by the extrahaustorial matrix (Fig. 16), which appears to be empty in some areas but may contain densely stained deposits. The extrahaustorial matrix thickness appeared to change (Figs. 13, 14, 15) as the haustoria matured (Figs. 12, 16).

An apparent break in the haustorial wall (Fig. 6) formed a channel which seemed to connect haustorial material to the tubular vesicles bounded by the extrahaustorial sheath. No other similar openings were found on the walls of the haustoria examined, therefore it is difficult to assume that it is similar to the channel-like areas reported for P. graminis, by Ehlrich and Ehlrich (22).

Ultrastructure of the Intercellular Hyphae. The intercellular hyphae grow between the host cells and may form haustorial mother cells that penetrate adjacent host cell walls. The cellular contents of intercellular hyphae are similar to the haustoria with few basic differences. The nuclear condition of these hyphae is dikaryotic (Figs. 11, 27-B, 29), but no nuclei were observed in any of the haustorial mother cells examined. The mitochondria of the intercellular hyphae assume many shapes, which range from irregularly-elongated to spherical. Several mitochondria are shown (Fig. 29, 31, 32) with their centers filled with invaginated cytoplasm that appears less dense than the haustorial cytoplasm. Van Dyke and Hooker (87), observed swollen distorted mitochondria in haustoria of incompatible interaction but did not comment on the presence of invaginated mitochondria in their Fig. 9. The occurrence of "pockets" in thin sections of cucumber

glyoxysomes (microbodies) has been reported by Trelease et al., (1971). They showed that the invaginations occurred at a particular time after germination during the peak of glyoxylate cycle activity. Trelease and his co-workers suggested that such occurrence of a morphological feature in a specific type of organelle must have a structural-functional relationship. Mitochondrial invaginations apparently occurred in actively growing vegetative hyphae, which contain dense cytoplasm full of ribosomes. These invaginations might have a role in the growth and reproduction of mitochondria, or in the formations of other organelles.

The occurrence of septa of different stages of development were shown (Figs. 4-A, 7-B, 11, 26-C, 27-B, 27-C, 27-D, 28-A, 30, and 31). These septa are similar to other rust fungi described by Ehrlich et al., (23), Coffey et al., (16, 17), Littlefield and Bracker (54), Littlefield and Heath (56), however a few differences did exist. I observed mitochondria and glycogen bodies (Figs. 27-A, 27-B), within the pore matrix that Ehrlich et al.,(23) did not observe for P. graminis and P. recondita. Coffey et al., (16) showed several septa sections, but none ap-peared to have mitochondria in the pore region. They did however, show the existence of microtubules in the pore region that I did not find. The occurrence of filaments in the intercellular hyphae, surrounded by ribosomes and parallel to the invaginated fungal plasmalemma are shown (Fig. 19). These filaments appear to be arranged in pairs. Heath and Heath (44) showed the existence of such filaments associated with some cytoplasmic microtubules in U. phaseoli var. vignae. Structures not commonly known in other fungi exist in Fig.

7-B, where small tubule-like bodies with darker centers are clumped together, and linked to the endoplasmic reticulum. These structures apparently are similar to that described by Harder (39) for P. coronata avenae, where tubular vesicles (a component of the endoplasmic reticulum complex) were found in the extra haustorial matrix in host cytoplasm around the haustoria. Another unusual but unique structure (Fig. 24-A) was observed at a penetration site of an epidermal cell of wheat leaf. The area of contact between the host cell wall and the haustorial mother cell appears to have been expanded, exerting pressure on the fungal wall at the thickened area causing it to rupture and form a "cap-like bulge". The cell wall shows no obvious structural change. The reasons for the expansion at the area of contact are not known.

There seems to be an agreement (56) that enzymatic action is involved during the penetration of host cell wall. However, a physical force has been reported by Rijo and Sargent (80) to be involved in causing the outward bulging of the coffee cell wall infected with Hemileia vastatrix. My results showed that the bulging occurred in the fungal wall. Therefore the involvement of both chemical and physical actions cannot be ruled out.

Virus-like Particles. This is the first report on the occurrence of virus-like particles (VLPs) in wheat leaf rust. The existence of virus and VLPs in fungi has long been established. Lemke (52) and Ghabrial (32) reviewed the literature on viruses in Eukaryotic organisms, and the effect of those viruses on their hosts. However, several studies concerning the association of VLPs with many plant pathogenic fungi were not included in either review.

Rawlinson and Maclean (78) observed that P. graminis tritici failed to grow on axenic culture from urediospores, and those isolates which grew produced a range of different types of colonies. Rawlinson and Maclean examined their cultures for virus particles, since Bozarth et al., (6) showed that VLPs caused cultural variation in virulent strains of Helminthosporium maydis. Rawlinson and Maclean (78) showed that isometric virus-like particles were present in all colonies but were located in the cytoplasm of several different hyphae. In 1973 Yarwood and Hect-Poinar (92) found VLPs resembling tobacco mosaic virus (TMV) in five rust species and two species of powdery mildews; attempts to produce virus-like infections using spores or juice preparations of diseased tissue were not successful. McDonald and Heath (68) reported on the occurrence of three types of rod-shaped virus-like particles and spherical VLPs in the extract of urediospores, germ tubes, and pustules of U. phaseoli var. vignae. The zoospores of the fungus Polymyxa graminia has been confirmed as the vector of soil-borne wheat mosaic virus (SBWMV) by Estes and Brakke (28) and Rao and Brakke (77). The association of the virus with its fungus-vector was thought be internal. However, Lagenberg and Giunchedi (51) observed that SBWMV was in close contact with its vector in the host tissue, but virus particles were not found within the fungal propagules.

Aside from plant pathogenic fungi, there are other economically important species for which virus-like particles have been reported to exist. Dieleman-Vanzaayen et al., (21) reported on the appearance of rod-shaped virus-like particles in Peziza ostracoderma (a contaminant fungus), in mushroom nurseries. Filamentous and polyhedral virus-like

particles were extracted and purified from wild-growing but edible mushroom Boletus edulis by Huttinga et al., (48).

In leaf rust of wheat several types of particles mostly of the rod-shape type are shown to exist in haustoria and intercellular hyphae. No particles were observed in urediospores. In the cytoplasm of a haustorial lobe (Fig. 2-B), short rod particles are seen, those particles appear to have no pattern of arrangement, but they are apparently localized on an axis and not randomly distributed. The rod-shaped particles (Fig. 3-B) which are present in the haustorium cytoplasm in the wheat mesophyll cell are obviously parallel to each other. They resemble those particles shown in Bos (5), Fig. 34 for tobacco etch virus laminated aggregates in their arrangement and appearance in thin sections. The haustorium vacuole in Fig. 4-B has at least two types of particles enclosed in a membrane. A short rod-type, and spherical particles intermixed, and the whole structure is thought to be as an invaginated fungal plasmalemma, but the presence of discernable particles, and the inability to seperate the tonoplast from the fungal plasma membrane especially at the area marked with stars near haustorial wall make that unreasonable or unlikely. Tubular and vesicular elements were shown to exist in vacuoles of U. fabae haustorium by Abu-Zinada et al., (1). They provided no detailed micrograph of those elements, but from their description, the structure in (Fig. 4-B) has no similarities to their multivesicular bodies. The center of some of the spehrical particles contains darkly stained bodies, which are easily seen in the larger spheres. The rod-shaped particles have similarities with the short rigid rods described by McDonald and Heath

(68), which were extracted from cowpea rust. The cytoplasm of the haustorium (Fig. 7-A) and the intercellular hyphae (Fig. 7-B) shows rod-type particles, that differ in their arrangement, but they otherwise appear similar to the beet necrotic yellow vein virus shown by Langenberg and Giunchedi (51) in their electron micrograph (Fig. 6). The rod-type particles in Fig. 7-A apparently cross other longer particles, which are adjacent to the nuclear membrane. The short rod-type particles (Fig. 7-B) are arranged in a different manner, where the particles are intercrossed with each other forming a characteristic chevron-shaped aggregate (51). There is, however another type of arrangement in Fig. 7-B, and in Fig. 12, where the particles appear to radiate from a common center (star). The haustorium in Fig. 14 is a serial section of that in Fig. 13-A. The haustorium is present in a mesophyll cell which contains many particles of wheat streak mosaic virus (WSMV), and few inclusion bodies. Adjacent to the fungal nuclear envelope, darkly stained particles are arranged around a lighter center. Fig. 13-B shows an enlargement of those particles surrounding the centers. The particles in Fig. 14 are exactly positioned in the same location, but apparently are displayed in a longitudinal plane of section in variable length. The particles in both figures are similar to the WSMV particles in the host cytoplasm, and contrast deminishes between the particles in cross section (Fig. 13). The vacuoles appear to have disrupted membranes (Fig. 14), but contain spherical particle aggregates with darkly stained centers (between stars). Those spherical particles resemble the virus-like particles in the intercellular hyphae of cowpea rust described by McDonald and Heath (68).

The discussion of the different particles in P. recondita is based entirely on examinations of thin section of wheat leaf tissue infected with the fungus and the virus. No extraction or purification methods were employed, nor measurement of dimensions were taken or provided. It is therefore proper to refer to them as virus-like particles until the questions of their nature, and how they get inside the fungus are solved.

Several attempts have been made to determine whether urediospores of P. recondita transmit wheat streak mosaic virus. This was based on the fact that several fungi are known to vector viruses, yet other fungi were themselves hosts for viruses according to Grogan and Campbell (35). Erasmus and Wechmar (26) reported that the stem and leaf rust fungi of wheat did transmit brome mosaic virus (BMV) through urediospores, and later they showed that the BMV was carried externally on urediospores (27).

I conducted repeated experiments to test the hypothesis that urediospores of P. recondita transmit WSMV in greenhouse inoculated plants. None of the test plants showed typical symptoms, and only few of the inoculated leaves had chlorotic areas. Those leaves were embedded, and sectioned as described previously, but none of the sections were examined in the electron microscope.

Invaginated Fungal Plasmalemma. The invaginated fungal plasmalemma (IFP) occurred in all fungal-cell types examined in P. recondita. Their occurrence appears to be a result of extensions in the plasma membrane followed by enfolding of the membrane on itself, forming complex membranous structures. The term which I am proposing to use is

the "invaginated fungal plasmalemma" (IFP). The term carries a descriptive meaning rather than the other terminology previously used. The invaginated fungal plasmalemma should be applied to those obvious structures that are directly connected to or shown next to the plasma membrane where connections may be present but are not seen in the plane of sectioning.

Several terms are now used in the ultrastructure literature of fungi to describe the invaginations of the fungal plasma membrane, and in many instances, different names were applied to what appears to be the same structure, by different workers, and in other cases the same author used different terminology for the same structure. Moore and McAlear (67) reported the occurrence of sponge-like structures continuous with fungal wall and their interior limits were defined by the plasma membrane. They named such structures as lomasomes. This was the first report of the existence of those structures in fungi. Those authors thought that lomasomes were exclusive in fungi, but their claim was proven to be erroneous, since similar structures were found in higher plants and algae (3, 62).

The occurrence of invaginated fungal plasmalemma in different fungal species is well-documented and shown in many electron microscopic studies by Moore and McAlear (67), Bracker (7), Marchant and Robards (62) and Van Dyke and Hooker (87), but their function and exact origin remained uncertain. Ehrlich et al. (24), and Calonge (11) observed the formation of lomasomes at the area of contact between the HMC and the host cells, where penetration is expected, and predicted that lomasomes were the first host cell reaction to infection. However, Manocha

and Shaw (57) showed the existence of lomasomes in cells of disease-free "Khapli" wheat. The frequency of the occurrence of IFP in the rust fungi infecting various crops is as different as the terms used to describe them. Shaw and Manocha (82) and Manocha and Shaw (58) noticed that the plasma membrane in the haustoria of P. graminis tritici in wheat was often invaginated by lomasomes. Van Dyke and Hooker (87) found fungal plasma membrane extensions (lomasomes) in haustoria and intercellular hyphae of the compatible interaction of P. sorghi in maize, but no such structures were present in the incompatible interactions. Hardwick et al., (41) reported that typical lomasomes were present in mycelium, but were rare in the haustorium of U. appendiculatus in bean. In safflower infected with P. carthami, Zimmer (93) observed lomasomes in both hyphae and haustoria, but they were more abundant in the hyphae suggesting that their role as a major absorptive bodies is diminished. Al-Kheragi and Losel (2) noted an occasional presence of lomasomes in haustoria of P. poarum only. Coffey et al., (17) described a cluster of convoluted membranes, which were darkly stained in the haustorial neck of Melampsora lini. No specific term was given but they mentioned the similarity of those membranes to lomasomes. Rijo and Sargent (80) showed that coffee leaf rust haustoria and intercellular hyphae contained a tubular complex and lomasomes, and they made a distinction between them based on their association with the plasma membrane.

The association of the membranous structures formed as a result of invagination of the fungal plasma membrane to the plasmalemma was not always clear. Therefore, several systems were proposed to name

those structures. Marchant and Robards (62) suggested that all membranous or vesicular structures associated with the plasmalemma can be classified under the general term paramural body regardless of their origin. Paramural bodies were then separated into two subclasses based on their derivation: plasmalemmasomes, in which the membranes are formed completely from plasma membranes, and lomasomes, which are derived entirely from cytoplasmic vesicles. Brushaber and Jenkins (8) proposed the use of the term lomasomes for the membranous structures associated with eukaryotic cell wall and multivesicular bodies be used for structures not associated with the plasma membrane. In a three paper series Harder (36, 37, 38) described the cytoplasm of the intercellular hyphae and the sporogenous cells of P. coronata to contain multivesicular bodies or membranous complexes without specification of which was associated with the plasmalemma. On the contrary, Ramberg and McLaughlin (76) observed the presence of membrane complexes distributed randomly through the cytoplasm which were occasionally associated with the plasmalemma of Ustilago maydis. They referred to the structures near the plasmalemma of the forming septa as multivesicular bodies.

In P. recondita of wheat, the invaginated fungal plasmalemma are clearly demonstrated to occur in haustoria and haustorial necks (Figs. 2-A, 4-B, 15, 16, 17, 18,), and the intercullular hyphae (Figs. 12, 19-A, 26-A and C, 28-A, 29, 30, 31, and 32). My results agree with Van Dyke and Hooker (87), Zimmer (93), and Rijo and Sargent (80), but my observations are different from Shaw and Manocha (82), Hardwick et al. (41), Coffey et al., (16), and Al-Khesraji and Losel (2) who observed

that the invaginated fungal plasmalemma (lomasomes) occurred only in the fungal haustoria. The appearance IFP in urediospores (Figs. 35-B, and 36) confirm the observations of Ehrlich and Ehrlich (25) on Puccinia graminis tritici of wheat and disagree with Moor and McAlear (67) and Hess and Weber (45) who failed to observe lomasomes in spores.

The direct connection of the invaginated fungal plasmalemma at more than one site to the plasma membrane in both haustoria and intercellular hyphae in the figures mentioned above, illustrates that IFP membranous structures are all originated from the plasma membrane. The other membranous structures, however, observed near the plasmalemma and which contain tubules or vesicles (Figs. 11 and 16), but where the clear link to the plasma membrane is lacking may in fact be connected based on their trilaminar structure, and asymmetry arrangement of the membrane similar to that displayed in the plasmalemma at higher magnification as showing by Brushaber and Jenkins (8).

Fungal and Host Microbodies. Electron microscopic examinations of thin sections of wheat leaf cells infected with P. recondita reveal that microbodies do occur in haustoria, intercellular hyphae and urediospores. Those fungal organelles possess a single smooth membrane surrounding a matrix of moderate electron opacity, similar to the descriptions given to the other microbodies observed in glutaraldehyde-fixed materials by Frederick et al., (30), Maxwell et al., (64), de Duve, (20), and Huang et al., (47). Inspite of the appearance of microbodies in both haustoria (Figs. 7-A, 8, 9, 10, 12, and 16) and intercellular hyphae (Figs. 7-B, and 27-A and 27-C), they were more numerous in haustoria in the sections examined. The number of microbodies per

haustorium was variable and in some instances (Figs. 7-A, 8, and 9) exceeded the mitochondria count. The common occurrence of microbodies observed here does not agree with Maxwell et al., (65), who generalized that microbodies are scarce in haustoria and intercellular hyphae of biotrophic plant pathogens (obligate parasites including rusts). My findings, however, are in agreement with several other rust studies reported by Coffey et al., (16, 17), Littlefield and Bracker (55), Heath and Heath (42), and Al-Khesragi and Losel (2). Microbodies of the leaf rust of wheat are of two types: crystalline and non-crystalline. The first type is found in few haustoria (Figs. 8, 9) and in the membrane-bound cytoplasm region around the pore apparatus of the intercellular hyphae (Figs. 27-A and 27-C). The crystals are located in the center of the microbodies. The non-crystalline microbodies existed in all haustoria observed (including Figs. 8 and 9) and in the intercellular hyphae (Fig. 7-B). The association of microbodies with endoplasmic reticulum and mitochondria in haustoria and intercellular hyphae is illustrated clearly (Figs. 7, 8, 9, 10, 12, 27-A, and 27-C). In addition, lipid-like bodies are present near the microbodies (Figs. 7-A, 9, 10). The size of the microbodies in all the sections examined for P. recondita, based on a visual estimations only, was smaller than the mitochondria. On the contrary, wheat leaf microbodies were larger than the mitochondria in all cells. Frederick and Newcomb (29) observed that all four festucoid species including wheat contained microbodies, which had fibrils with a definite structure. However, the presence of crystals was never detected in wheat microbodies of this study.

Fine Structure of Urediospores. The ultrastructure of

urediospores of P. recondita resembles that of P. graminis tritici described by Williams and Ledingham (90), Thomas and Isaac (85), Ehrlich and Ehrlich (25), and except for a few details, is similar to urediospores of Melampsora lini described by Manocha and Shaw (60) and P. coronata reported by Harder (38).

Different stages of maturity in urediospores of P. recondita are shown in Fig. 33. The urediospore wall appears to thicken, with an increase in lipid droplets and cytoplasm density are some of the maturity signs that are evident in Figs. 33-A, 33-B, and 33-C. A noticeable increase in spore wall thickness accompanied with visible spines (Fig. 33-D) represent an advanced stage of mature urediospores. These maturity features are similar to urediospores of P. coronata described by Harder (38), and Littlefield and Bracker (53) for M. lini. Spine development in P. recondita appears to start inside the spore between the plasmalemma and the inner surface of the wall (Fig. 34-A), where the endoplasmic reticulum appears to form a layer of membranes adjacent to and parallel to the spine base. The double flap of endoplasmic reticulum was first described by Ehrlich and Ehrlich (25) in P. graminis. Later, Littlefield and Bracker (53) showed the existence of small cisternae of the endoplasmic reticulum associated with the plasma membrane before spine initials were formed in M. lini. The spine appeared to be separated from the spore plasma membrane by deposition of wall material at the base of the spine, which pushed it outward (Fig. 34-B), and was accompanied by an increase in the amount of endoplasmic reticulum near the base adjacent to the plasma membrane. Spine development is an important feature in spore maturation, and as

the spore matures its wall becomes thick and spines increase in size. Thomas and Isaac (85) found that spines developed to mature size below the urediospore wall, and during spore maturation and expansion the spines pass through the wall. The mitochondria of maturing spores elongate, twist around each other, and aggregate in the periphery of the cytoplasm (Figs. 35-B and 36). Mitochondria were not seen to encircle lipid bodies or glycogen granules, but they assume dumbbell shapes as reported by Ehrlich and Ehrlich (25) for P. graminis. A recent study by Salako (81) for urediospores of P. recondita, described several features such as the foamy appearance of cytoplasm and folded membranes distributed around the periphery of germinating urediospores. These were not seen in any of the spores that I examined, possibly due to maturity difference. Invaginated fungal plasmalemmas in the urediospore were not frequently found as Ehrlich and Ehrlich (25) reported for P. graminis, but their existence in P. recondita is illustrated in Fig. 35-B. Nucleoli were frequently found (Figs. 35-A, 35-B) in developing urediospores of P. recondita, which resembles the finding of Manocha and Shaw (60) in M. lini. Nucleoli were not observed in urediospores of P. graminis tritici by Williams and Ledingham, (90), and Manocha and Wisdom, (61), and mature urediospores of M. lini by Manocha and Shaw, (60).

LITERATURE CITED

1. Abu-zinada, A. H., Cobb, A., and Boulter, D. 1975. An electron-microscopic study of the effects of parasite interaction between Vicia faba L. and Uromyces fabae. Physiol. Plant Pathol. 5: 113-118.

2. Al-Khesragi, T. O., and Losel, D. M. 1981. The fine structure of haustoria, intracellular hyphae and intercellular hyphae of Puccinia poarum. Physiol. Plant Pathol. 19: 301-311.

3. Barton, R. 1965. Electron microscopic studies on surface activity in cells of Chara vulgaris. Planta 66: 95-105.

4. Beeves, Harvy. 1979. Microbodies in higher plants. Annu. Rev. of Plant Physiol. 30: 159-193.

5. Bos, 1983. Introduction to plant virology. Longman, London and New York. 160 pp.

6. Bozarth, R. F., Wood, H. A., and Nelson, R. R. 1972. Virus-like particles in virulent strains of Helminthosporium maydis. (Abstr.) Phytopathology 62: 748.

7. Bracker, C. E. 1967. Ultrastructure of fungi. Annu. Rev. of Phytopathol. 5: 343-374.

8. Brushaper, J. A., and Jenkins, Jr., S. F. 1971. Lomasomes and vesicles in Poria monticola. Can. J. Bot. 49: 2075-2079.

9. Burleigh, J. R., Roelfs, A. P., and Eversmeyer. 1972. Estimating damage to wheat caused by Puccinia recondita tritici. Phytopathology 62: 944-946.

10. Bushnell, W. R. 1972. Physiology of fungal haustoria. Annu. Rev. Phytopathol. 10: 151-176.

11. Calonge, F. D. 1969. Ultrastructure of the haustoria or intracellular hyphae in four different fungi. Arch. Mikrobiol. 67: 209-225.

12. Carr, R. J., and Kim, K. S. 1983. Ultrastructure of mixed plant virus infection: Bean yellow mosaic virus with cowpea severe mosaic virus or cowpea mosaic virus in bean. Virology 124: 338-348.

13. Chong, J., and Harder, D. E. 1980. Ultrastructure of haustorium development in Puccinia coronata avenae. I. Cytochemistry and electron probe X-ray analysis of the haustorial neck ring. Can. J. Bot. 58: 2496-2505.

14. Chong, J., Harder, D. E., and Rohringer, R. 1981. Ontogeny of mono-and dikaryotic rust haustoria: Cytochemical and ultrastructure studies. Phytopathology 71: 975-983.

15. Chong, J., and Harder, D. E. 1982. Ultrastructure of haustorium development in Puccinia coronata avenae: Some host responses. Phytopathology 72: 1527-1531.

16. Coffey, M. D., Palevitz, B. A., and Allen, P. J. 1972. The fine structure of two rust fungi, Puccinia helianthi, and Melampsora lini. Can. J. Bot. 50: 231-240.

17. Coffey, M. D., Palevitz, B. A., and Allen, P. J. 1972. Ultrastructural changes in rust-infected tissues of flax and sunflower. Can. J. Bot. 50: 1485-1492.

18. Coffey, M. D., and Wilson, U. E. 1983. An ultrastructural study of the late-blight fungus Phytopthora infestans and its interaction with the foliage of two potato cultivars possessing different levels of general (field) resistance. Can. J. Bot. 61: 2669-2685.

19. Cole, G. T., and Aldrich, H. C. 1970. Ultrastructure of conidiogenesis in Scopulariopsis brevicaulis. Can. J. Bot. 49: 745-755.

20. de Duve, C. 1983. Microbodies in living cells. Scientific American. 248 (May): 74-84.

21. Dieleman-Vanzaayen, A. I., and Finch, J. T. 1970. Intracellular appearance and some morphological features of virus-like particles in an ascomycete fungus. Virology 42: 534-537.

22. Ehrlich, H. G., and Ehrlich, A. M. 1963. Electron microscopy of the host-parasite relationships in stem rust of wheat. Amer. J. Bot. 50: 123-130.

23. Ehrlich, M. A., Ehrlich, H. G., and Schaffer, J. F. 1968. Septal pores in the Heterobasidiomycetidae, P. graminis and P. recondita. Amer. J. Bot. 55: 1020-1027.

24. Ehrlich, M. A., Schaffer, J. F. and Ehrlich, H. G. 1968. Lomasomes in wheat leaves infected by Puccinia graminis and P. recondita. Can. J. Bot. 46: 17-20.

25. Ehrlich, M. A., and Ehrlich, H. G. 1969. Urediospore development in P. graminis. Can. J. Bot. 47: 2061-2064.

26. Erasmus, D. S., and Von Wechmar, M. B. 1983. The association of brome mosaic virus and wheat rusts: I. Transmission of BMV by uredospores of wheat stem and leaf rust. Phytopathol. Z. 108: 26-33.

27. Erasmus, D. S., Rybicki, E. P., and Von Wechmar, M. B. 1983. The association of brome mosaic virus and wheat rusts. II. Detection of BMV in/or uredospores of wheat stem rust. Phytopathol. Z. 108: 34-40.

28. Este, A. P., and Brakke, M. K. 1969. Correlation of Polymyxa graminis with transmission of soil-borne wheat mosaic virus. Virology 28: 772-774.

29. Frederick, S. E., and Newcomb, E. H. 1971. Ultrastructure and distribution of microbodies in leaves of grasses with and without CO_2 photorespiration. Planta 96: 152-174.

30. Frederick, S. E., Gruber, P. J., and Newcomb, E. H. 1975. Plant-microbodies. Protoplasma 84: 1-29.

31. Gerhardt, B. 1978. Microbodies/Peroxisomen pflazlicher zeller. "Cell biology monographs" Vol. 5, 283 pp. Wein: Springer.

32. Ghabrial, S. A. 1980. Effects of fungal viruses on their hosts. Annu. Rev. Phytopathol. 18: 441-461.

33. Gold, R. E., Littlefield, L. J., and Statler, G. D. 1978. Ultra-structure of pycnial and aecial stages of Puccinia recondita. Can. J. Bot. 57: 74-86.

34. Gray, D. J., Amerson, H. V., and Van Dyke, C. G. 1982. An ultra-structural comparison of monokaryotic and dikaryotic haustoria formed in the fusiform rust fungus. Cornartium quercuum f. sp. fusiforme. Can. J. Bot. 60: 2914-2922.

35. Grogan, R. G., and Campbell, R. N. 1966. Fungi as vectors and hosts of viruses. Annu. Rev. Phytopathol. 4: 29-51.

36. Harder, D. E. 1976. Mitosis and cell division in some cereal rust fungi. I. Fine structure of the interphase and promitotic nuclei. Can. J. Bot. 54: 981-994.

37. Harder, D. E. 1976. Mitosis and cell division in some cereal rust fungi. II. The processes of mitosis and cytokinesis. Can. J. Bot. 54: 995-1009.

38. Harder, D. E. 1976. Electron microscopy of urediospore formation in Puccinia coronata avenae and P. graminis avenae. Can. J. Bot. 54: 1010-1019.

39. Harder, D. E. 1978. Comparative ultrastructure of the haustoria in uredial and pycnial infections of Puccinia coronata avenae. Can. J. Bot. 56: 214-228.

40. Harder, D. E., Rohringer, R., Samborski, D. J., Kim, W. K., and Chong, J. 1978. Electron microscopy of susceptible and resistant near-isogenic (sr6/Sr6) lines of wheat infected by Puccinia graminis tritici. I. The host pathogen interface in the compatible (sr6/P6) interaction. Can. J. Bot. 56: 2955-2966.

41. Hardwick, N. V., Greenwood, A. D., and Wood, R. K. S. 1971. The fine structure of Uromyces appendiculatus in Phaselus vulgaris. Can. J. Bot. 49: 383-390.

42. Heath, M. E., and Heath, I. B. 1975. Ultrastructural changes associated with the haustorial mother cell during haustorium formation in Uromyces phaseoli var. vignae. Protoplasma 84: 297-314.

43. Heath, Michele. 1976. Ultrastructural and functional similarity of the haustorial neckband of the rust fungi and the casparian strip of vascular plants. Can. J. Bot. 54: 2484-2489.

44. Heath, M. C., and Heath, I. B. 1978. Microtubules and organelle movement in the rust fungus Uromyces phaseoli var. vignae. Cytobiologie 16: 393-411.

45. Hess, W. M., and Weber, D. J. 1973. Ultrastructure of dormant and germinated sporangiospores of Rhizopus arrhizus. Protoplasma 77: 15-33.

46. Hollings, M. 1962. Viruses associated with a die-back disease of cultivated mushroom. Nature 196: 963-965.

47. Huang, A. H. C., Trelease, R. N., and Moore, Jr. T. S. 1983. Plant Peroxisomes. American Society of Plant Physiologists. Academic Press, New York, London, San Francisco. 252 pp.

48. Huttinga, H., Wichers, H. J., and Zaayen, A. D. 1975. Filamentous and polyhedral virus-like particles in Boletus edulis. Neth. J. Plant Pathol. 81: 102-106.

49. Johnston, C. O. 1931. Effects of leaf rust infection on yield of certain varieties of wheat. J. Amer. Soc. Agron. 23: 1-12.

50. Kim, K. S., and Fulton, J. P. 1973. Plant virus-induced cell wall overgrowth and associated membrane elaboration. J. Ultrastruct. Res. 45: 328-342.

51. Langenberg, W. G., and Giunchedi, L. 1982. Ultrastructure of fungal plant virus vectors Polymyxa graminis in soil borne wheat mosaic virus-infected wheat and P. betae in beet necrotic yellow vein virus-infected sugarbeet. Phytopathology 72: 1152-1158.

52. Lemke, Paul, A. 1976. Viruses of Eukaryotic microorganisms. Annu. Rev. Microbiol. 30: 105-145.

53. Littlefield, L. J., and Bracker, C. E. 1971. Ultrastructure and development of urediospore ornamentation in Melampsora lini. Can. J. Bot. 49: 2067-2073.

54. Littlefield, L. J., and Bracker, C. E. 1971. Ultrastructure of septa in Melampsora lini. Trans. Br. Mycol. Soc. 56: 181-188.

55. Littlefield, L. J., and Bracker, C. E. 1972. Ultrastructure specialization at the host-pathogen interface in rust-infected flax. Protoplasma 74: 271-305.

56. Littlefield, L. J., and Heath, M. C. 1979. Ultrastructure of rust fungi. Academic Press, New York, San Francisco, London. 277 pp.

57. Manocha, M. S., and Shaw, M. 1964. Occurrence of lomasomes in mesophyll cells of 'Khapli' wheat. Nature 203 (4952): 1402- 1403.

58. Manocha, M. S. 1966. Fine structure of rust haustoria in susceptible and resistant wheat. Indian Phytopathol. 19: 159-161.

59. Manocha, M. S., and Shaw, M. 1966. The physiology of host-parasite relations. XVI. Fine structure of the nucleus in the rust-infected mesophyll cells of wheat. Can. J. Bot. 44: 669-673.

60. Manocha, M. S., and Shaw, M. 1967. Electron microscopy of urediospores of Melampsora lini of rust infected flax. Can. J. Bot. 45: 1575-1582.

61. Manocha, M. S., and Wisdom, C. J. 1971. Ultrastructural studies on the uredial stage of wheat stem rust. Phytopathol. Z. 70: 263-273.

62. Marchant, R., and Robards, A. W. 1968. Membrane systems associated with the plasma lemma of plant cells. Ann. Bot. 32: 457-471.

63. Maxwell, D. P., Williams, P. H., and Maxwell, M. D. 1970. Microbodies and lipid bodies in hyphal tips of Sclerotinia sclerotiorum. Can. J. Bot. 48: 1689-1691.

64. Maxwell, D. P., Maxwell, M. D., Hanssler, G., Armentrout, V. N., Murray, G. M., and Hoch, H. C. 1975. Microbodies and glyoxylate cycle enzyme activities in filamentous fungi. Planta 124: 109-123.

65. Maxwell, D. P., Armentrout, V. N., and Graves, L. B. 1977. Microbodies in plant pathogenic fungi. Annu. Rev. Phytopathol 15: 119-134.

66. Mollenhauer, H. H., Moore, D. J., and Kelley, A. G. 1966. The widespread occurrence of plant cytosomes resembling animal microbodies. Protoplasma 62: 44-52.

67. Moore, T. R., and McAlear, J. H. 1961. Fine structure of mycota. 5. Lomasomes - previously uncharacterized hyphal structures. Mycologia 53: 194-200.

68. McDonald, J. G., and Heath, M. C. 1978. Rod-shaped and spherical virus-like particles in cowpea rust fungus. Can. J. Bot. 56: 963-975.

69. McMullen, C. R., Gardner, W. S., and Myers, G. A. 1977. Ultrastructure of cell-wall thickenings and paramural bodies induced by barley stripe mosaic virus. Phytopathology 67: 462-267.

70. McMullen, C. R., and Gardner, W. S. 1980. Cytoplasmic inclusions induced by wheat streak mosaic virus. J. Ultrastruct. Res. 72: 65-75.

71. Peresypkin, V. F., Loban, V. L., and Volvoshin, N. V. 1979. Ultrastructure of haustoria and intercellular hyphae of Puccinia triticinia Erikss. Mycelium. Mikobiologicheskii Zhurnal 41: 245-247.

72. Peyton, G. A., and Bowen, C. C. 1963. The host-parasite interface of Peronospora manshurica, on Glycine max. Amer. J. Bot. 50: 787-799.

73. Pring, R. J. 1980. A fine structural study of the infection of leaves of Phaseolus vulgaris by urediospores of Uromyces phaseoli. Physiol. Plant Pathol. 17: 269-276.

74. Pring, R. J. 1984. Effects of triadimefon on the ultrastructure of rust fungi infecting leaves of wheat and broad bean Vicia faba. Pesticide Biochemistry and Physiology 21: 127-137.

75. Raju, D. G., Sill, Jr., W. H., and Browder, L. E. 1969. The combined effects of two viral diseases and leaf rust on wheat. Phytopathology 59: 1488-1492.

76. Ramberg, J. E., and McLaughlin, D. J. 1980. Ultrastructure study of promycelial development and basidiospore initiation in Ustilago maydis. Can. J. Bot. 58: 1548-1561.

77. Rao, A. S., and Brakke, M. K. 1969. Relation of soil-borne wheat mosaic virus and its fungal vector, Polymyxa graminis. Phytopathology 59: 581-587.

78. Rawlinson, C. J., and Maclean, D. J. 1973. Virus-like particles in axenic cultures of Puccinia graminis tritici. Trans. Br. Mycol. Soc. 61: 590-593.

79. Rice, M. A. 1927. The haustoria of certain rusts and the relation between host and pathogen. Bull. Torrey Bot. Club. 54: 63-153.

80. Rijo, L., and Sargent, J. A. 1974. The fine structure of the coffee leaf rust, Hemileia vastatrix. Can. J. Bot. 52: 1363-1367.

81. Salako, E. A. 1981. The ultrastructure of the uredospores of Puccinia recondita. Mycopathologia 76: 3-12.

82. Shaw, M., and Manocha, M. S. 1965. The physiology of host-parasite relations. XV. Fine structure in rust infected wheat leaves. Can. J. Bot. 43: 1285-1292.

83. Skipp, R. A., Harder, D. E., and Samborski, D. J. 1974. Electron microscopy studies on infection of resistant (Sr6 gene) and susceptible near isogenic wheat lines by Puccinia graminis f. sp. tritici. Can. J. Bot. 52: 2615-2620.

84. Takatashi, O., Toshikazu, T., and Hirosuke, S. 1984. The interface between fungus and host cell in crown-rust infected oat leaves. Scanning and transmission electron microscopic observations. Ann. Phytopathol. Soc. Japan 50: 10-18.

85. Thomas, P. L., and Isaac, P. K. 1967. The development of echinulation in uredospores of wheat stem rust. Can. J. Bot. 45: 287-289.

86. Trelease, R. N., Becker, W. M., Gruber, P. J., and Newcomb, E. H. 1971. Microbodies (glyoxysomes and peroxisomes) in cucumber cotyledons. Correlative biochemical and ultrastructural study in light and dark-grown seedlings. Plant Physiol. 48: 461-475.

87. Van Dyke, C. G., and Hooker, A. L. 1969. Ultrastructure of host and parasite interactions of Zea mays with Puccinia sorghi. Phytopathology 59: 1934-1946.

88. Wechmar, M. B. von. 1980. Transmission of brome mosaic virus by Puccinia graminis tritici. Phytopathol. Z. 99: 289-293.

89. Wiese, M. V. 1977. Compendium of wheat diseases - American Phyto-Pathological Society, St. Paul, MN. 106 pp.

90. Williams, P. G., and Ledingham, G. A. 1964. Fine structure of wheat stem rust urediospores. Can. J. Bot. 42: 1503-1508.

91. Wilsenach, R., and Kessel, M. 1965. The role of lomasomes in wall formation in Penicillium vermiculatum. J. Gen. Microbiol. 40: 401-404.

92. Yarwood, C. E., and Hect-Poinar, E. 1973. Viruses from rusts and mildews. Phytopathology 63: 1111-1115.

93. Zimmer, D. E. 1970. Fine structure of Puccinia carthami and the ultrastructural nature of exclusionary seedling-rust resistance of safflower. Phytopathology 60: 1157-1163.

ABBREVIATIONS USED IN FIGURES

B	Band
C	Collar
Ch	Chloroplast
Cp	Plastid
Cu	Cuticle
D	Dictyosome
ER	Endoplasmic Reticulum
ERC	Endoplasmic Reticulum Complex
EHM	Extrahaustorial Membrane
EHS	Extrahaustorial Sheath
FC	Fungal Cytoplasm
FD	Fungal Dictyosome
FL	Fungal Lipid Droplet
FMB	Fungal Microbody
FM	Fungal Mitochondrion
FN	Fungal Nucleus
FNE	Fungal Nuclear Envelope
FLP	Fungal Plasmalemma
FV	Fungal Vacuole
FW	Fungal Wall
G	Glycogen
GC	Guard Cell
H	Haustorium
HMC	Haustorial Mother Cell
HNK	Haustorial Neck
HC	Host Cytoplasm
HL	Host Lipid Droplet
HMB	Host Microbody
HM	Host Mitochondrion
HN	Host Nucleus
HPL	Host Plasma Lemma
HV	Host Vacuole
IB	Inclusion Body (Virus)
ICH	Intercellular Hyphae
IS	Intercellular Space
IFP	Invaginated Fungal Plasmalemma
Nu	Nucleolus
O	Osmiophillic Body
PD	Pedicel
PW	Pinwheel Inclusion
R	Ribosomes
SC	Subsidiary Cell
Sep	Septum
Sp	Spine
TM	Thylakoid Membrane
U	Urediospore
Vi	Virus Particles
W	Wall of Host Cell

Figure 1. Cross sections of wheat mesophyll cells mechanically inoculated with WSMV.

A) Showing pinwheels, laminated aggregates (arrow heads), and scroll (arrow) in host cytoplasm between the chloroplast and the nucleus.

B) Similar to A except the absence of pinwheels and more laminated aggregates (arrowheads) distributed throughout the cytoplasm.

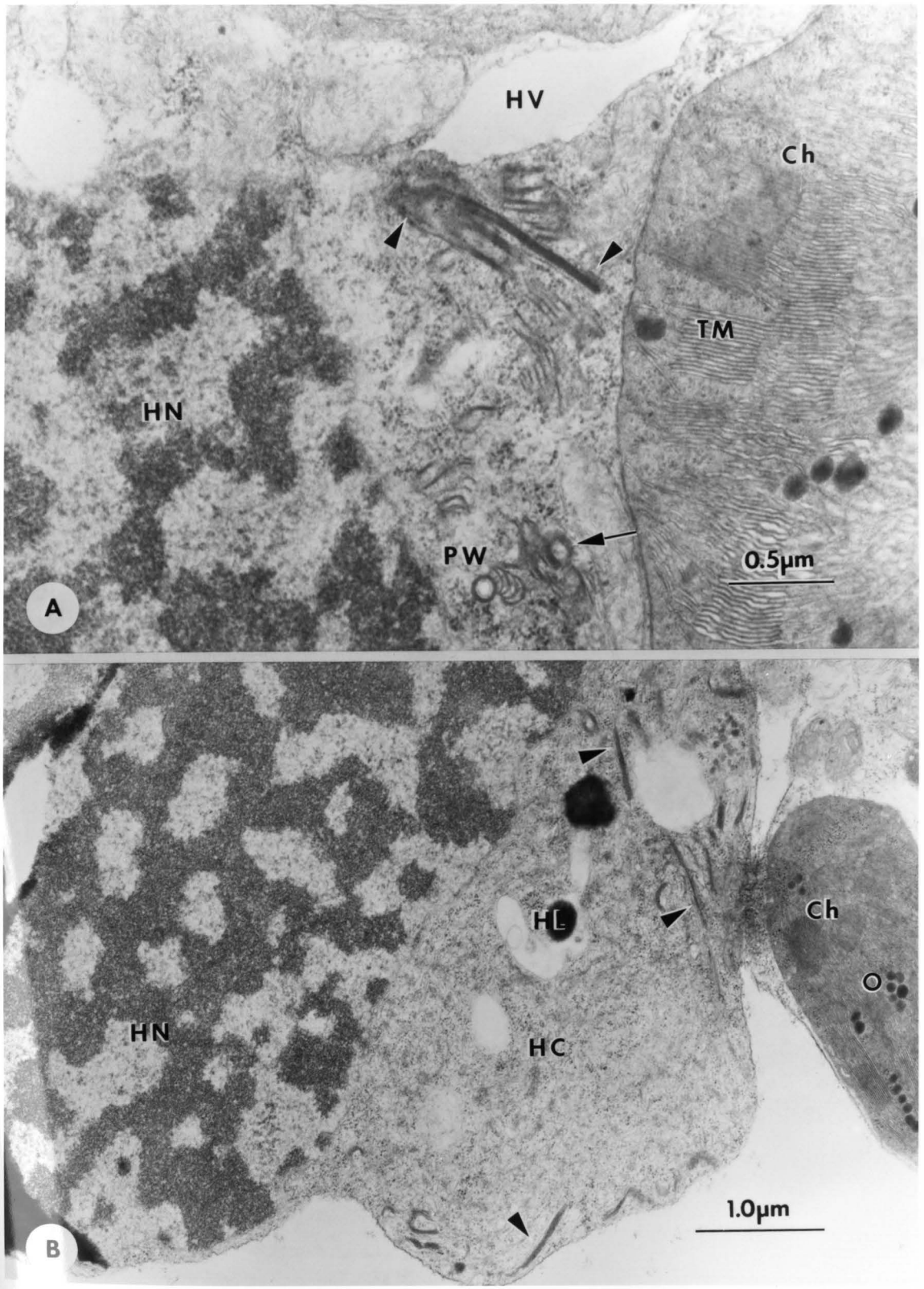
HV
Ch
TM
HN
PW
0.5μm
A
HL
Ch
O
HN
HC
1.0μm
B

Figure 2. A) This portion of a mesophyll cell contains transverse profiles of haustorial lobes, a longitudinal section of an intercellular hypha, a host nucleus, and vaculated cytoplasm. The lower haustorium has a large vacuole and an invaginated fungal plasma lemma.

B) An enlargement of the left side of the lower haustorium showing darkly stained particles in the cytoplasm (arrowheads). Note the darkly staining wavy fungal tonoplast (arrow).

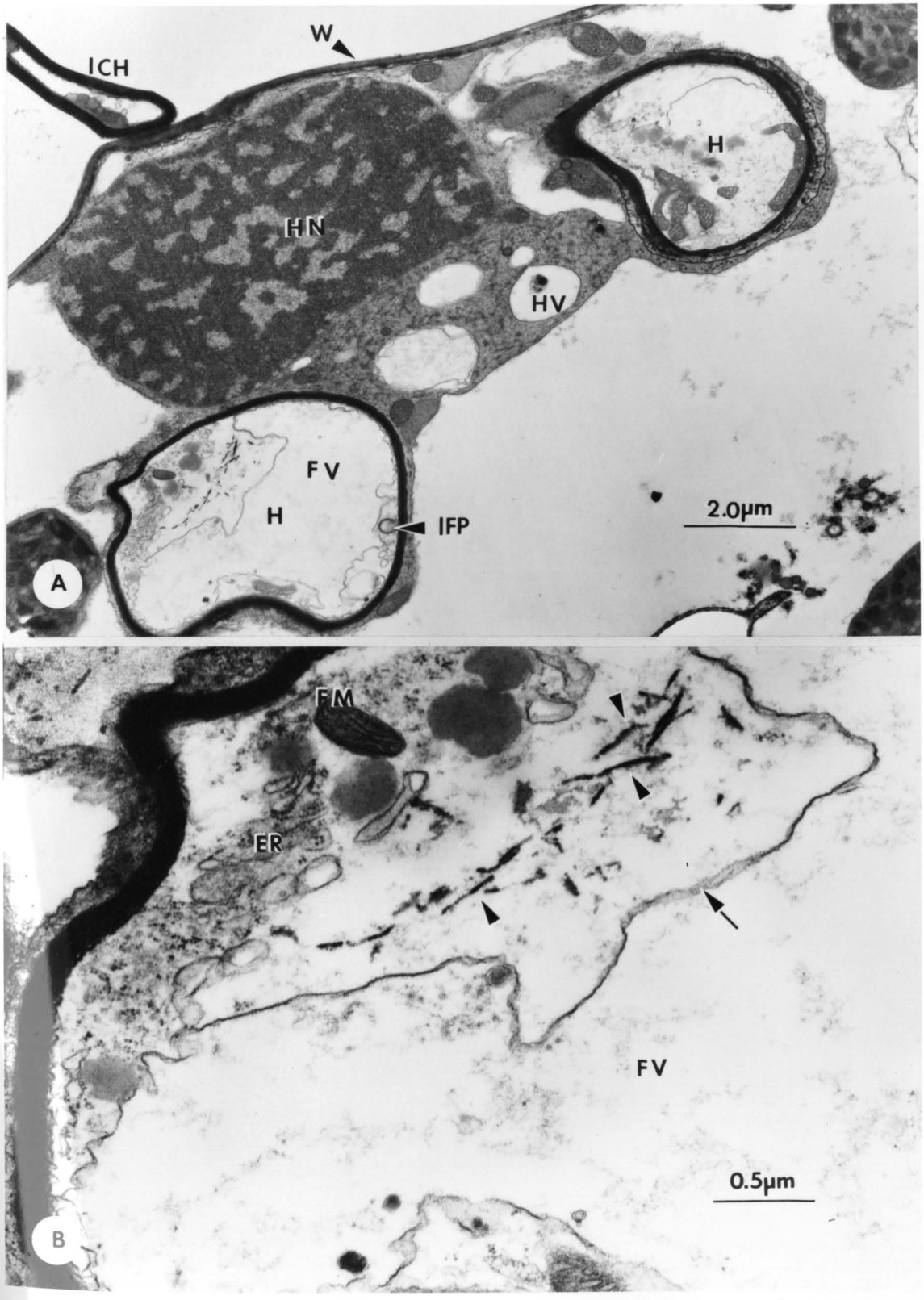
W
ICH
H
HN
HV
FV
H
IFP
2.0μm
A
FM
ER
FV
0.5μm
B

Figure 3. A) A thin section through part of a haustorium in a wheat mesophyll cell, clearly demonstrates the occurrence of rod-shaped particles, mitochondria and thylakoid membranes (TM) in chloroplasts.

B) An enlargement of the haustorial part, where rod-shaped particles (arrowheads) occur in the fungal cytoplasm. Note the wavy appearance of the fungal plasma membrane.

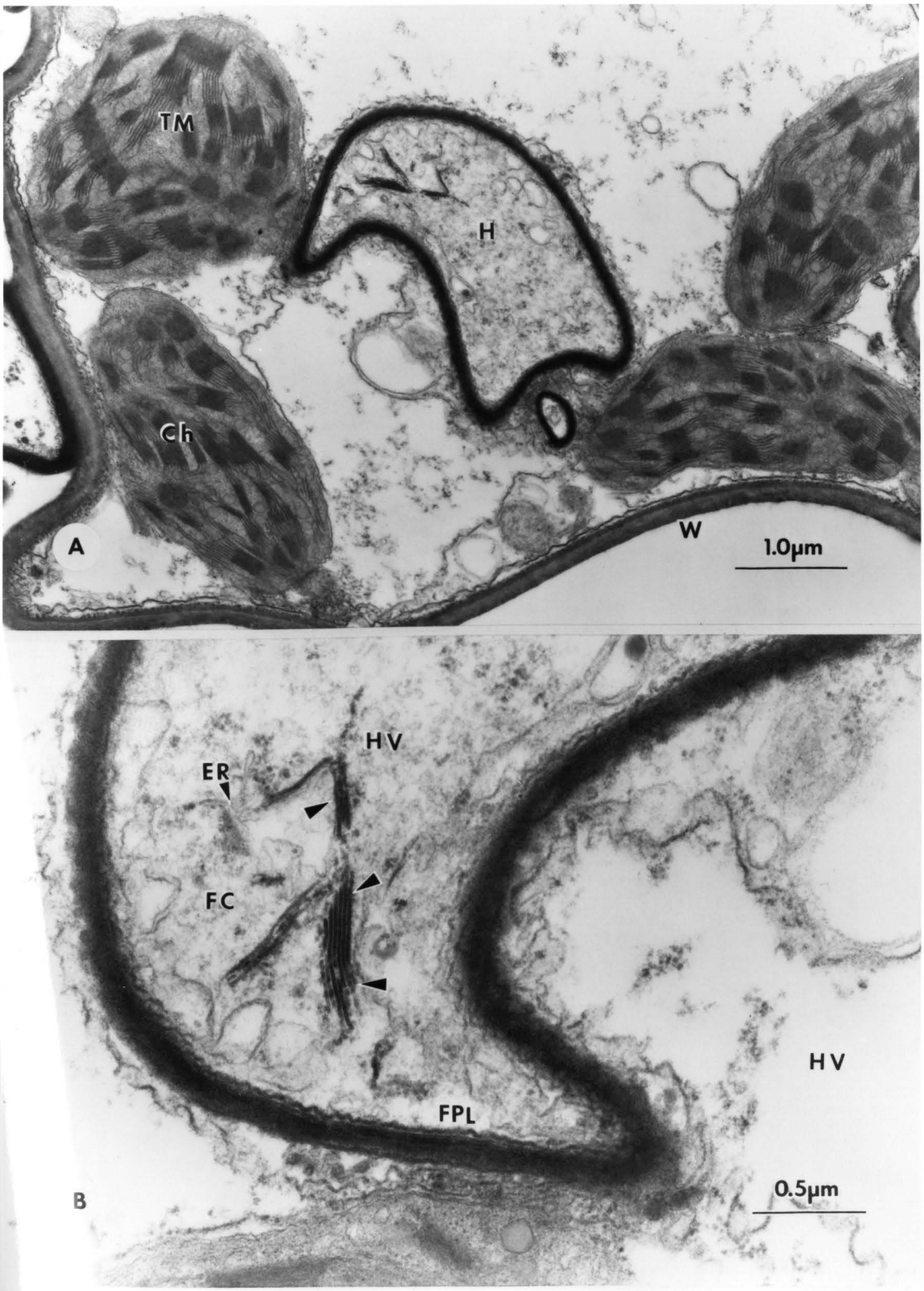
TM
H
Ch
A
W
1.0μm
HV
ER
FC
HV
FPL
B
0.5μm

Figure 4. A) A transverse and a longitudinal section of a haustorium, and intercellular hyphae respectively. Illustrates the association of the haustorium with the host nucleus, numerous mitochondria grouped in one side of the haustorium and a mixture of rod and spherical-shaped particles present in the other side.

B) An enlargement of the lower side of the haustorium shown in A, contains rod and spherical-shaped particles (arrowheads), which appeared to be bounded by a membrane and present in the fungal vacuole. Note the dissolution of the membranes in the area between the stars.

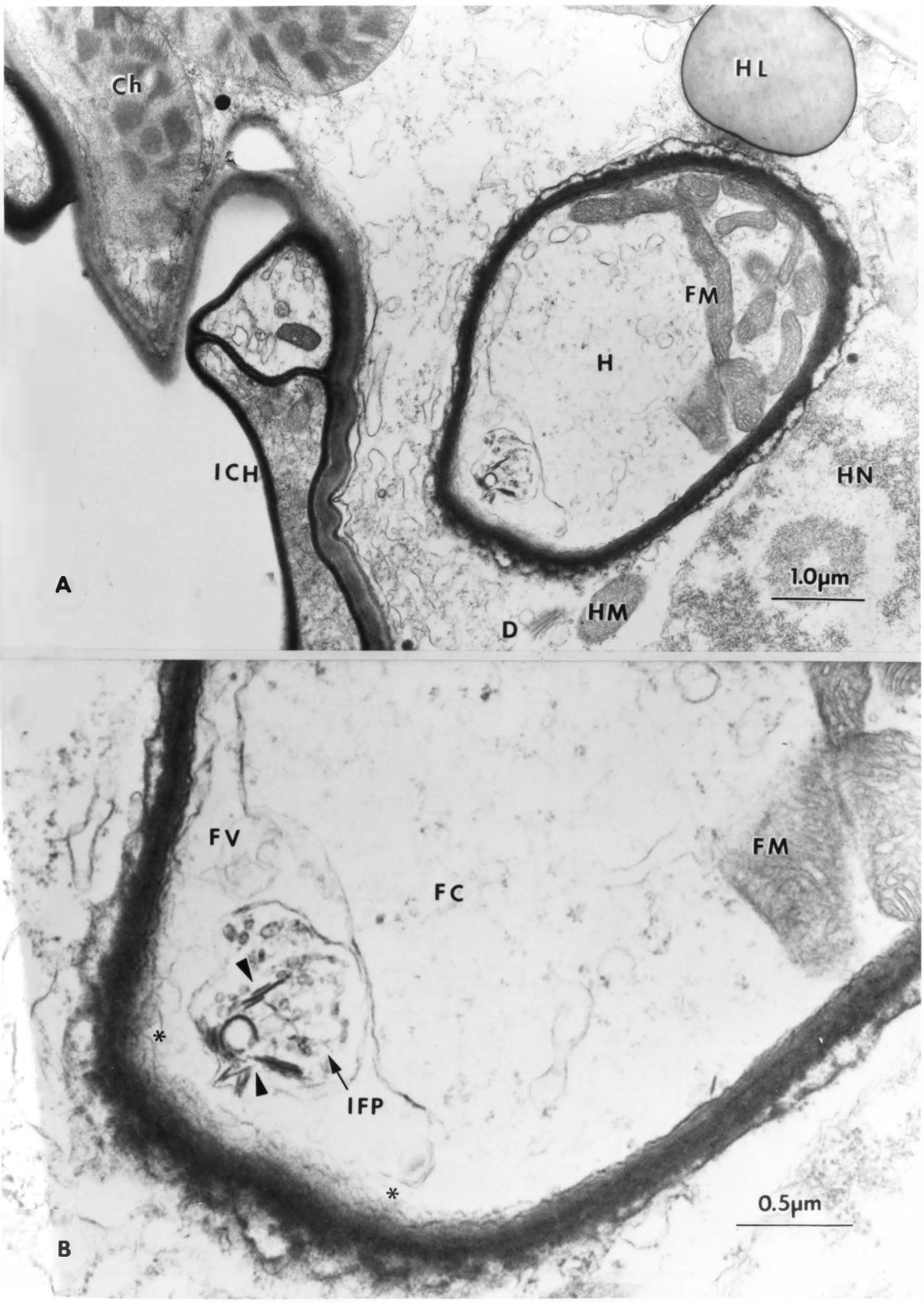
Ch
HL
FM
H
ICH
HN
A
1.0μm
D
HM
FV
FC
FM
IFP
B
0.5μm

Figure 5. A) Ultrastructural profile of haustorial lobes in a mesophyll cell, reveals mitochondria in the lobe on the left, a large vacuole, and an unusual clump of material on the outside end of the haustorial wall (arrowheads).

B) An enlargement of the clump of material shown in A, indicates that it consists of a granular matrix (arrowheads) and tubular matrix (arrow).

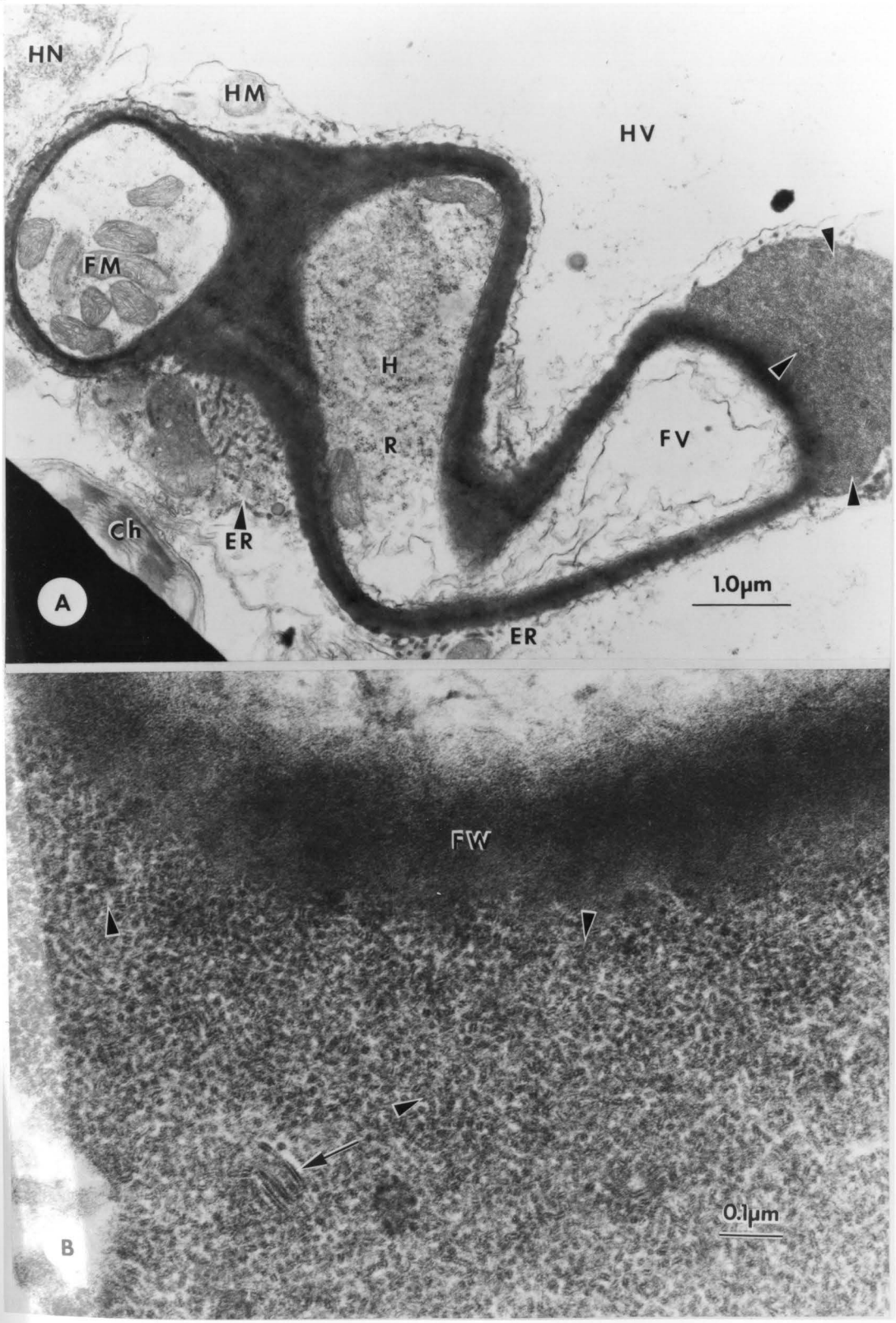
HN
HM
HV
FM
H
R
FV
Ch
ER
A
1.0μm
ER
FW
0.1μm
B

Figure 6. A) Ultrastructure of a cross section of a partial haustorium, showing numerous ribosomes in vacuolated cytoplasm, and a dense membranous structure on the haustorial wall (arrowheads). Note the partial opening and break in the fungal wall between stars, and the ends of the membrane appear to be connected with the host plasmalemma.

B) An enlargement of A, shows numerous host ribosomes, cross sections of WSMV (Vi) and tubular vesicles bounded by the plasmalemma of the host.

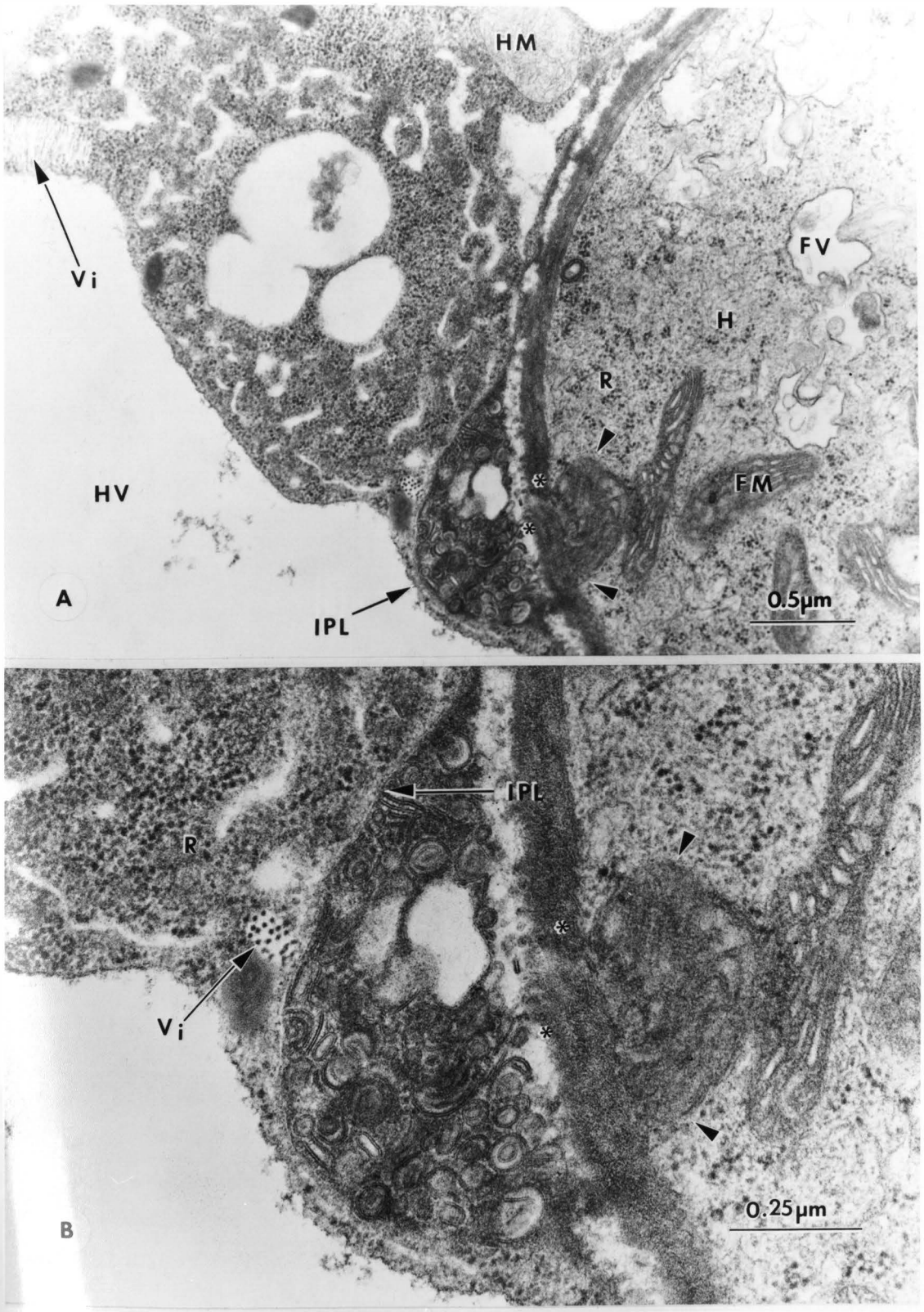
HM
Vi
FV
H
R
HV
FM
A
IPL
0.5µm
IPL
R
Vi
B
0.25µm

Figure 7. A) A transverse section of a haustorium in the cytoplasm of a wheat mesophyll cell shows an elongated mitochondrion, and microbodies. Note the presence of particles of a short-rod type (arrows), and two darkly stained bodies similar to lipid droplets.

B) A section through septated intercellular hyphae revealing several microbodies, mitochondria, large vacuoles, and short-rod particles in the fungal cytoplasm (arrows). Note the presence of "fungal endoplasmic reticulum complexes" between stars.

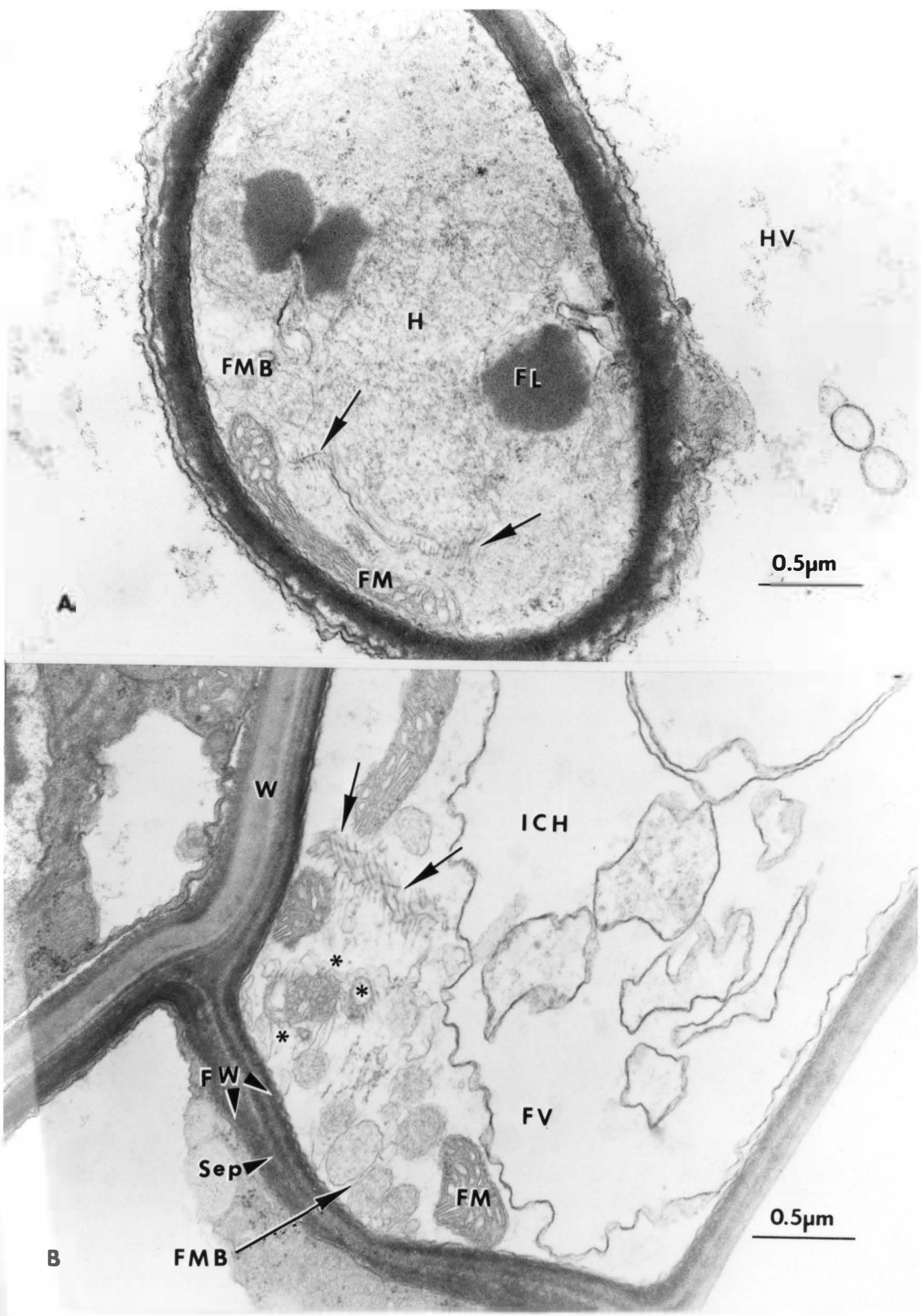
HV
H
FMB
FL
FM
0.5µm
A
W
ICH
*
*
*
FW
FV
Sep
FM
FMB
0.5µm
B

Figure 8. Ultrastructure of a haustorium and intercellular hypha of a P. recondita - infected flag leaf of wheat. The haustorium contains several microbodies, some with crystals, elongated possibly dividing mitochondria, and endoplasmic reticulum. The intercellular hypha is closely appressed to the host cell wall. Note the presence of the host endoplasmic reticulum complex (arrowheads) with small tubules of darkly stained material. The mesophyll host cell also shows microbodies, mitochondria and chloroplasts.

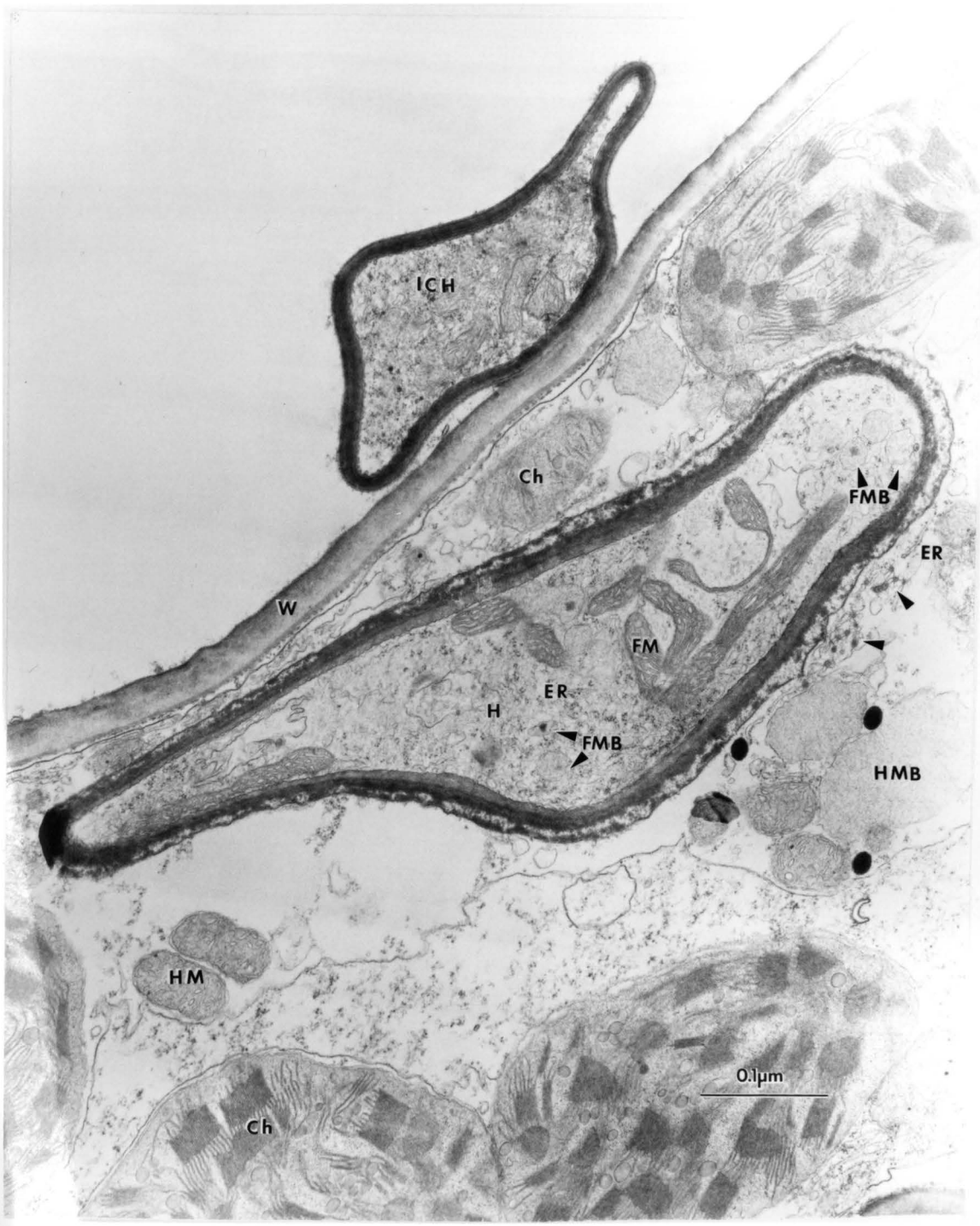
ICH
Ch
FMB
ER
W
FM
ER
H
FMB
HMB
HM
0.1μm
Ch

Figure 9. Ultrastructure of a wheat mesophyll cell infected with a combination of WSMV and P. recondita. Organelles in the haustorium include microbodies, mitochondria, lipid droplets, and ribosomes. Virus particles are present in the host cytoplasm between the haustorium and the chloroplast.

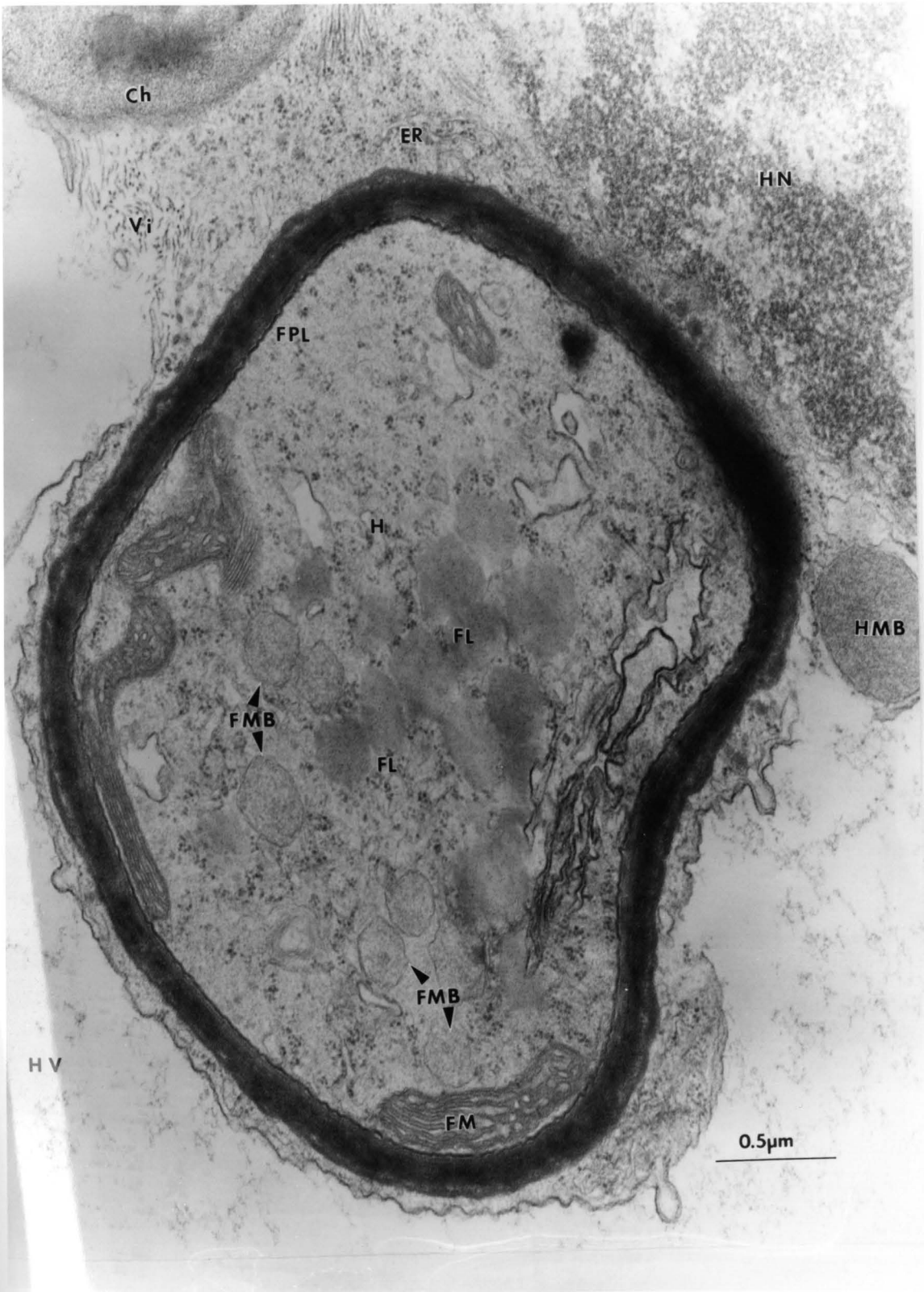
Ch
ER
HN
Vi
FPL
H
FL
HMB
FMB
FL
FMB
HV
FM
0.5μm

Figure 10. A transverse section of a haustorium in the cytoplasm of wheat leaf infected with WSMV, shows extrahaustorial sheath (EHS) surrounding the haustorium. Note the arrangement of endoplasmic reticulum complexes (small arrows). The lower portion of the haustorium is extended, exerting pressure on the EHS which appears to be stretched and broken.

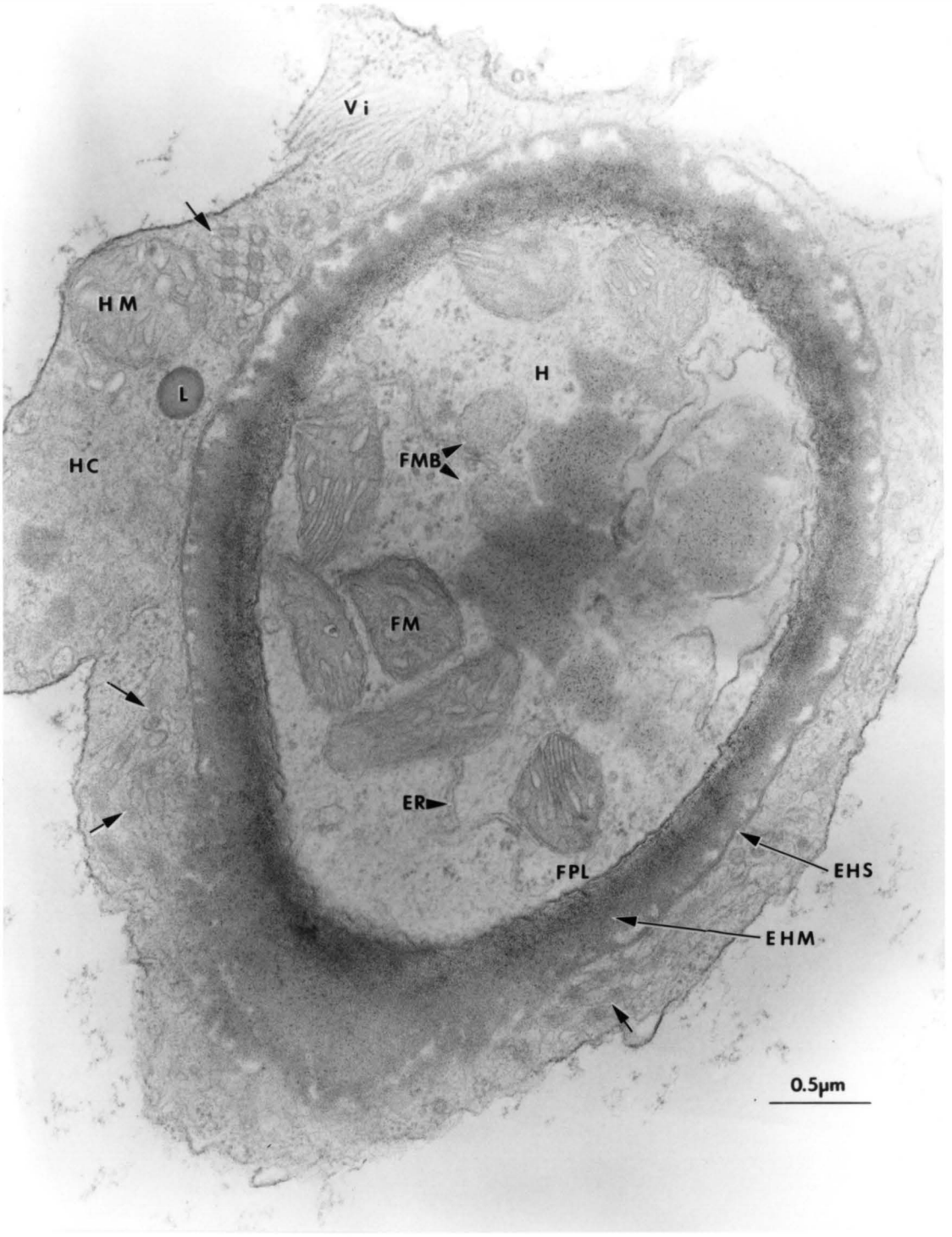
Vi
HM
L
H
HC
FMB
FM
ER
FPL
EHS
EHM
0.5µm

Figure 11. A longitudinal and a transverse section of wheat leaf rust, showing a partially septate intercellular hypha with two nuclei one of which appears to be passing through the septal pore, and an invaginated fungal membranous structure (star). The section also shows a cross section of a haustorium inside the host mesophyll cell. Note the presence of plasmodesmata (arrowheads) between two cells.


FN
FN
FV
*
Sep
I
C
H
FW
Ch
HM
Ch
W
H
1.0µm

Figure 12. Ultrastructure of a transverse section of a leaf rust haustorium contains several mitochondria, microbodies, ribosomes, and a small structure of short-rod particles arranged around a common center (arrowhead). Note the relative size of fungal mitochondria and microbodies to that of the host.

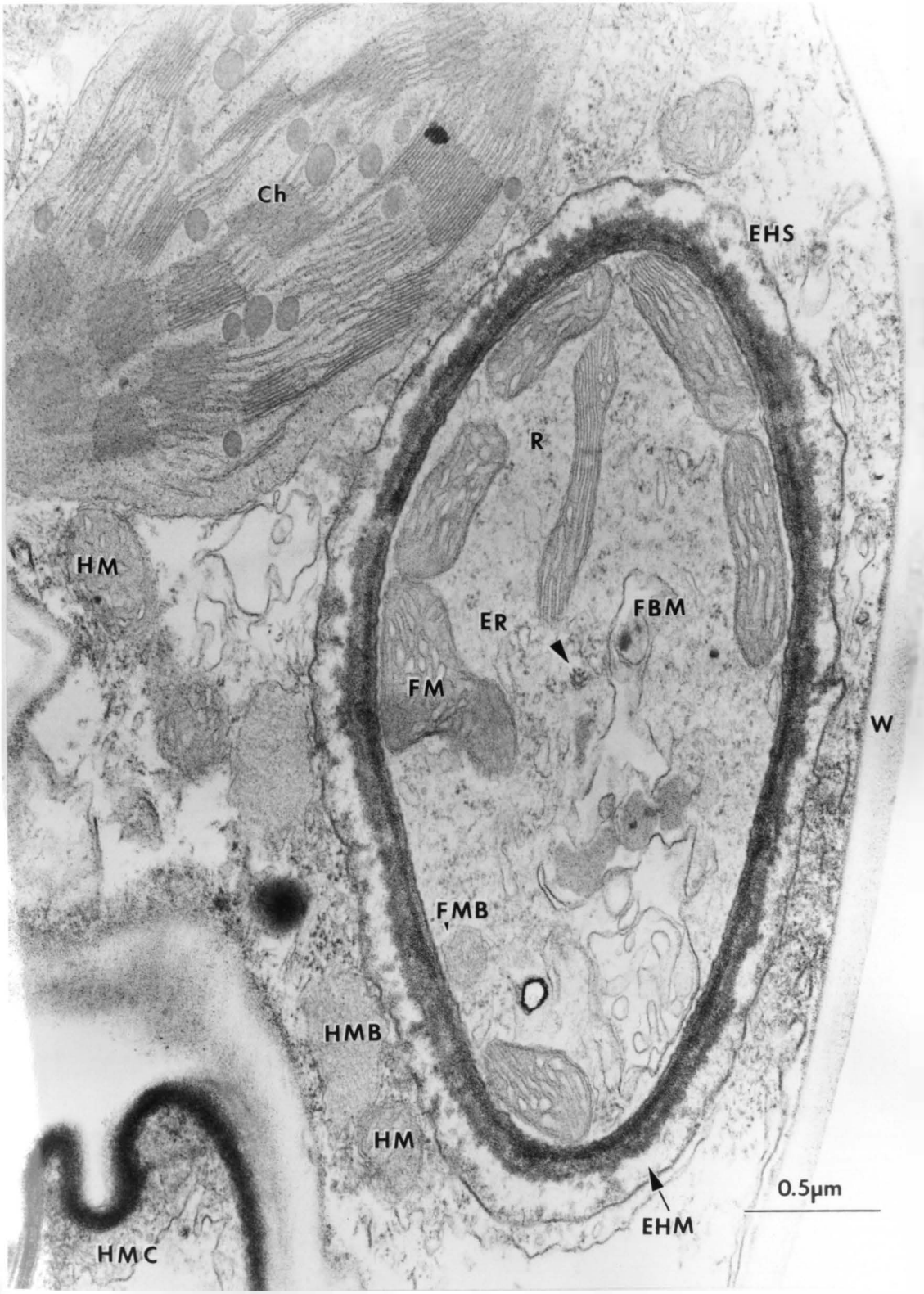
Ch
EHS
R
HM
ER
FBM
FM
W
FMB
HMB
HM
0.5µm
EHM
HMC

Figure 13. A) Ultrastructure of a wheat leaf cell infected with P. recondita and WSMV. Darkly stained particles in cross section are present in the fungus haustorium (arrowheads).

B) An enlargement of those particles shown in A, where a circular structure is surrounded by number of particles. Note the size similarity between these particles, and the virus in cross section in the host cytoplasm shown in A. Pinwheels, scrolls, tubes and other configurations of cylindrical inclusions also occur in the host cytoplasm.

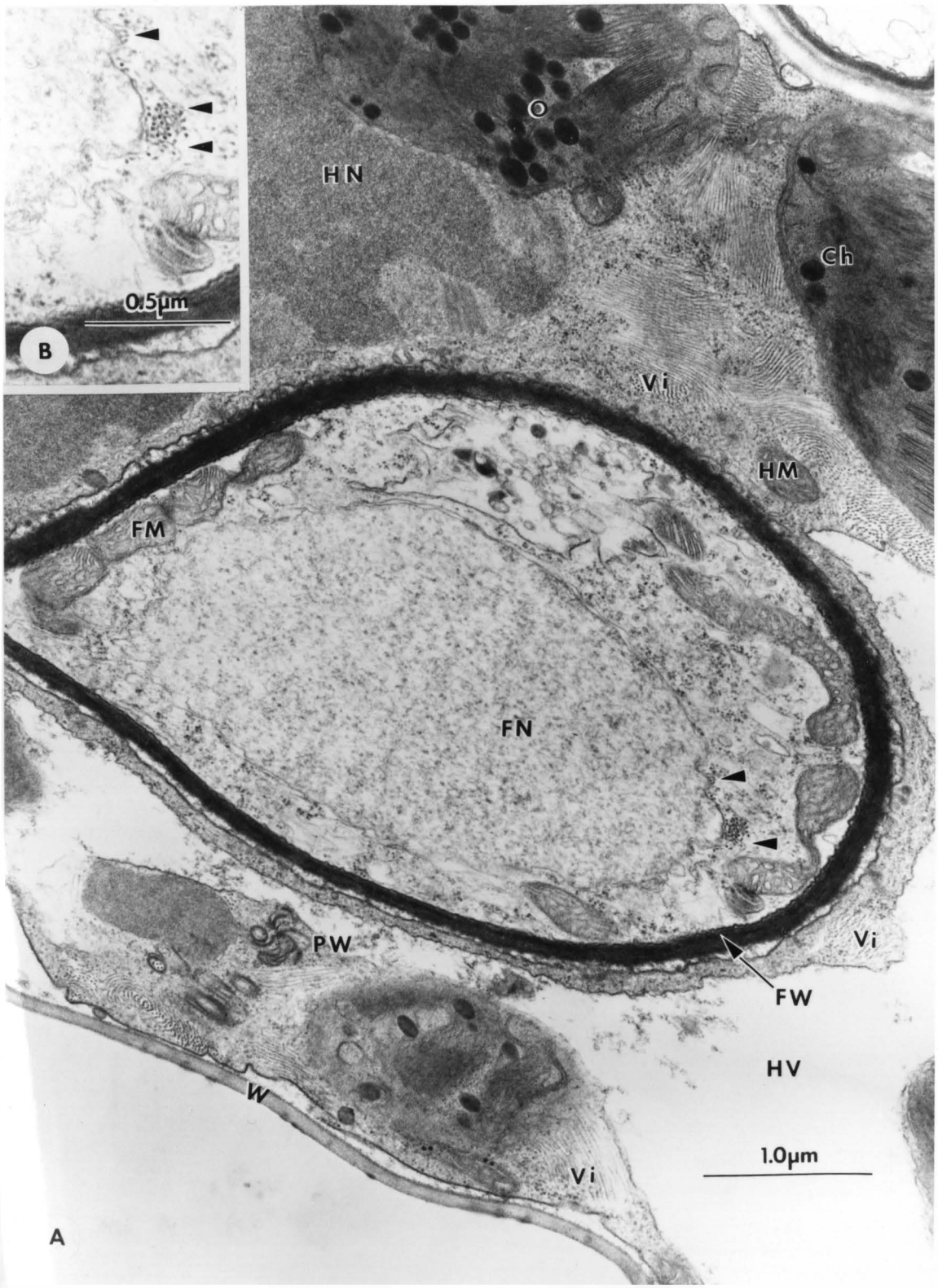
O
HN
Ch
0.5μm
B
Vi
HM
FM
FN
PW
Vi
FW
HV
W
1.0μm
Vi
A

Figure 14. A serial section of the haustorium in Figure 13-A, shows longitudinal and cross sections of the particles (small arrowheads) present next to the nuclear envelope (big arrowheads). Note the presence of various shaped vesicles which contain dark centers similar to the "fungal endoplasmic reticulum complex" in Figure 7-B. Other organelles evident in the host cytoplasm are a pycnotic nucleus, a large mass of WSMV and scrolls (small arrow).

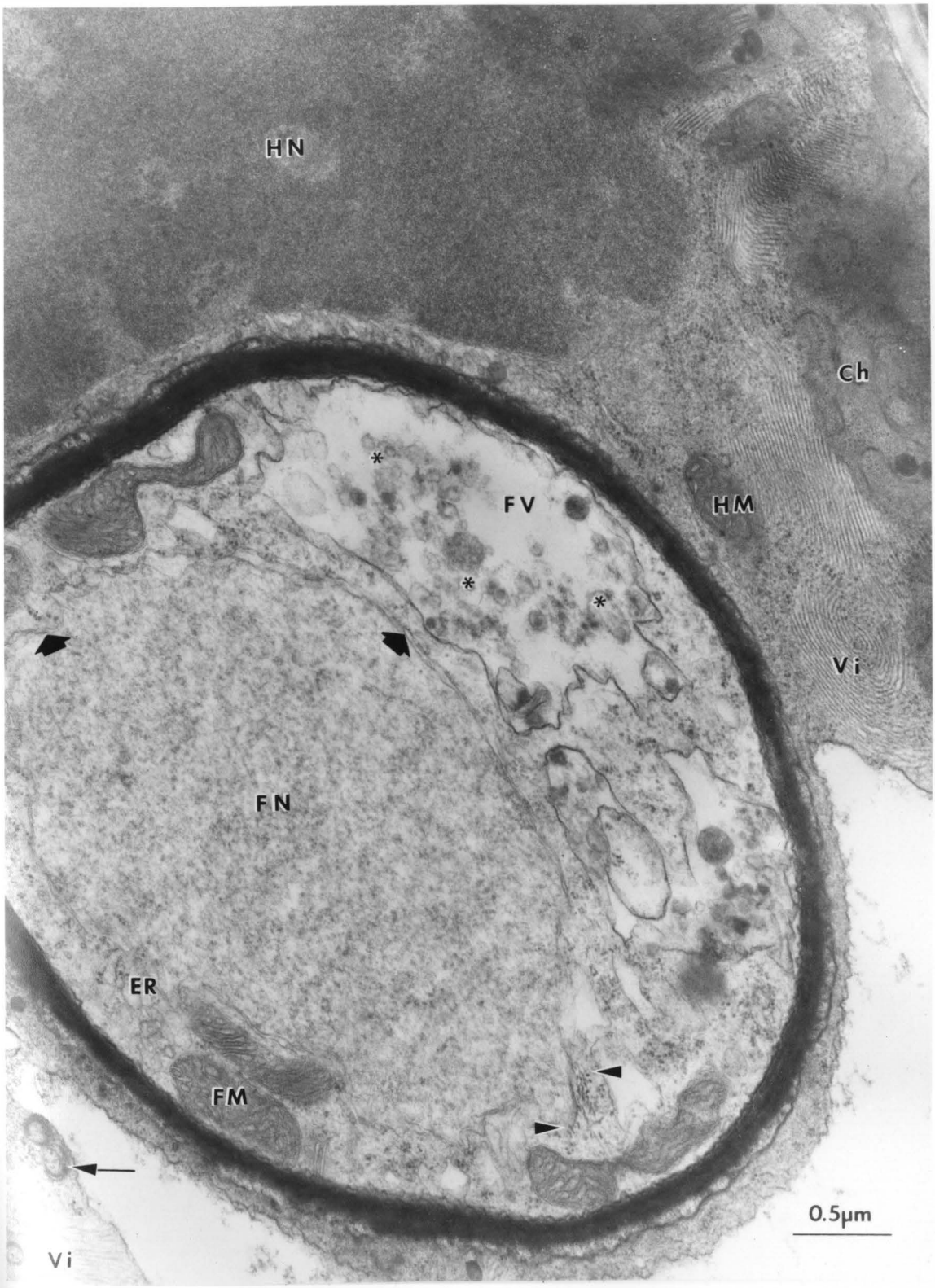
HN
Ch
FV
HM
Vi
FN
ER
FM
0.5μm
Vi

Figure 15. A section through a haustorium where the fungal plasma lemma (FPL) is connected directly to both ends of the invaginated fungal plasmalemma (IFP). The mitochondria are positioned on one side of the haustorium opposite to the IFP. Note the stretched mitochondria, and the thin connection (arrowheads), and a large vacuole with scattered vesicles.

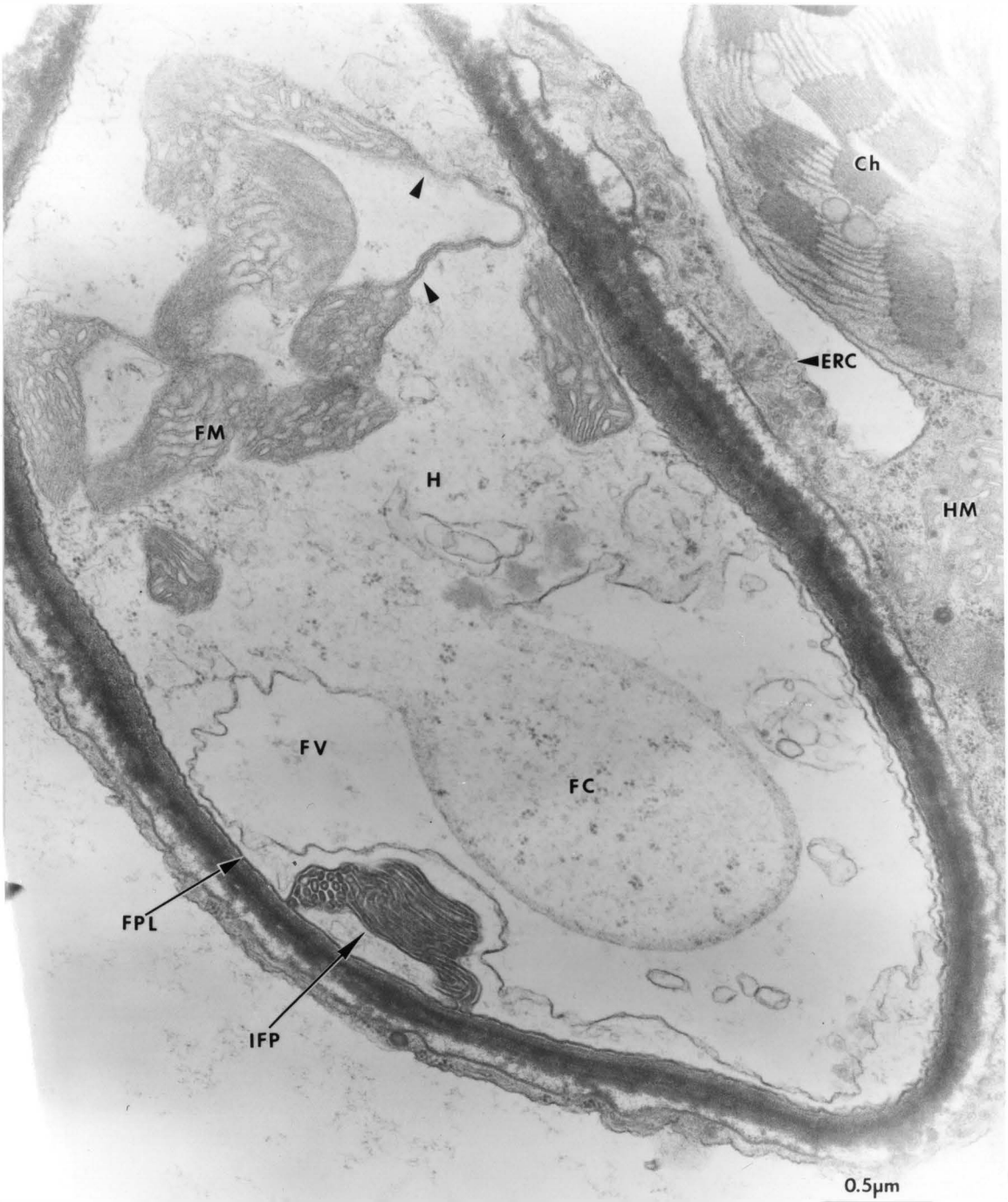
Ch
ERC
FM
H
HM
FV
FC
FPL
IFP
0.5µm

Figure 16. A transverse section of a leaf rust haustorium in an epidermal cell of wheat leaf, where an invaginated fungal plasma lemma appears next to, but not clearly connected to the fungal plasma membrane. An unusual pleomorphic membranous structure is present in the haustorium cytoplasm (stars). Note the double membrane around the fungal mitochondria (arrowheads).

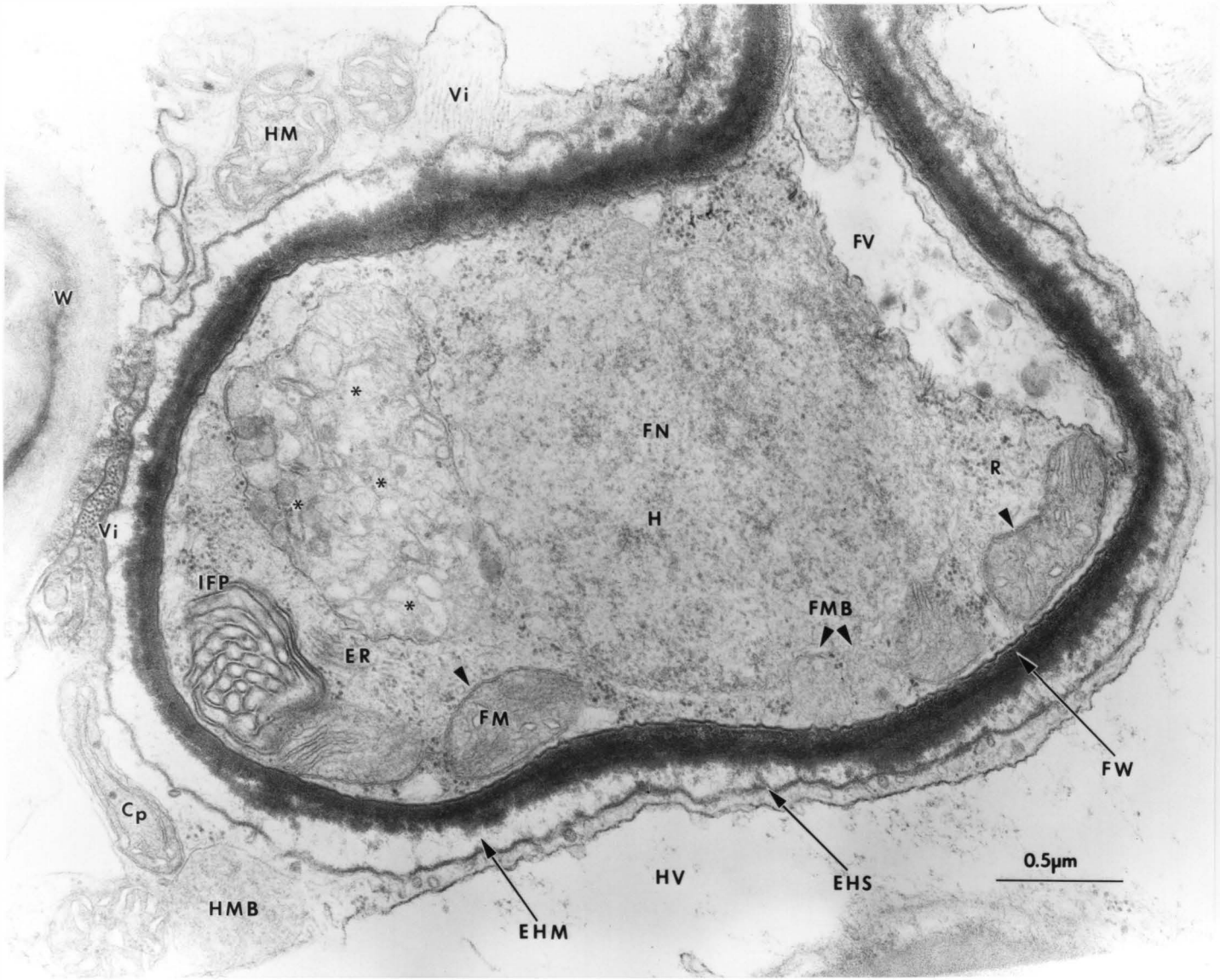
Vi
HM
FV
W
FN
R
H
Vi
IFP
FMB
ER
FM
FW
Cp
0.5μm
HV
EHS
HMB
EHM

Figure 17. Ultrastructure of a wheat mesophyll cell showing haustorial mother cell, haustorium and virus particles. A near complete penetration process, contains a haustorium with haustorial neck (HNK), a mitochondrion passing through the neck, and an invaginated plasmalemma (arrow) in the neck. Note the darkly stained neck band (B) shown only in one side.


Ch
HMC
W
Vi
FM
B
HNK
HM
FPL
0.5μm
H

Figure 18-A. A section through a haustorial mother cell (HMC) that is penetrating the host cell, the HMC wall is thickened around what would be the penetration pore (arrowheads). A haustorium with a haustorial neck is in the wheat mesophyll cell.

Figure 18-B. An enlargement of the haustorial neck and part of the haustorium where a massive invaginated fungal plasmalemma has developed (arrowheads).

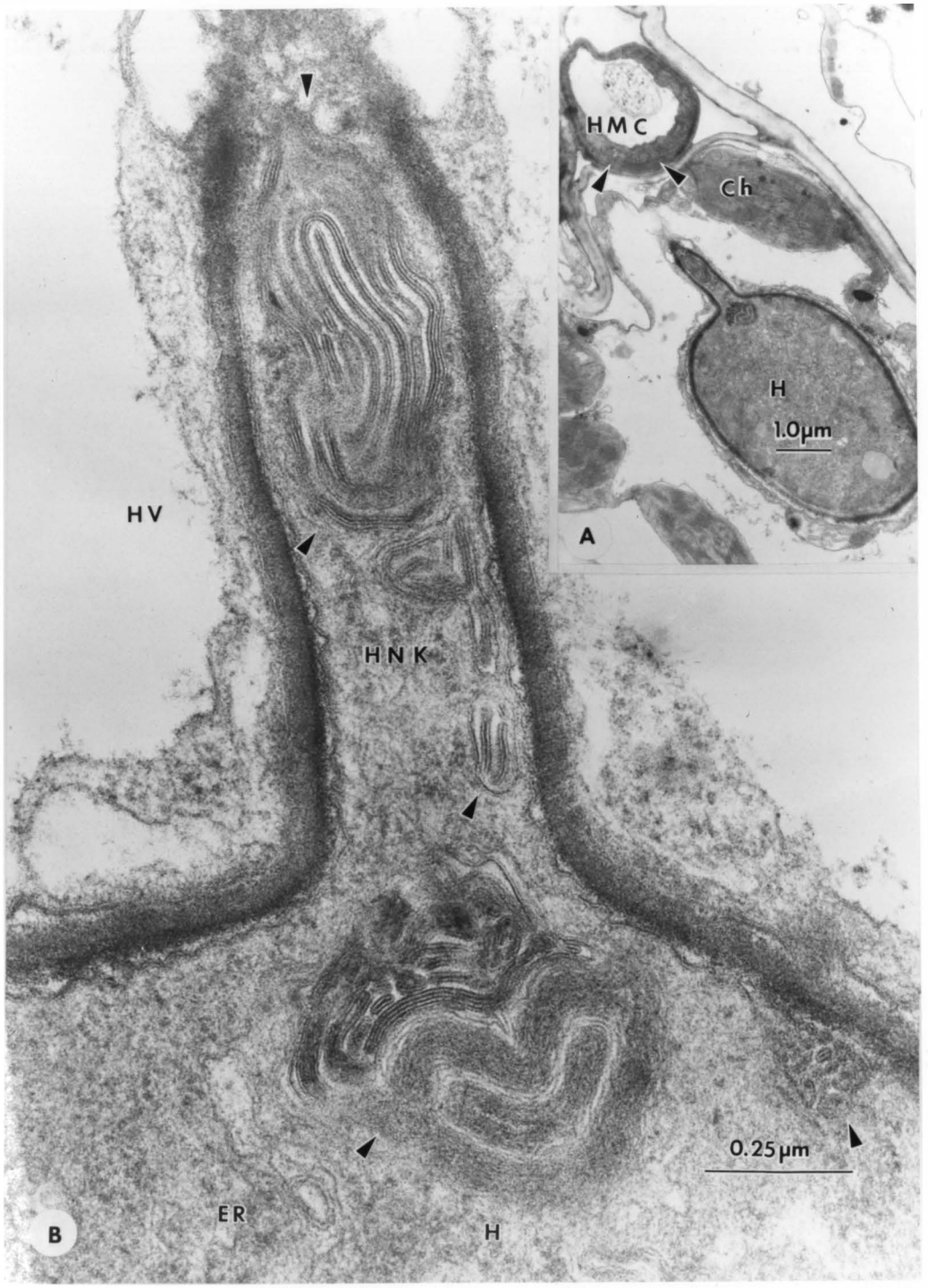
HMC
Ch
H
1.0μm
A
HV
HNK
0.25μm
ER
H
B

Figure 19-A. Invaginated fungal plasmalemma in an intercellular hypha directly formed on the plasma membrane. A great amount of ribosomes are present as well as paired filaments (arrowheads). Note the amorphous material present between fungal wall and host cell wall (stars).

Figure 19-B. An enlargement of A in the area of the invaginated plasmalemma revealing a different membrane configuration, and continuous filaments around the IFP (arrowheads).

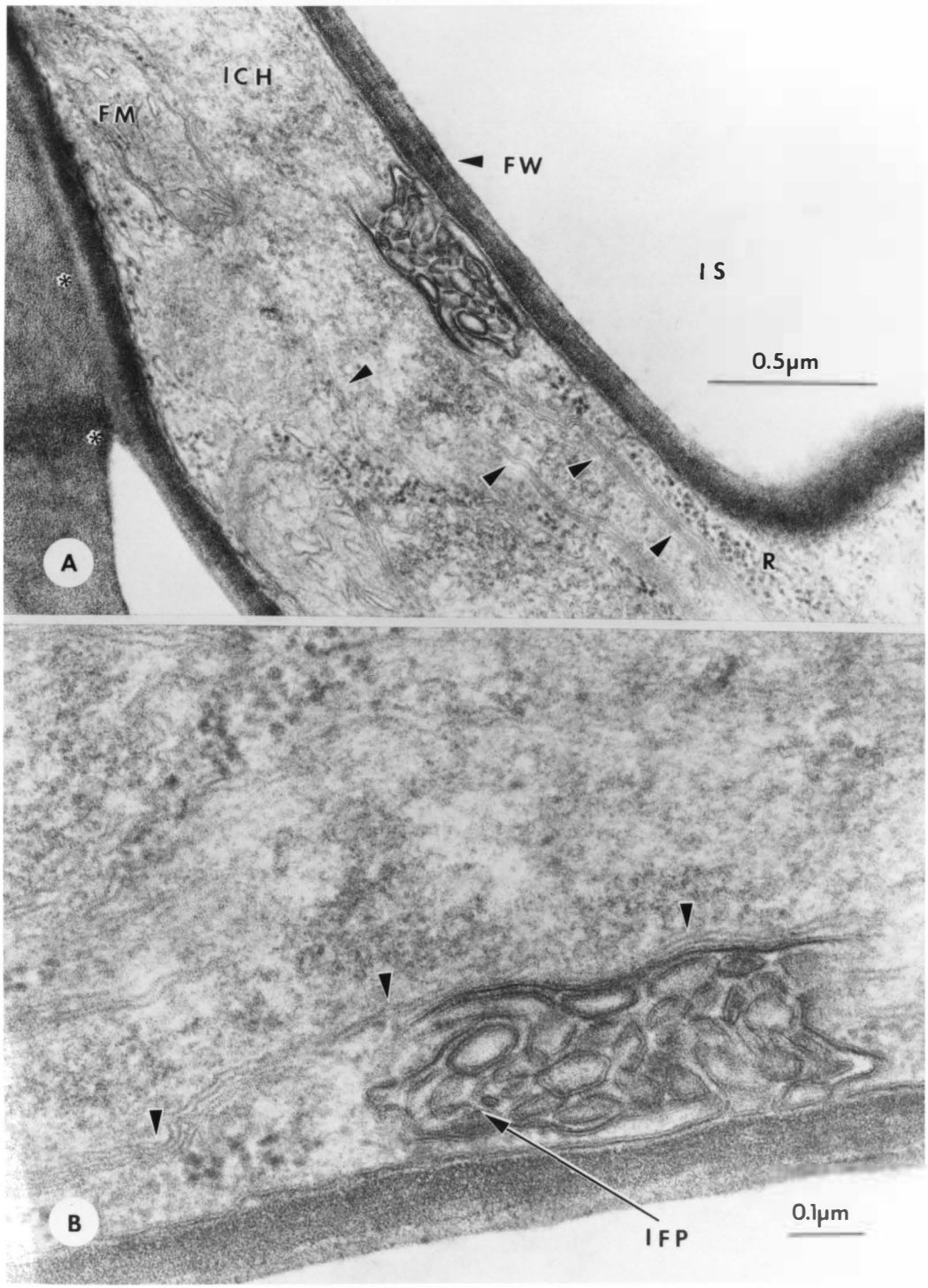
ICH
FM
FW
IS
0.5μm
A
R
B
IFP
0.1μm

Figure 20. Serial sections of the penetration process of a haustorial mother cell through the mesophyll cell of wheat.

A) Is a HMC with a thickened wall around the penetration pore (arrowhead).

B) A partial opening through the host cell wall.

C) Similar to B, but with an almost closed pore, and partial appearance of the collar around the haustorial neck (arrowhead). Note the host plasma membrane around the collar.

D & E) HMC without the penetration pore, with a thickened wall at the surface adjacent to the host cell wall, a complete view of the collar surrounding the HNK (arrowhead), and the host plasma membrane encircling them. Note IFP in D (arrow) in the HMC, and less mitochondria, and more glycogen in E.

F) HMC with a thinner wall, and fewer mitochondria. Note the host plasma membrane is not surrounding the collar (arrowhead), and the appearance of several host mitochondria next to the chloroplasts.

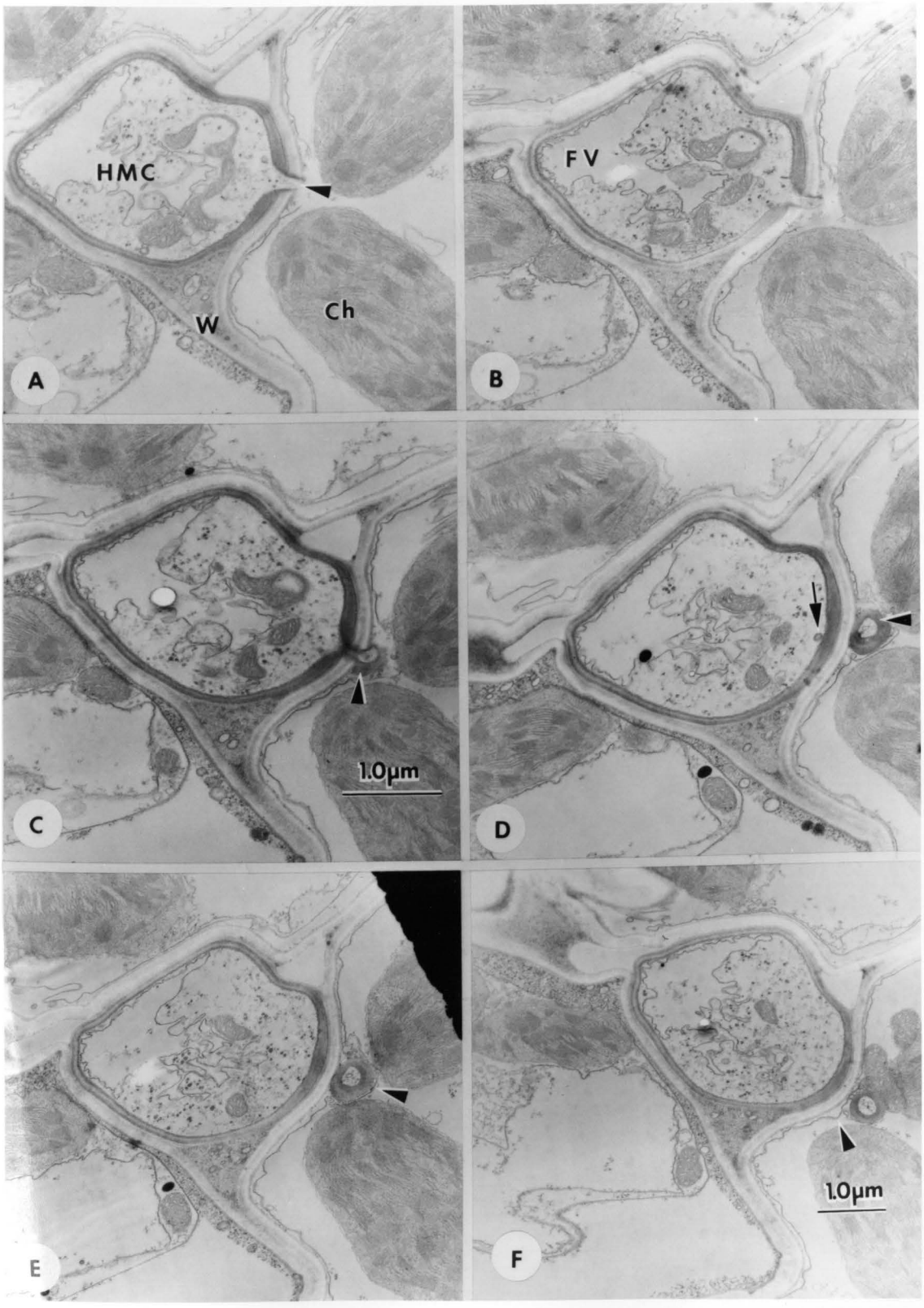
HMC
W
Ch
A
FV
B
1.0µm
C
D
E
1.0µm
F

Figure 21. An enlargement of a cross sectioned HMC in Figure 20-F. A haustorial mother cell with slight thickened fungal wall around the would be penetration pore contains scattered glycogen granules. The collar (arrowhead) surrounds the haustorial neck (stars), and the host plasma membrane is located between the host cell wall and the collar.

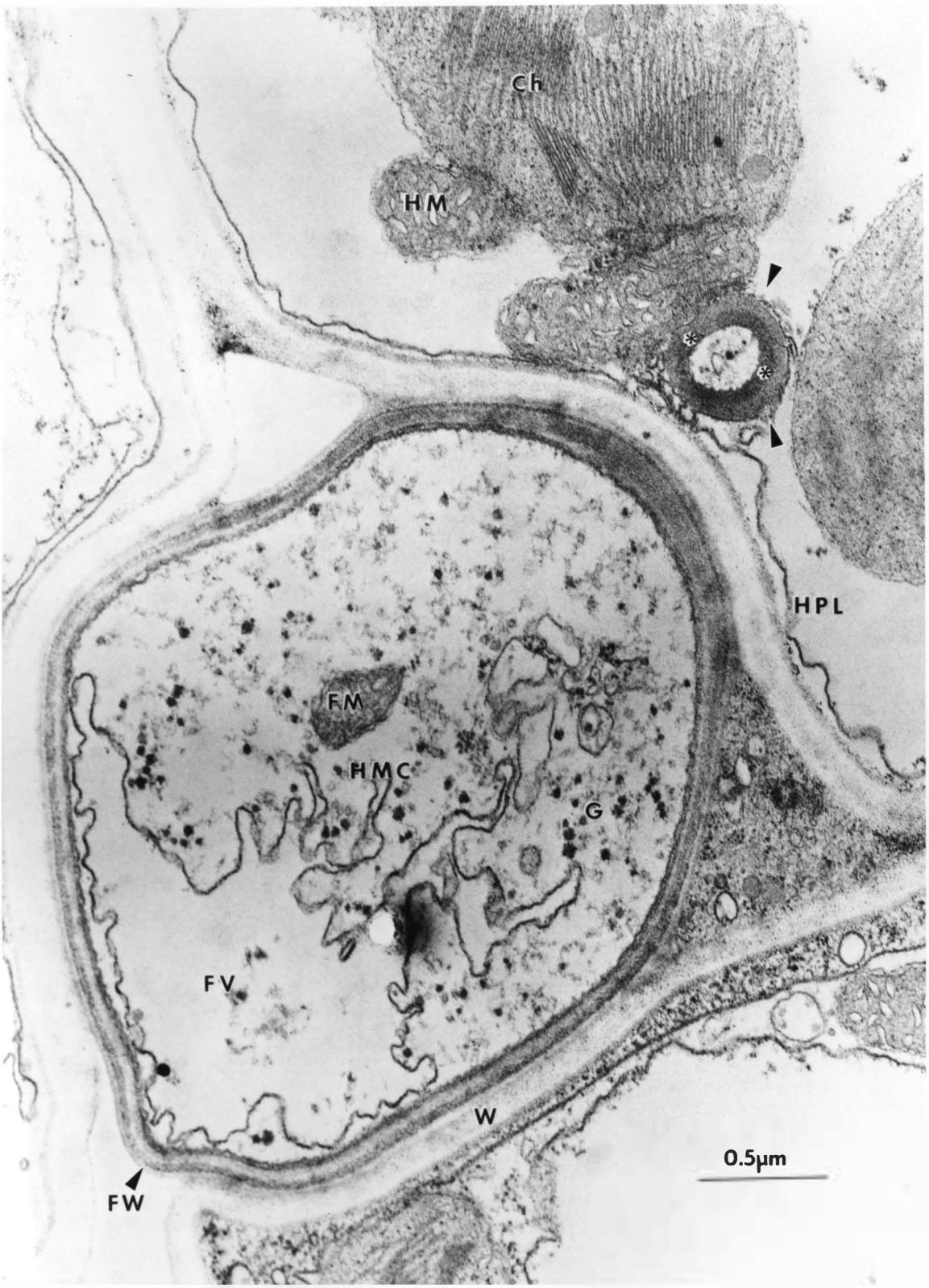
Ch
HM
HPL
FM
HMC
G
FV
W
FW
0.5µm

Figure 22. Longitudinal serial sections through penetration sites.

A & B) Are electronmicrograph of the same penetration site. The HNK is lacking in A, but B shows a median longitudinal section through the haustorial neck. The HMC is penetrating the host cell wall in B.

C) Shows a section through a different site of penetration. The haustorial mother cell is an indeterminate type, with a clear cut opening through the cell wall, and an incomplete HNK with an apparent neck band (stars). Note the collar area slightly showing in B, but more obvious in C (arrows).

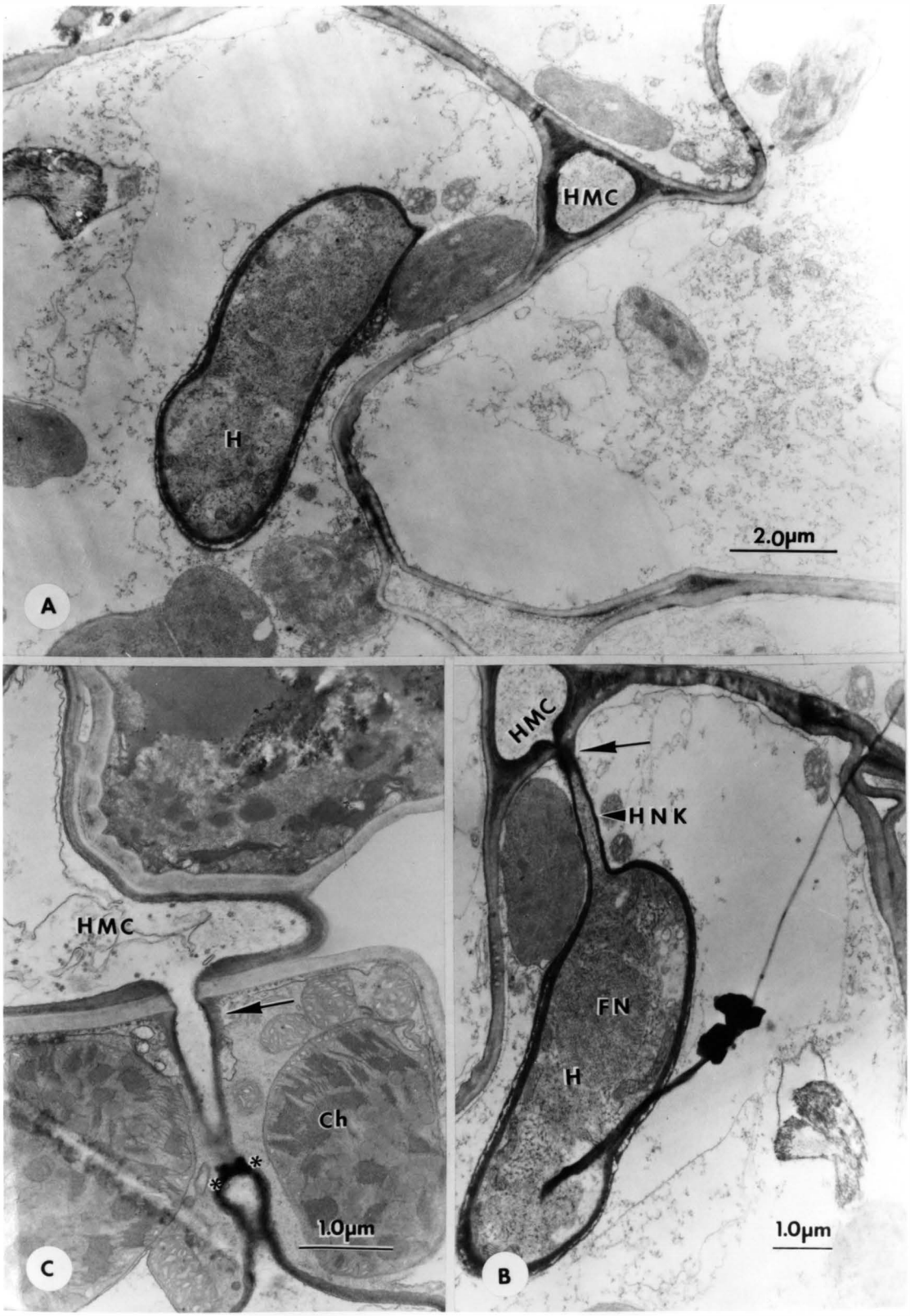
HMC
H
2.0μm
A
HMC
HNK
FN
H
1.0μm
B
HMC
Ch
1.0μm
C

Figure 23. Two views of haustorial mother cell penetrations and haustorial formations.

A) Cross section of HMC penetrating the host cell wall shows a well-developed collar bounded by HPL around the HNK. Note the deposited material (arrowheads) continuous with the collar.

B) A complete penetration process of HMC with a HNK connected to the haustorium. Note the neck bank (small arrows) in both A & B, and the different collar types formed around the the upper part of each HNK.

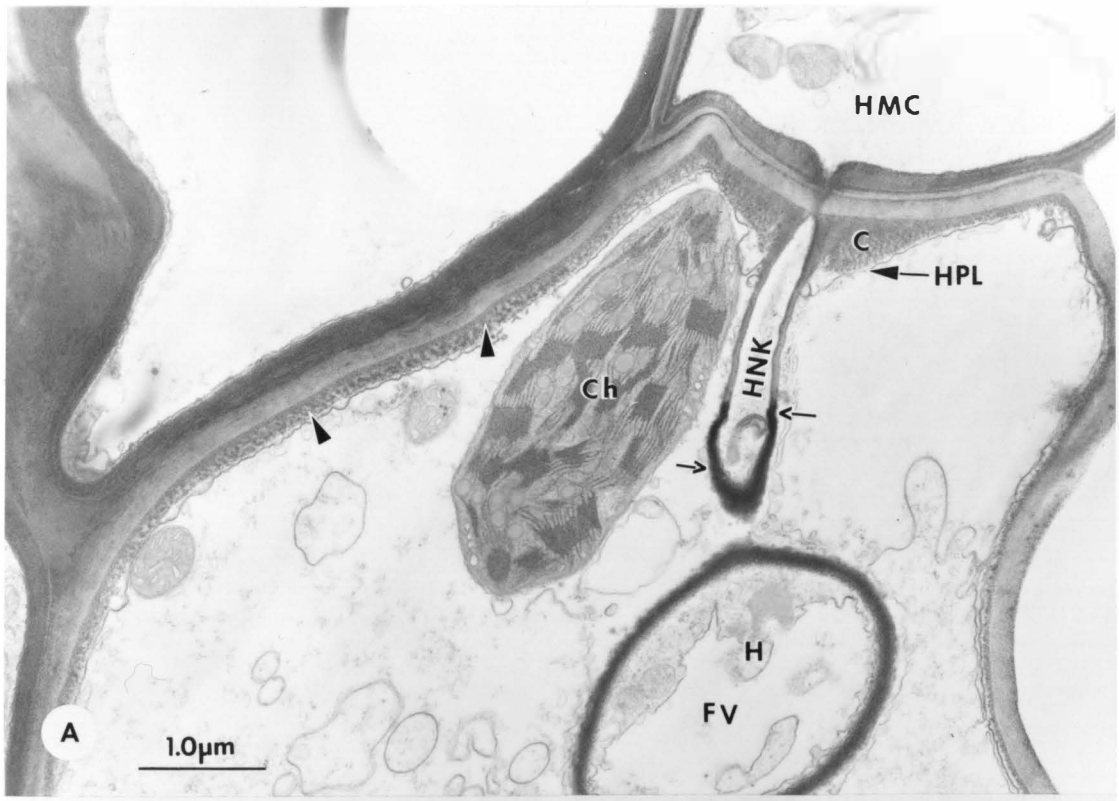
HMC
C
HPL
HNK
Ch
H
FV
A
1.0μm

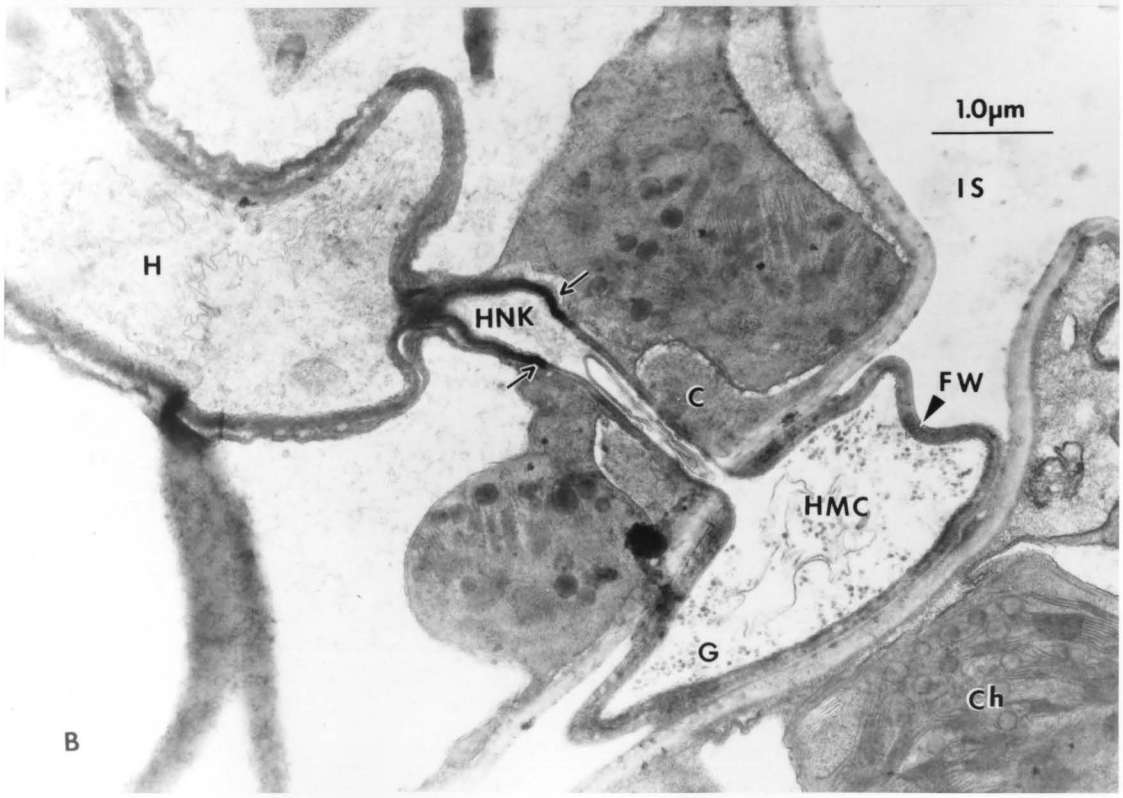
1.0μm
IS
H
HNK
C
FW
HMC
G
Ch
B

Figure 24. A transverse section through leaf rust penetration site in wheat epidermal cells.

A) Shows a haustorium with lower part of the HNK (small arrows), and HMC with thickened wall near penetration site (arrowhead).

B) An enlargement of the area around the penetration showing a "cap-like bulge" in the fungal wall of the HMC (arrowheads). Note the dense layer (stars) between host cell and fungal wall.

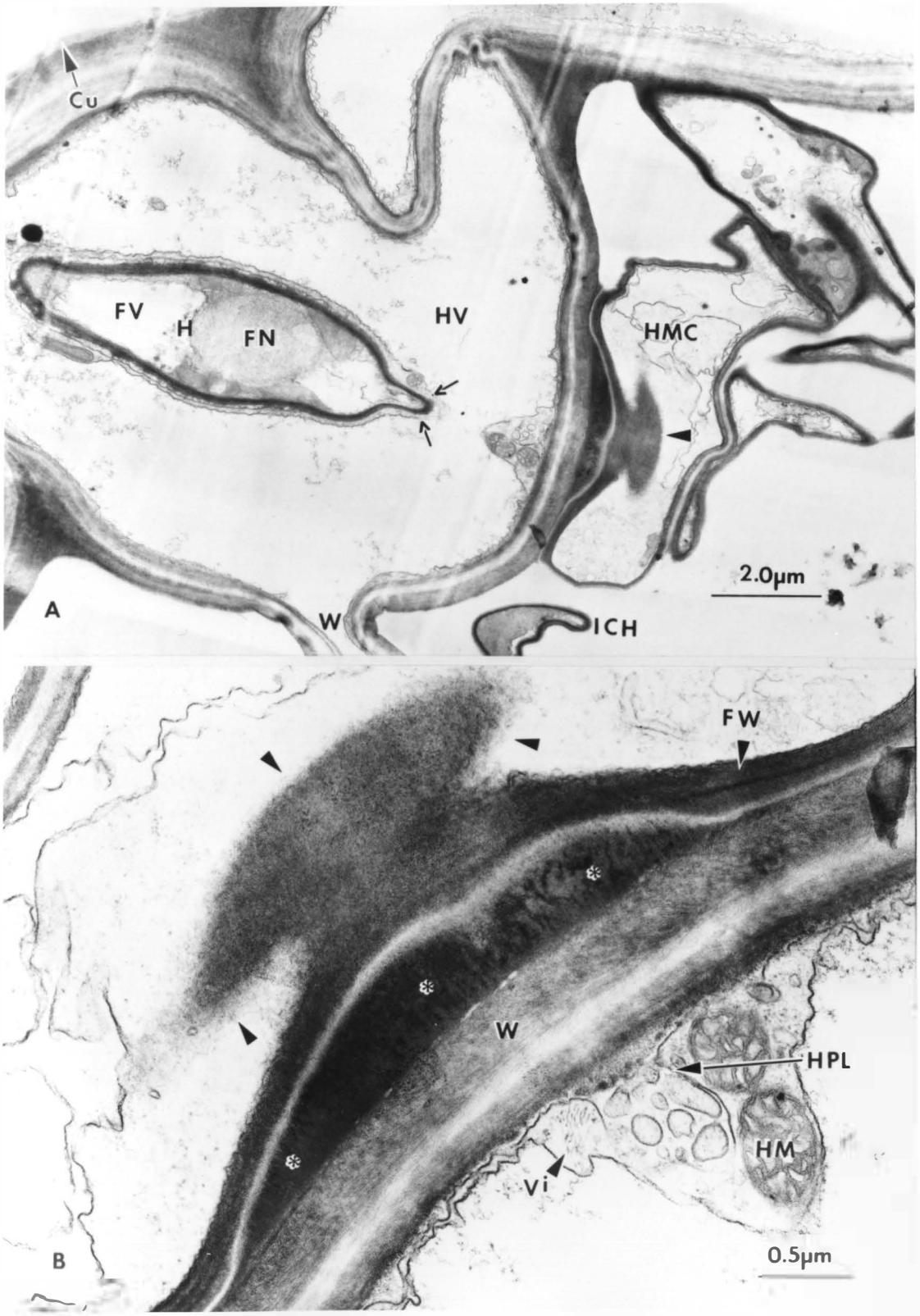
Cu
FV
H
FN
HV
HMC
2.0μm
A
W
ICH
FW
W
HPL
HM
Vi
B
0.5μm

Figure 25. A section through the epidermal area of a wheat leaf infected with leaf rust, showing nucleated guard cells with thick and thin areas on the cell wall. A subsidiary cell contains a haustorium, apparently vacuolated, next to the nucleus. Note the cuticle between the arrowheads.


SC
H
H N
ICH
W
Cu
GC
1.0µm

Figure 26. Longitudinal serial sections of the septal pore apparatus in an intercellular hypha of P. recondita.

A) A section apparently away from the septal pore area.

B) Almost median section through the plugged pore (arrowhead). Note the disappearance of the invaginated fungal plasmalemma (IFP) in the section.

C) A median section through the septal pore. Note the bilateral infolding of the hyphal wall centripetally, leaving a wide pore.

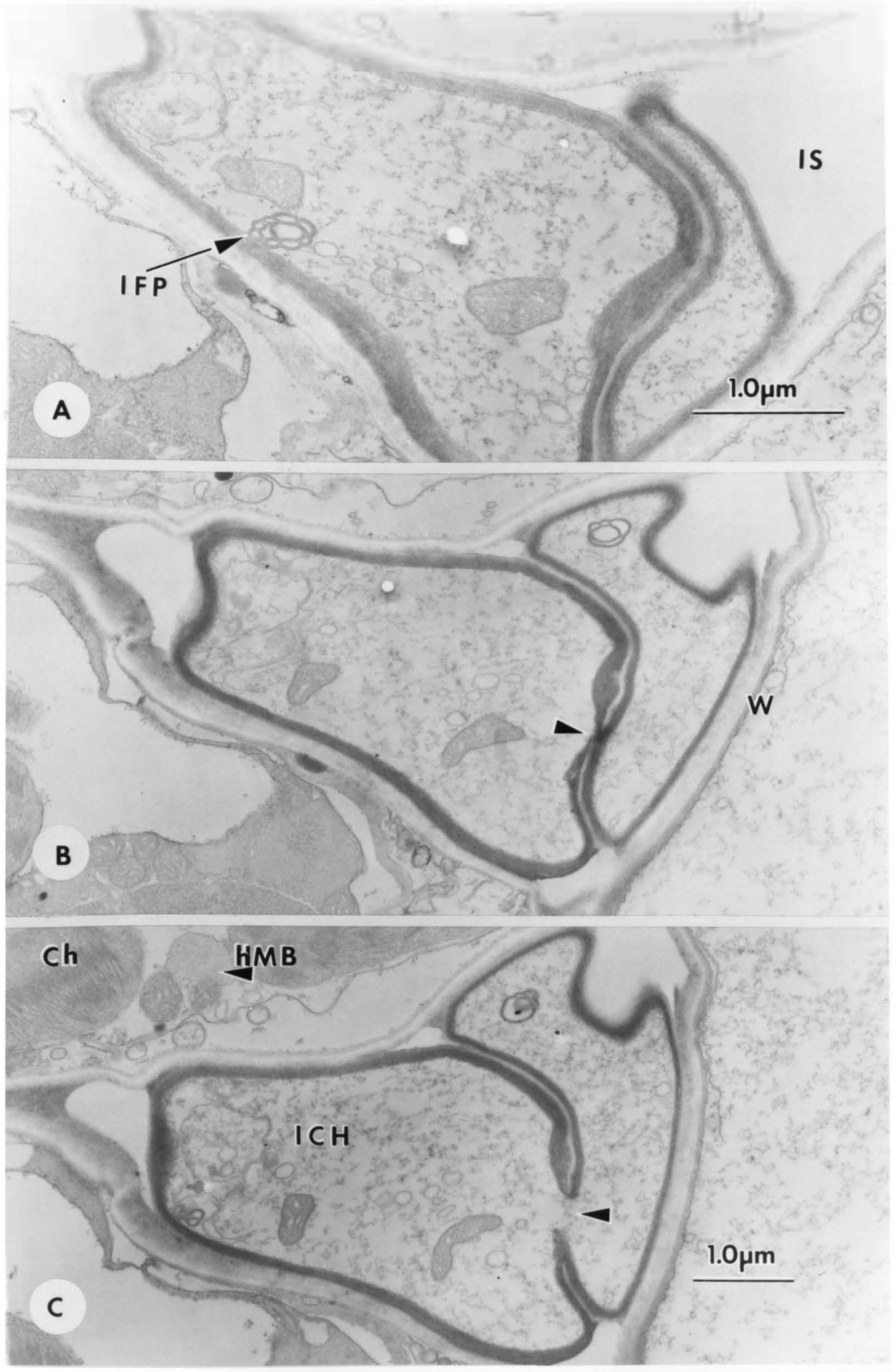
IS
IFP
A
1.0µm
W
B
Ch
HMB
ICH
1.0µm
C

Figure 27. Sections through different septal types of uredial mycelium.

A) A non-perforated septum, surrounded by crystalline and non-crystalline microbodies, mitochondria, and glycogen bodies all bounded by a membrane from the rest of the cytoplasm.

B) A perforated septum, showing a pore and plug (arrowheads). The hypha above the septum is binucleate. Note the presence of mitochondria around the septal pore region in A & B.

C & D) Partial septa in intercellular hyphae. Both pores are open and the passage of organelles is evident. Note the invaginated fungal plasmalemma in A & D (arrows).

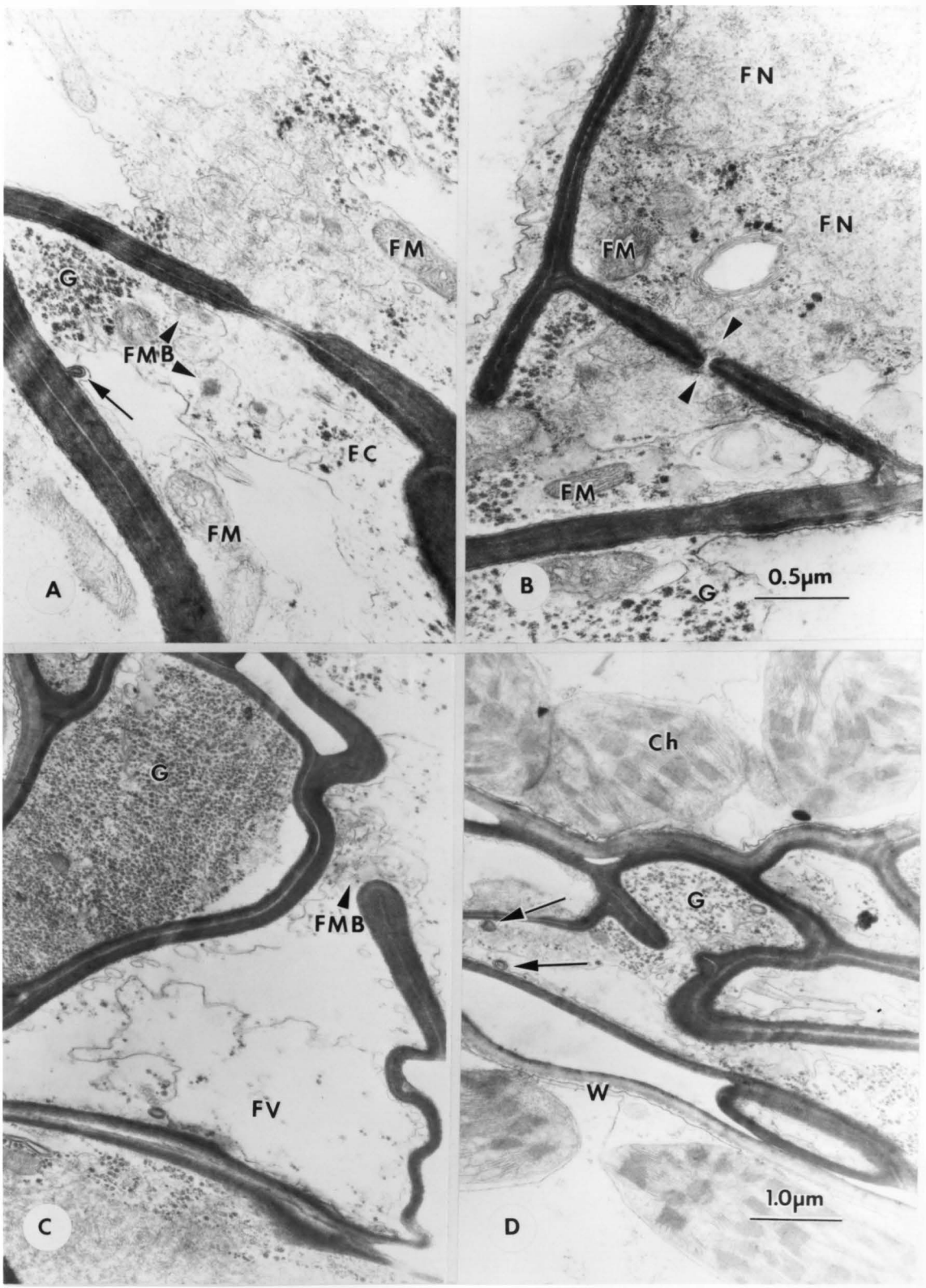
FM
G
FMB
EC
FM
A
FN
FN
FM
FM
G
B
0.5μm
G
FMB
FV
C
Ch
G
W
D
1.0μm

Figure 28-A. A longitudinal section through an intercellular vegetative hypha, showing the close contact to the cell wall on one side. The cells are rich in ribosomes, and mitochondria.

28-B. An enlargement of A, the lower cell shows a little lump on the outside surface (arrowheads), with a cementing material between the cells (stars). Note the invaginated fungal plasmalemma (arrows).

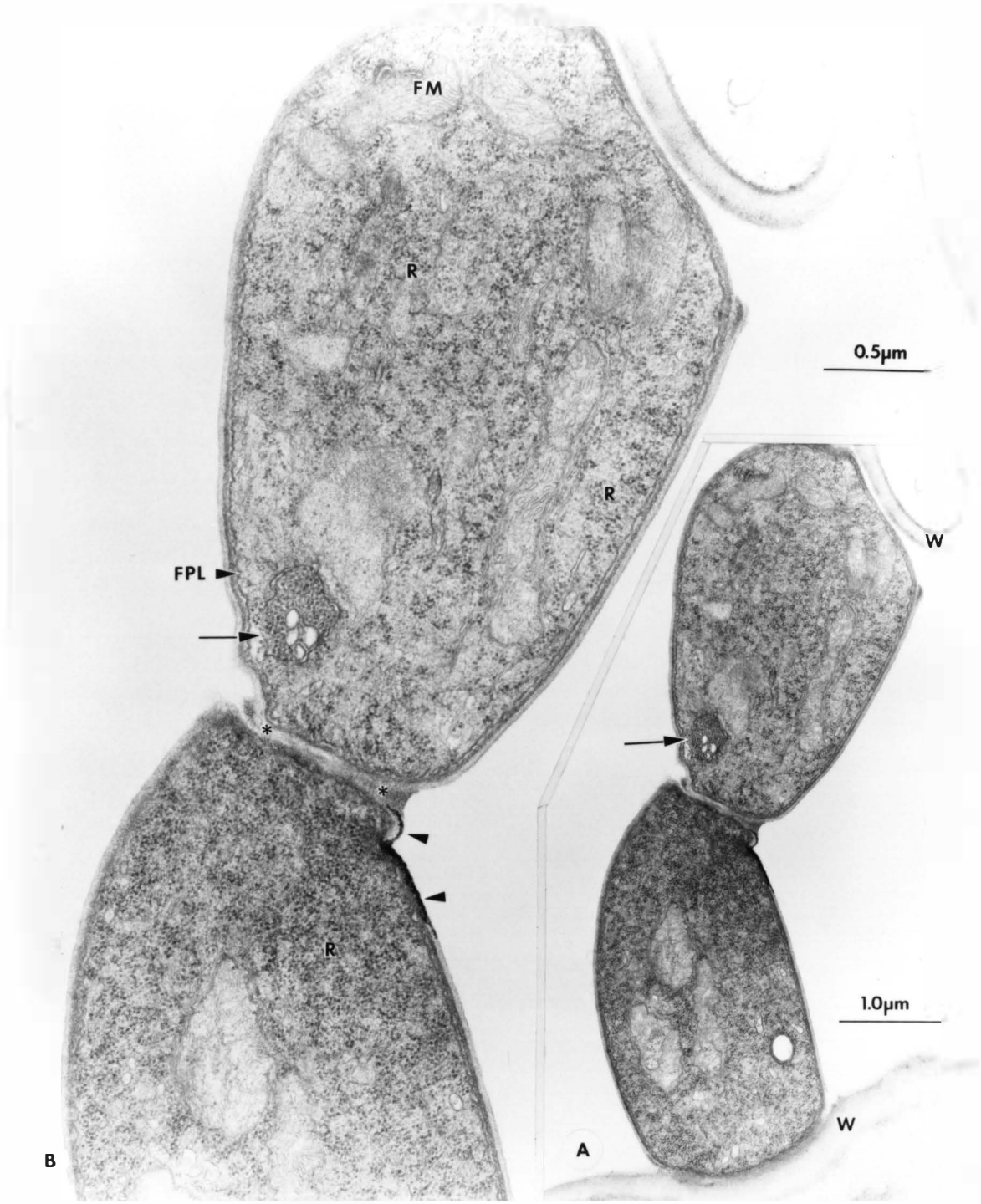
FM
R
R
R
0.5μm
FPL
W
*
*
1.0μm
W
B
A

Figure 29. A cross section of a hyphal cell showing an intercellular binucleate mycelium that contains an extensive amount of ribosomes, and mitochondria with cytoplasmic invaginations (big arrows). Note the close contact between the hypha and the host cell wall (stars).

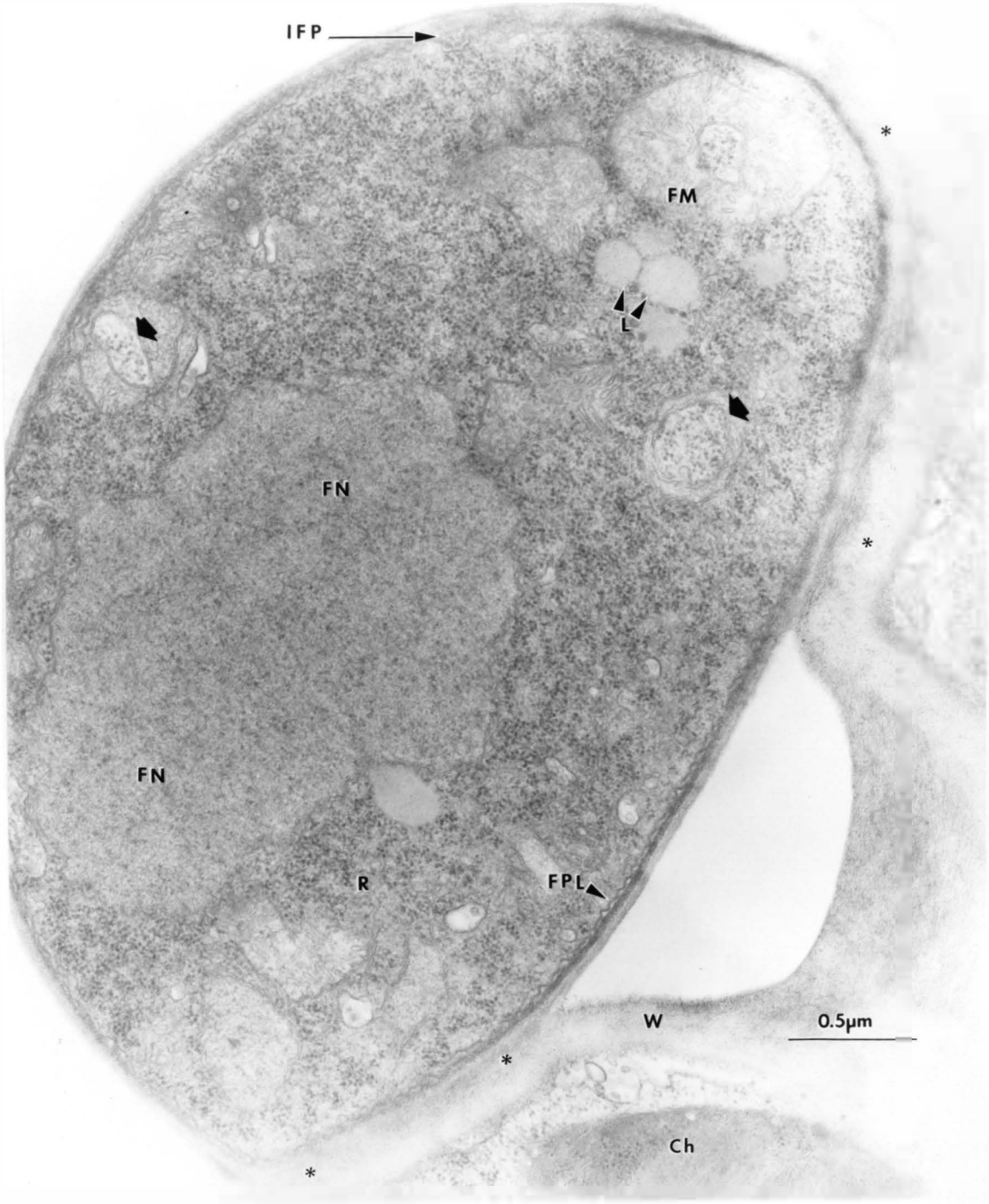
IFP
FM
L
FN
FN
R
FPL
W
0.5µm
Ch

Figure 30. A cross section of branched intercellular hyphae between wheat leaf mesophyll cells showing densely stained cytoplasm with ribosomes, nuclei, a nucleolus, and mitochondria. Most hyphal branches include an invaginated fungal plasma lemma (arrows). Part of the mesophyll cell contains chloroplasts. Note the presence of a structure similar to a dictyosome (arrowhead).

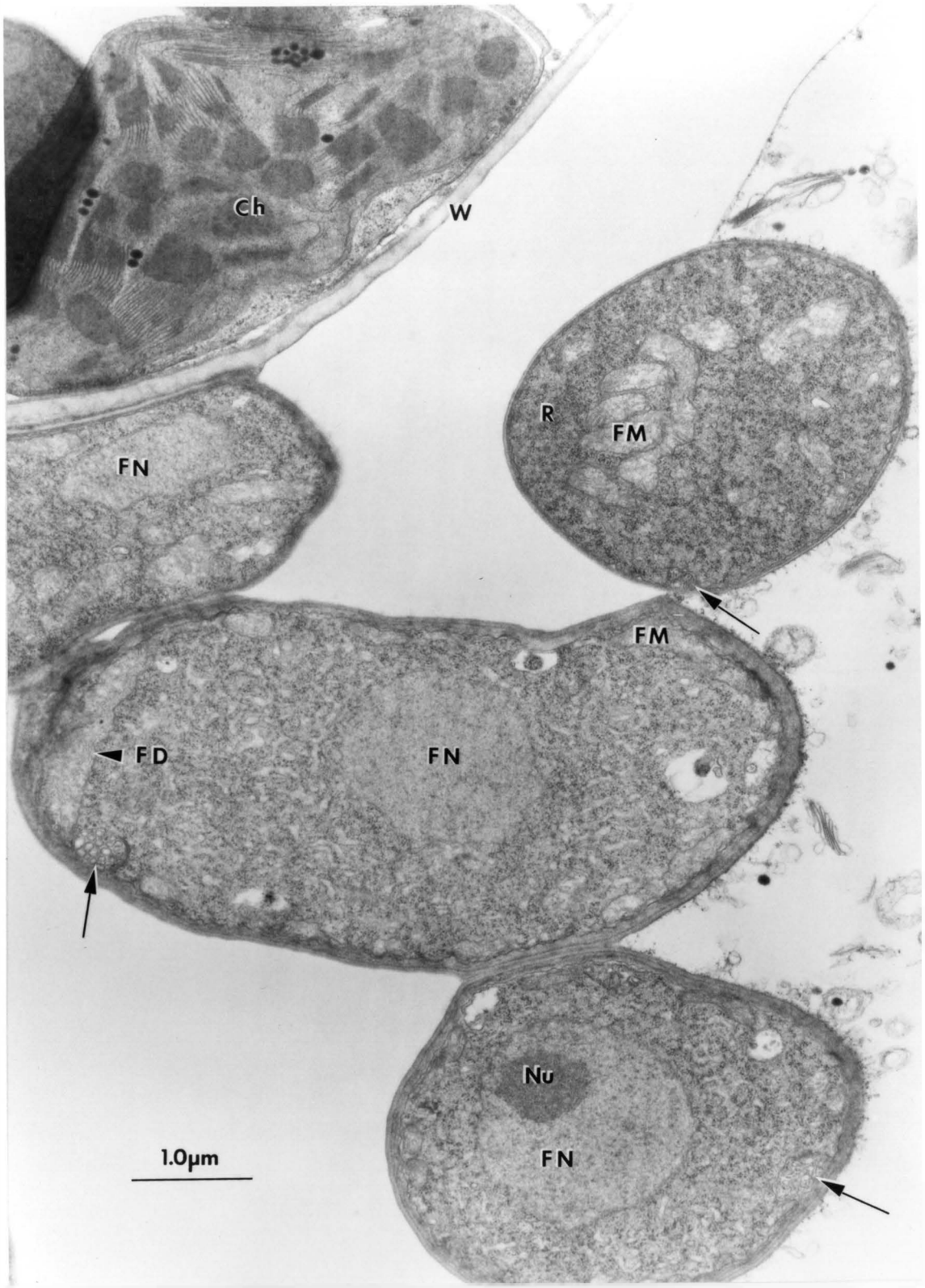
Ch
W
R
FM
FN
FM
FD
FN
Nu
FN
1.0μm

Figure 31. Ultrastructure of a septate intercellular hypha, very high in ribosome content. The plasmalemma is very much invaginated (arrows). Note the rounded mitochondria with cytoplasm enclosed in their centers (arrowheads), and a cementing-like material between the host cell wall and fungal wall (stars).

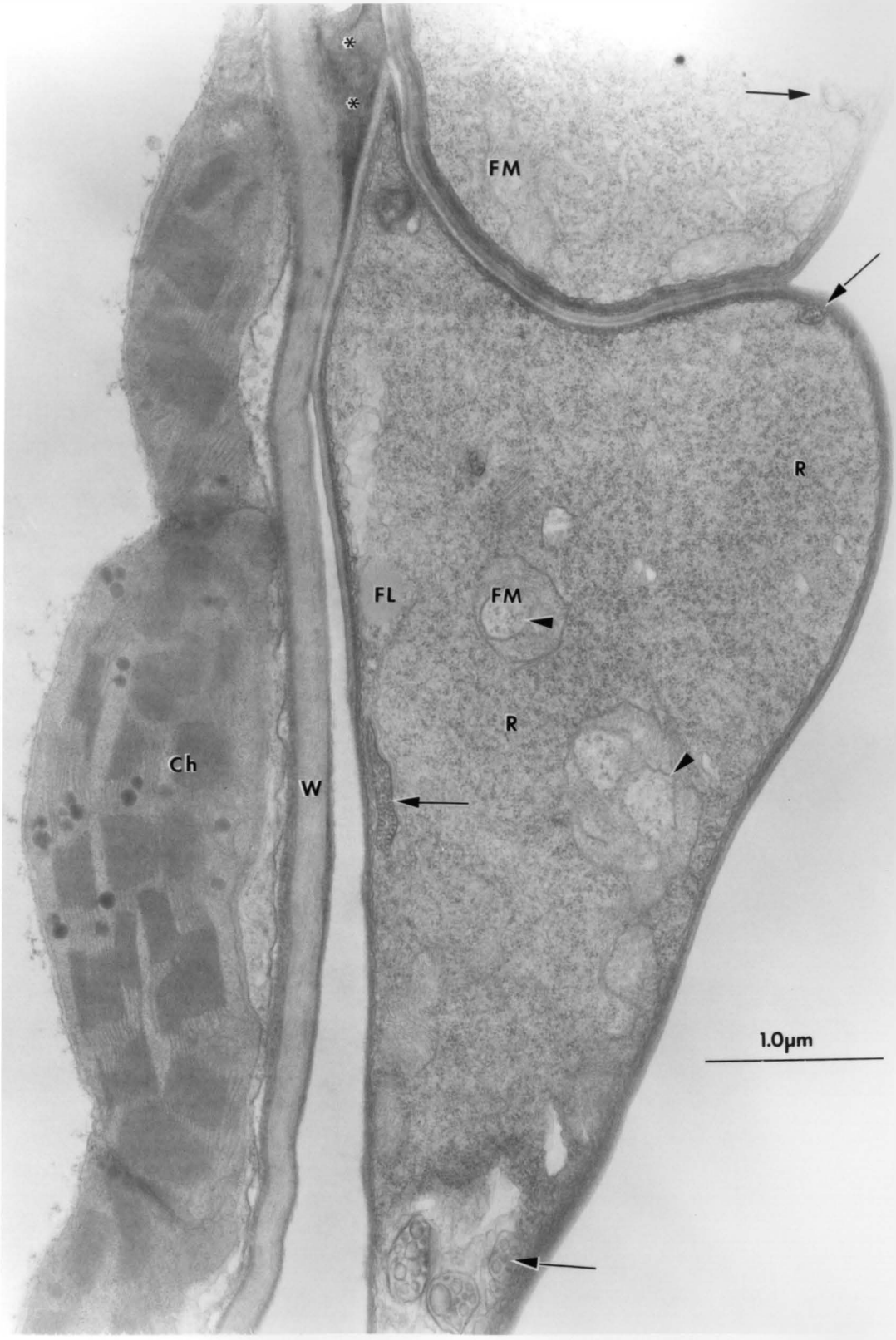
FM
R
FL
FM
R
Ch
W
1.0μm

Figure 32. Ultrastructure of an intercellular hypha, that is a continuous section of Figure 31. The fungal plasmalemma is highly invaginated (arrows). Note the amount of ribosomes, and the mitochondria with invaginated cytoplasm.


IFP
FPL
FM
W
FV
W
R
Ch
0.5µm

Figure 33. Cross sections through different maturity stages of uridiospores.

A) Section through two adjacent immature spores showing spines below spore wall.

B) Enlarged view of an immature spore with spines (Sp) still under the surface,high amount of lipid, ribosomes, and mitochondria.

C) A median section showing the origin of spines.

D) A mature highly vaculated urediospore with spines at the spore surface. Note the wall thickness between the arrowheads.

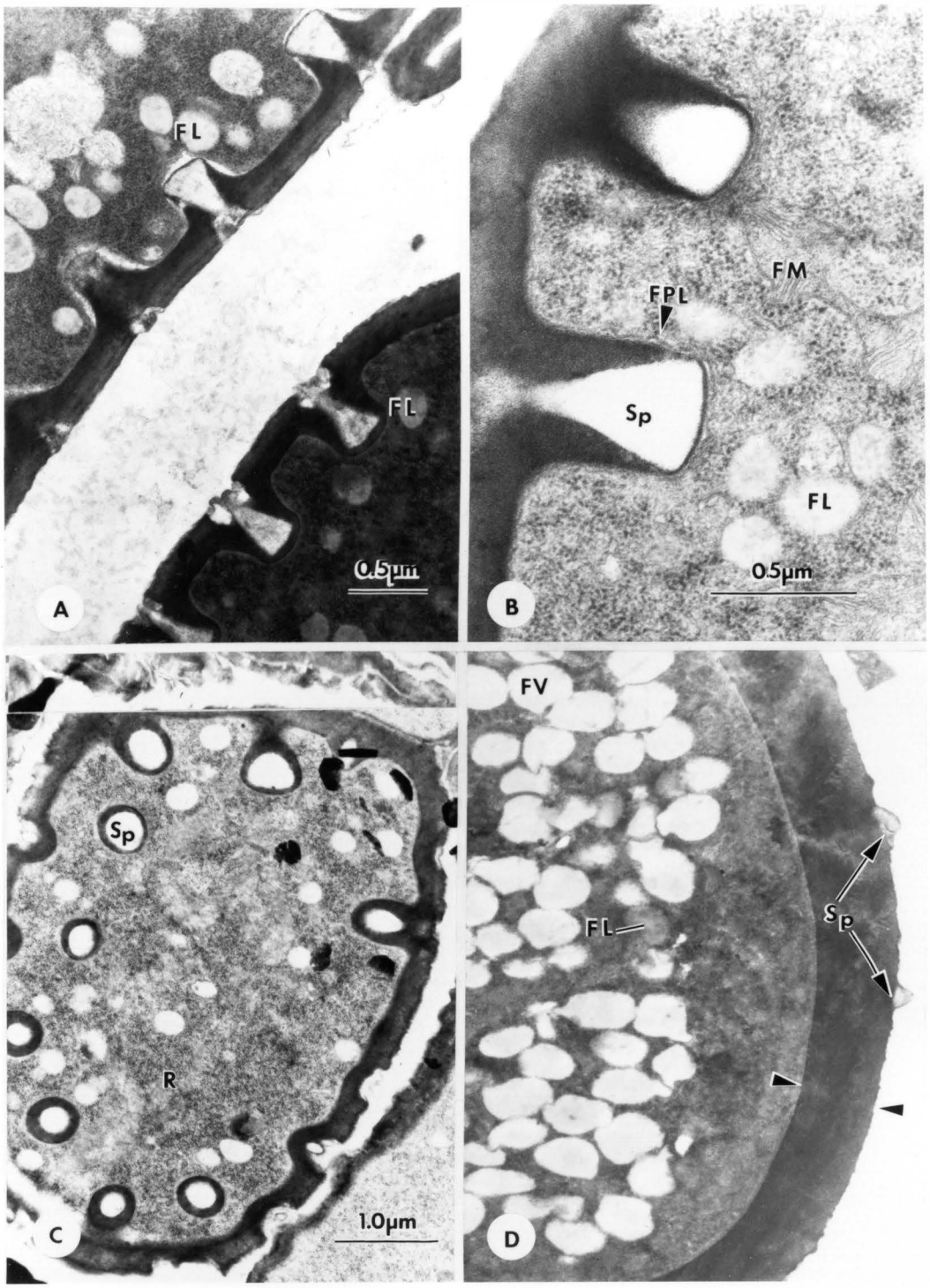
FL
FL
0.5μm
A
FM
FPL
Sp
FL
0.5μm
B
Sp
R
1.0μm
C
FV
FL
Sp
D

Figure 34. Sections through developing spines of urediospores in P. recondita of wheat.

A) A profile of an immature urediospore reveals two spines at different levels from the surface, fungal plasmalemma, mitochondria, and dense cytoplasm rich in ribosomes (R). Note the occurrence of a "flap" of endoplasmic reticulum at the base of the spines (arrows).

B) Section through a developing spine pushing toward the spore surface, and a dense wall-like material (stars) separate the spine from the plasmalemma. A large amount of ER persists at the base of the spine (arrows).

C & D) Enlargement of spines in A, clearly illustrates the presence of endoplasmic reticulum-like membranes near the fungal plasma membrane (arrowheads).

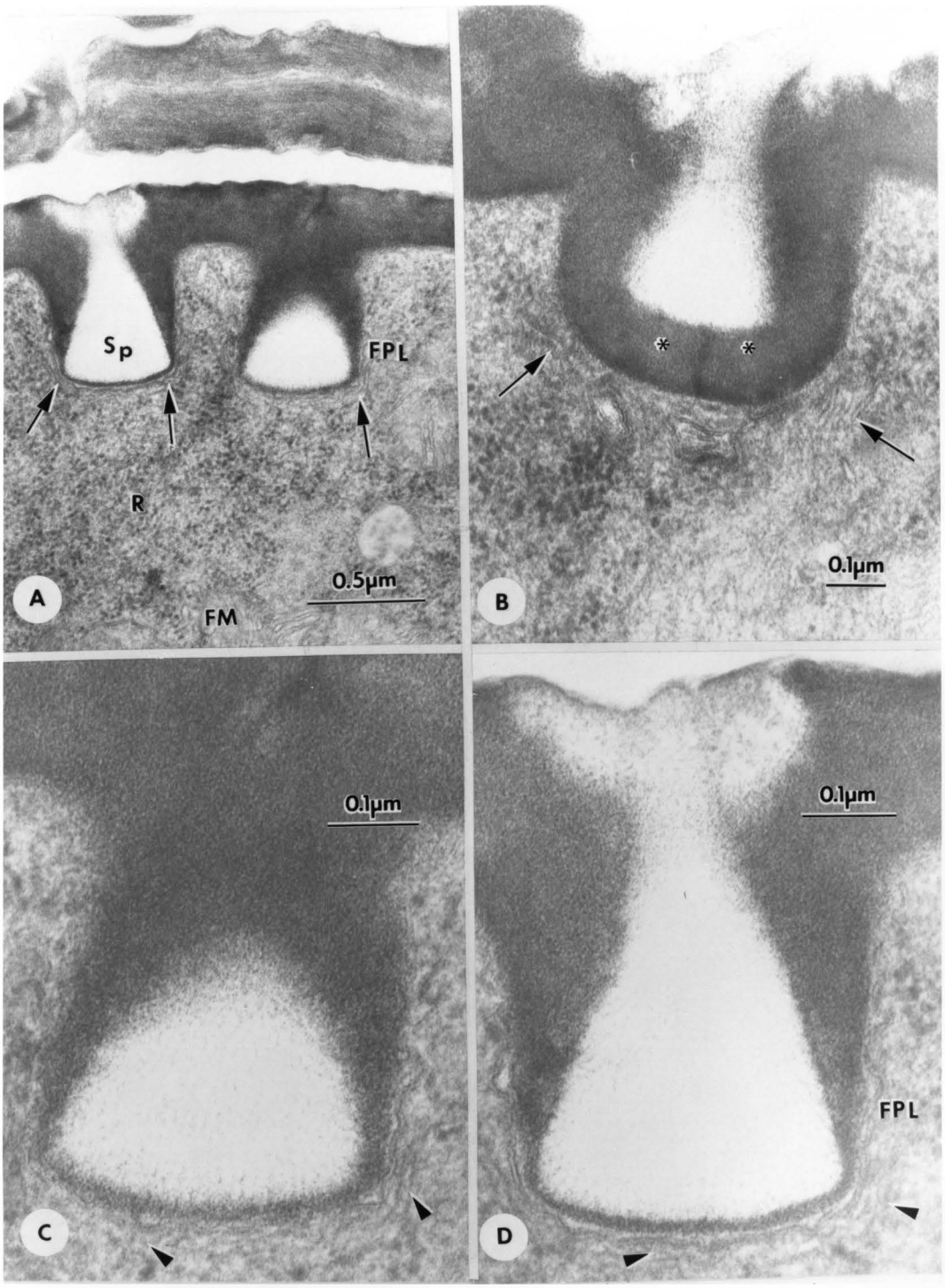
Sp
FPL
R
0.5μm
A
FM
0.1μm
B
0.1μm
C
0.1μm
FPL
D

Figure 35. Ultrastructure of urediospore formation and maturation.

A) Two different stages of urediospore development. The spore on the left is more mature, with spines emerged to the surface (arrowheads), a thicker cell wall. The lipid droplets are large and numerous. The spore on the right has most of the characteristics mentioned, but appears less mature, and contains a nucleus with nucleolus (arrowhead). The spore is still attached to its pedicle.

B) An immature binucleate spore, with a prominent nucleolus, dense cytoplasm, small vacuole and invaginated fungal plasmalemma (arrowhead).


U
FN
2.0μm
U
PD
FL
A
Nu
FN
FV
FN
1.0μm
B

Figure 36. An enlargement of Figure 35-B showing details of a maturing urediospore with small vacuoles (FV), several mitochondria, two nuclei, a nucleolus, nuclear envelopes (big arrowheads), microbodies and enormous amount of ribosomes. Note the presence of invaginated fungal plasma lemma (arrow).

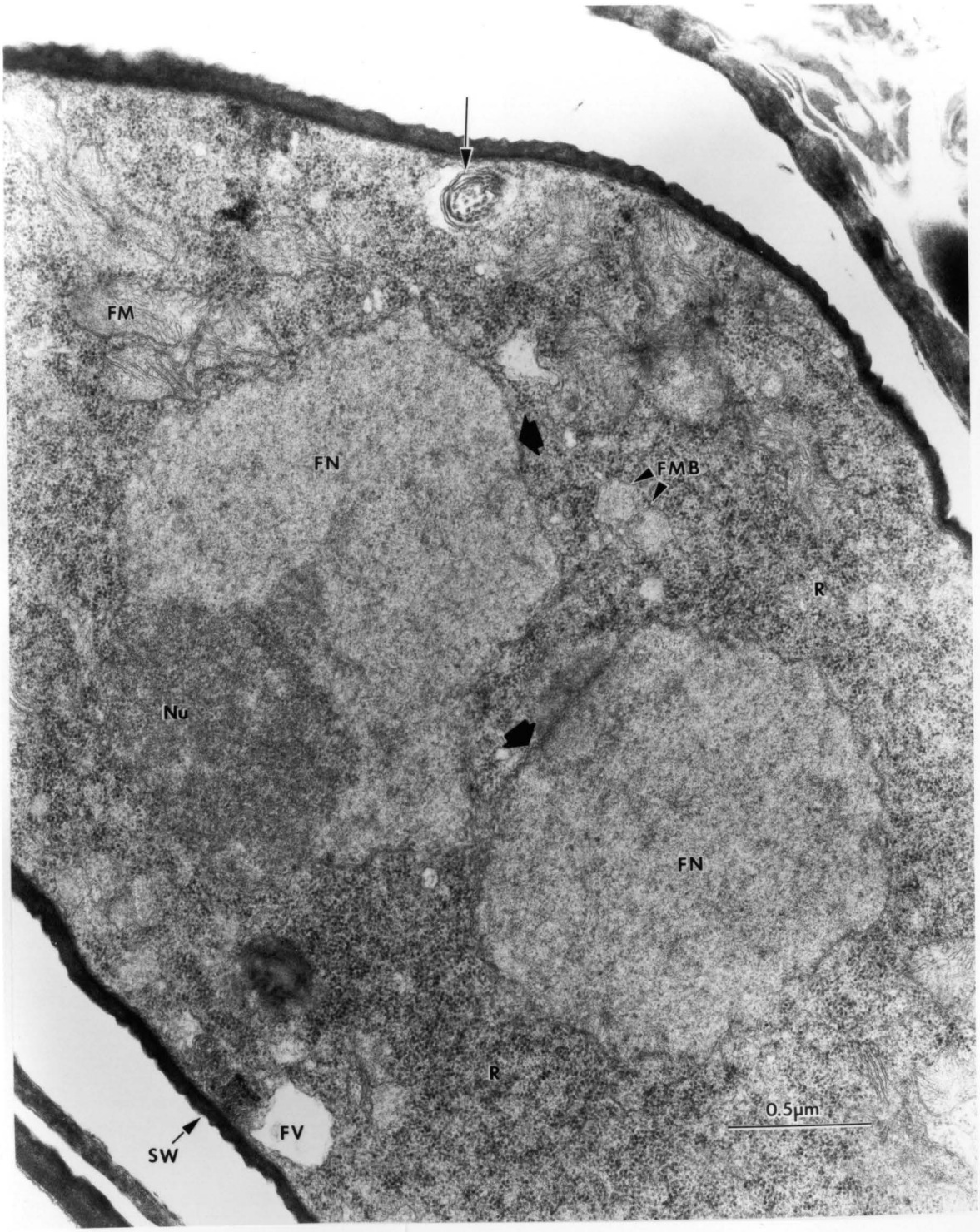
FM
FN
FMB
R
Nu
FN
R
FV
SW
0.5µm

Figure 37. Different views of the block trimming device.

A) A disk made from an acrylic sheet, mounted on a wooden table. The hole at its center is for block holding.

B) The disc is holding a specimen block with embedded tissue positioned in its center.

C) A side view of the block trimming device, fitted on the stage of a binocular microscope. Note the presence of two small handles in the disc used for rotation during trimming.

D) Top view of the "Swift Stero Eighty" binocular microscope. The white surface is part of the wooden table designed to fit over the microscope stage.

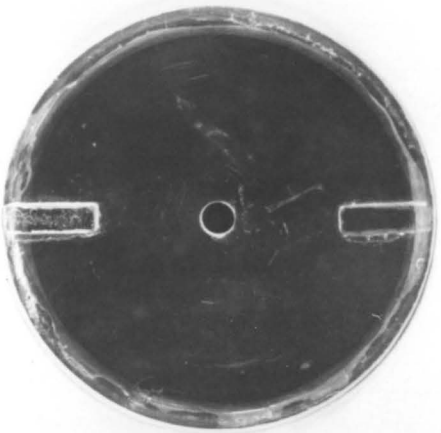

A

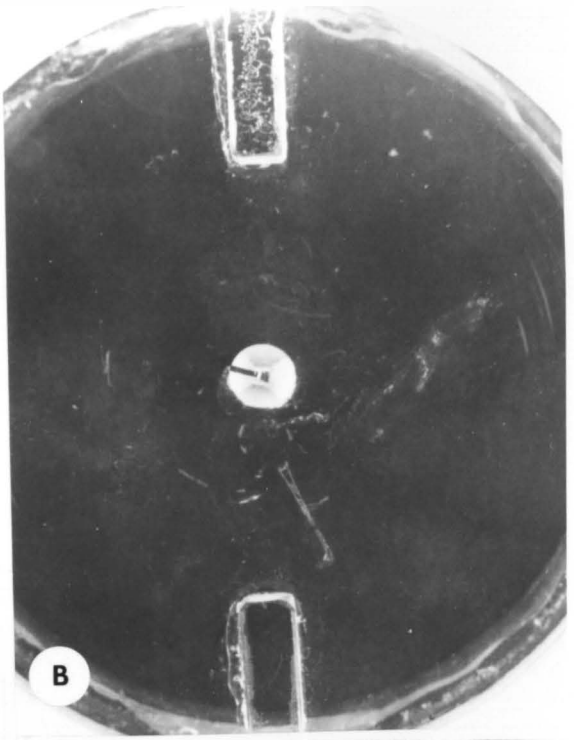

B

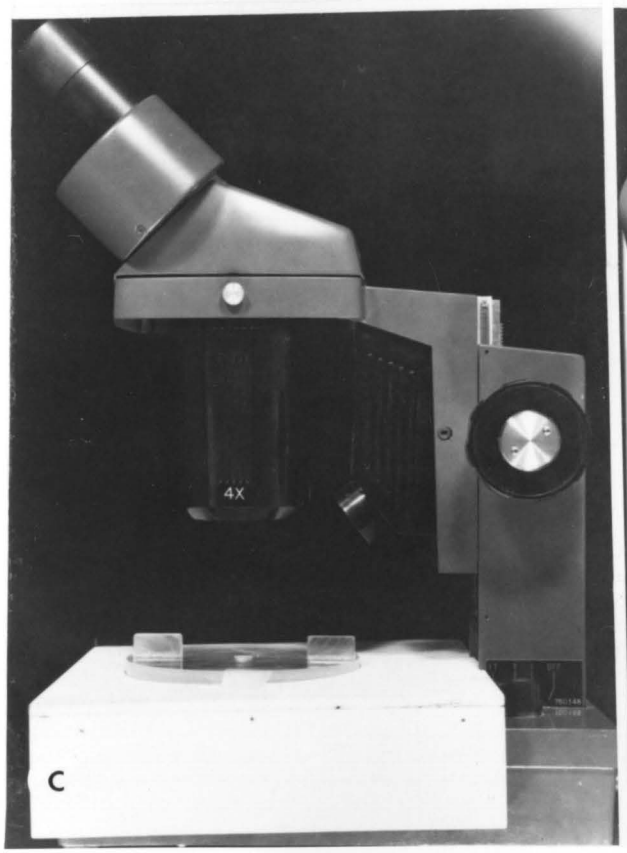

C

D